Differentiation and Cultivation of Retinal Cells in a Defined 3D Environment

Differenzierung und Kultivierung von retinalen Zellen in einer definierten 3D-Umgebung

Zur Erlangung des akademischen Grades eines
DOKTORS DER NATURWISSENSCHAFTEN
(Dr. rer. nat.)
von der KIT-Fakultät für Chemie und Biowissenschaften
des Karlsruher Instituts für Technologie (KIT)

genehmigte

Dissertation

von

Stephan Keppler
aus Schwäbisch Hall

Dekan: Prof. Dr. Manfred Wilhelm
Referent: Prof. Dr. Martin Bastmeyer
Korreferent: PD Dr. Dietmar Gradl
Tag der mündlichen Prüfung: 10.02.2021

Karlsruhe Institute of Technology

Erklärung

Der experimentelle Teil der vorliegenden Arbeit wurde in der Zeit von März 2017 bis September 2020 am Zoologischen Institut, Zell- und Neurobiologie des Karlsruher Instituts für Technologie (KIT) durchgeführt.

Ich versichere hiermit, dass ich diese Arbeit selbstständig verfasst habe und keine anderen als die angegebenen Quellen und Hinweise benutzt habe. Wörtliche oder inhaltlich übernommene Stellen sind als solche gekennzeichnet und die Satzung des Karlsruher Instituts für Technologie (KIT) zur Sicherung guter wissenschaftlicher Praxis habe ich in der gültigen Fassung beachtet. Diese Arbeit wurde in keiner Form einer anderen Prüfungsbehörde vorgelegt. Ich versichere außerdem, dass die beigelegte elektronische Version der Arbeit mit der schriftlichen übereinstimmt.

Karlsruhe, den 29.06.2021

Contents

Chapter 1

1 Abstract

Of the five senses, vision is probably of prime importance for most mammals. Central to visual perception is the retina, a stratified neurosensory tissue lining the back of the eye. It comprises one glial and six neural cell types and is embedded in the retinal pigment epithelium. Light is detected by photoreceptors, modulated by interneurons and forwarded to the brain via ganglion cells.

For decades, research was conducted on animal models, however, not all aspects of development and disease can be approximated therein. Recently, an *in vitro* cultivation system termed organoids was established. Mouse pluripotent stem cells have been aggregated and cultivated in the presence of extracellular matrix, leading to the differentiation of free-floating retina-like tissues. While organoids offer immense opportunities for research, they also have inherent limitations: they lack the retinal pigment epithelium cells, are developmentally restricted to stages comparable to early postnatal development, and their cultivation time is limited to approximately 30 days.

In this work, we sought to address these limitations and improve the organoid system. This should be achieved by a more complex *in vitro* cultivation system via the combination of retinal cells with micro-3D printed substrates. The established method of direct laser writing was employed to fabricate these 3D scaffolds. This method excels at generating larger-scaled substrates with an accuracy within the sub-micron range.

The differentiation and cultivation of retinal organoids was established and further improved by implementing modifications to published protocols. By this a significant increase in the efficiency of retinal induction was achieved.

Three-dimensional substrates consisting of pillar arrays with a height of 70 µm and a radius of 3.5 µm, distanced 20 µm from edge to edge were designed. These substrates were permissive to modifications via protein coating, thereby offering a suitable growth environment for cells.

In a next step, retinal organoids were enzymatically and mechanically dissociated to a single cell suspension and seeded on laminin-coated 3D substrates. Organoid-derived retinal tissues cultivated in 3D substrates were analysed for their viability, cellular composition and organization. The 3D substrates had

no adverse effect on the viability and all major retinal cell types were present. In some cases, a preferential organization in axial direction was observed with photoreceptor-like cells preferentially localizing to the upper part of the substrates. Furthermore, the cultivation time in the 3D substrates was prolonged to up to 50 days.

In this thesis, a long-term *in vitro* cultivation system combining retinal organoid-derived cells and direct laser writing-fabricated 3D substrates was successfully established. In successive work, further analyses and modifications of the system could be performed.

Chapter 2

2 Zusammenfassung

Unter den fünf Sinnesempfindungen nimmt das Sehen für die meisten Säugetiere die zentralste Rolle ein. Das Sehvermögen wird durch die Retina bewerkstelligt, einem geschichteten neurosensorischen Gewebe das den Augapfel auskleidet. Die Retina besteht aus Müller Gliazellen und sechs neuronalen Zelltypen und ist in das retinale Pigmentepithel eingebettet. Licht wird durch die Photorezeptoren detektiert, von Interneuronen verarbeitet und über die Ganglienzellen an das Gehirn weitergeleitet.

Seit Jahrzehnten werden für die Wissenschaft Tiermodelle verwendet, allerdings können diese nicht alle Aspekte der Entwicklung und Erscheinungsbilder von Erkrankungen widerspiegeln. Vor kurzem wurde ein *in vitro* Kultivierungssystem eingeführt, das als Organoide bezeichnet wird. Pluripotente Mausstammzellen wurden aggregiert und in der Gegenwart von Extrazellulärer Matrix weiter kultiviert. Dies führt zur Differenzierung von freischwimmendem Gewebe, das einer Retina ähnelt. Während Organoide unzählige Möglichkeiten für die Wissenschaft bieten, gehen sie auch mit einigen Beschränkungen einher: sie weisen nicht das retinale Pigmentepithel auf, sind von der Entwicklung auf frühe postnatale Stadien limitiert und ihre Kultivierungszeit ist auf ca. 30 Tage beschränkt.

In dieser Arbeit wurden Anstrengungen vorgenommen, die Beschränkungen des Organoid-Systems auszugleichen und zu verbessern. Dies sollte durch die Kombination mit mikro-3D gedruckten Substraten bewerkstelligt werden, um so ein komplexeres *in vitro* Kultivierungssystem zu erlangen. Zur Herstellung der Strukturen wurde die etablierte Methode des Direkten Laserschreibens verwendet. Diese Methode eignet sich hervorragend, um großflächige Substrate mit einer Genauigkeit jenseits der Mikrometer-Grenze, herzustellen.

Die Differenzierung und Kultivierung von retinalen Organoiden wurde etabliert und durch Modifikationen des ursprünglich publizierten Protokolls verbessert. Dadurch konnte die retinale Induktion in Organoiden signifikant verbessert werden.

Die dreidimensionalen Substrate bestehen aus Säulenfeldern mit einer Höhe von 70 µm, einem Radius von 3.5 µm und einem Kanten-zu-Kanten Abstand

von jeweils 20 µm. Ferner können diese Strukturen durch Proteinbeschichtungen weiter modifiziert werden, wodurch Zellen eine angemessene Wachstumsumgebung geboten wird.

In einem weiteren Schritt wurden retinale Organoide enzymatisch und mechanisch zu einer Einzelzellsuspension dissoziiert und auf Laminin-beschichteten 3D Substraten ausgesät. Von Organoiden abstammendes Gewebe in 3D Substraten wurde auf die Viabilität, die Zusammensetzung der Zelltypen und die Organisation der Zellen überprüft. Die 3D Substrate zeigten keinen negativen Einfluss auf die Viabilität der Zellen und alle Hauptklassen an retinalen Zellen waren vorhanden. In einigen Fällen konnte eine bevorzugte Orientierung in axialer Richtung beobachtet werden. Photorezeptor-ähnliche Zellen lokalisierten bevorzugt in den oberen Bereichen der Substrate. Außerdem konnte die Kultivierungszeit innerhalb der Strukturen auf bis zu 50 Tage ausgeweitet werden.

In dieser Dissertation wurde ein *in vitro* Kultivierungssystem erfolgreich eingeführt. Zur Verbesserung der Langzeitkultivierung wurden durch Direktes Laserschreiben hergestellte 3D Substrate mit von retinalen Organoiden abstammende Zellen kombiniert. In nachfolgenden Arbeiten kann das System weiter analysiert und Modifikationen vorgenommen werden.

Chapter 3
3 Introduction

Animals are relying on five senses to navigate through and interact with their surroundings. Depending on the various niches preferred by specific animals, the predominant senses also vary. For humans and many other animals, vision is the most important sense. It allows long- and short-range assessment of the environment, including animate and inanimate objects.

The importance of vision was a strong motivation for studying the eye, its morphology, composition, and development. Furthermore, its ease of accessibility in model animals combined with the same developmental origin as the brain, render the retina a suitable model system for morphological and developmental processes in complex neuronal tissues.

Notable structures of the eye are the cornea, ciliary body, iris, lens, and retina. The cornea is the outermost part of the eye. It is a transparent and avascular connective tissue, adopting functions such as the primary structural and infectious barrier (Eghrari et. al 2015). It is shaped flatter in the periphery and steeper towards the centre, creating an aspheric optical system. Typically, the cornea consists of an epithelium, stroma, and endothelium cell layer. Remarkably, the cornea is a transparent structure, with the transparency being achieved via the precise organization of stromal fibers and extracellular matrix (ECM) (DelMonte and T. Kim 2011). The iris is a thin annular structure, which controls the size and diameter of the pupil. Just behind the iris, the muscular structure of the ciliary body is located. It is composed of the ciliary muscle and ciliary epithelium. The muscle actively controls the shape of the lens, while the epithelium produces the aqueous humor, which regulates the intraocular pressure and provides nutrition to the avascular ocular tissue (Goel et. al 2013). Cornea, iris and ciliary body facilitate a functional unit to regulate the amount of light able to enter the eye.

3.1 Retinal Development *in Vivo*

The retina is the neurosensory part lining the back of the eye. It is comprised of three clearly distinguishable layers: the outer nuclear layer (ONL) with rod and

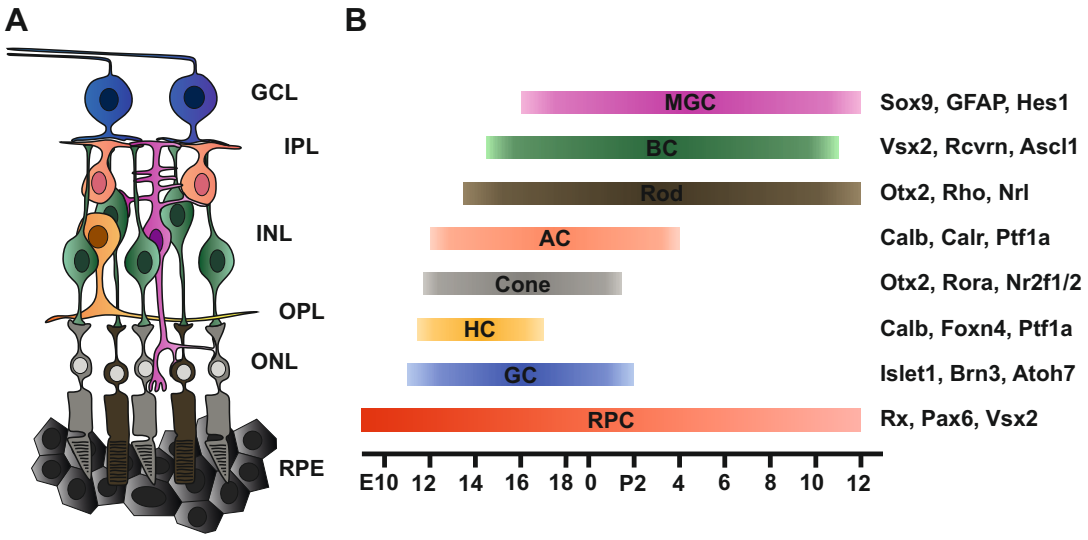

Figure 3.1: **Organization and cell type specification during retinogenesis.** (A) Schematic overview of retinal organization in axial direction. The retina is composed of three nuclear and two plexifom layers embedded in the RPE. (B) Temporal progression of retinal development starting with embryonic day 10 (E10) and lasting until postnatal day 12 (P12). For each cell type, three relevant markers are listed. GCL, ganglion cell layer; INL, inner nuclear layer; ONL, outer nuclear layer; IPL, inner plexiform layer; OPL, outer plexiform layer; RPE, retinal pigment epithelium; RPC, retinal progenitor cells; GC, ganglion cell; HC, horizontal cell; AC, amacrine cell; BC, bipolar cell; MGC, müller glial cell

cone photoreceptors (PR), the inner nuclear layer (INL) with bipolar, horizontal and amacrine cells, as well as Müller glial cells, and lastly the ganglion cell layer (GCL) with the retinal ganglion cells (GCs, Figure 3.1 A). Their axons coalesce and form the optic nerve. The layers are also defined by the corresponding cell's functions: the PRs in the ONL detect light via photosensitive proteins of the opsin family, the interneurons of the INL modulate, process and forward the stimuli detected by the PRs to the GCs in the GCL, which forward the information via the optic nerve to the superior colliculus in the brain (Barer and Sidman R. L. 1955; Scalia and Fite 1974). The general architecture and morphology of the eye is largely conserved throughout the animal kingdom.

The retina is not only strictly organized in axial direction, but also shows differential organization in lateral direction. Starting from the central point of vision, the fovea centralis, which is an area of closely packed cones right in the focus of the lens, the cellular composition shifts towards rod-domination in the periphery. Along with the central to peripheral changes in cell composition, the

retinal thickness also varies. While the retinal thickness is centrally at its lowest, it rapidly increases and slightly falls off towards the periphery (E. K. Kim et. al 2017).

Rod and cone PRs not only show differences in distribution, but are also responsible for vision in different light levels and circumstances. Rod PRs are highly sensitive and have Rhodopsin as light-sensitive photopigment. They function in dim light and are integral to animal's night vision. Cones are involved in colour and high-acuity vision. Depending on the species, several subtypes can be available, each containing one or more opsins sensitive to a different wave length (Brzezinski and Reh 2015; Yen and Fager 1984). In addition to the neuro retinal cells, the supportive monolayer of retinal pigment epithelium (RPE) is also part of the retina. PRs are in direct contact with the ciliated RPE, which adopts functions in metabolic support and in phagocytosis of spent outer segments. The subsequent regeneration of all-*trans*-retinol back to functional 11-*cis*-retinal is also mediated by the RPE (Kusakabe et. al 2009). Furthermore, the RPE also functions as a source of signaling during development (Ha et. al 2017).

Throughout development, retinal progenitor cells (RPC) continue to differentiate. This differentiation process follows a strict timeline. Progenitor cells can be subdivided into early and late progenitor cells, depending on the relative occurrence of their progeny. Birth-dating experiments in rat retina identified the progeny of single progenitor cells via the injection of low amounts of virus leading to the expression of β-galactosidase. Addition of a chromogenic substrate led to the formation of a blue dye in infected cells, allowing a clear characterization of cells via morphology and localization (Cepko et. al 1996; D. L. Turner and Cepko 1987). These experiments clearly showed the progeny of single progenitor cells, allowing conclusions about the time of occurrence of retinal cell types (Figure 3.1 B). Accordingly, GC are the first cell type to arise from early retinal progenitors, followed by horizontal, cone and amacrine cells. Late progenitor cells give rise to rods, bipolar and Müller glial cells (Bassett and Wallace 2012; Cepko et. al 1996).

3.1.1 Basic Steps in Retinal Development

The experimental focus of this thesis is on the development of retinal structures *in vitro*, therefore retinal development will be discussed in more detail in the following chapters.

The very early steps of retinal development are shortly after the gastrulation. In the anterior neural plate, the eye field is specified. This eye field contains all the progenitor cells giving rise to the future eye structures. However, this eye field is displaced shortly after gastrulation by prospective hypothalamic cells moving rostrally within the neural plate (H.-s. Li et. al 1997; Wilson S. W., Houart C. 2004). This displacement disrupts the eye field into two separate optic vesicles

(OVs) (Figure 3.2). A complex network of transcription factors is involved in specifying the eye field, called eye field transcription factors (EFTFs) (Zuber et. al 2003). These EFTFs comprise *Pax6, Six3, Six6, Rx, Lhx2* and *Otx2*. Most of these factors are also involved in the development of other neural structures, but their combined expression leads to the formation of the eye field (ibid.). The widespread expression of the EFTF in other tissues renders the analysis and characterization of their involvement during retinal differentiation more challenging.

Current models for establishing the eye field in mouse start with the presence of Otx2 and Sox2 in the anterior neural ectoderm at E7.0, leading to the expression of *Rx* at E7.5-E8.0, characterizing the prospective eye field. In the eye field, *Lhx2, Pax6, Six3* and *Rx* are expressed. Pax6 and Lhx2 work in concert to activate expression of *Six6*, while Six3 suppresses wingless and int-1 8b (Wnt8b), a process required to specify the anterior neural plate to neural retina fate (Heavner and Pevny 2012; W. Liu et. al 2010; Zuber et. al 2003). It could also be shown that the EFTFs are sufficient to generate eye fields by injecting their RNA simultaneously into one blastomere at the two-cell stage. This leads to the ectopic expression of RPE and even ectopic eyes in 20% of injected embryos. These eyes were detected near the central nervous system, but also in other areas of the embryo. EFTFs could also be induced via the combined action of Otx2 and the neural inducer and bone morphogenetic protein-inhibitor Noggin (Zuber et. al 2003).

EFTFs not only have important functions during the specification of the eye field, but they are also essential during eye development (Tétreault et. al 2009; Wawesik S., Maas R. L. 2000). Animals with defects in *Pax6, Lhx2* and *Six3* show malformations and developmental defects, ranging from microphthalmia to the arrest of development at optic cup (OC) stages (Glaser et. al 1994, 1992; Hägglund et. al 2011; Hever et. al 2006; Tétreault et. al 2009).

The central role of *Rx* during eye field establishment was shown in a Rx-deficient mouse model, where mice failed to establish the eye field and expression of EFTFs was lacking (Pariser et. al 2000). A potential function of *Rx* in cell sorting during formation of the eye field was indicated in chimeric mice, which contained wild-type and Rx deficient cells. The *Rx* deficient cells were segregated during early steps and were never included in the formation of eye structures (Medina-Martinez et. al 2009).

3.1.2 Formation of the Optic Vesicle and Optic Cup

After the eye field has been split into two domains and the walls of the diencephalon evaginate, the OVs form (Figure 3.2). During early stages of development, the pool of RPCs rapidly increases. Initially, this rise in proliferation was linked to

the morphogenic event of OV evagination. However, it was shown that drastic changes in cell morphology are central to the evagination events of the OV, along with alterations of the basal lamina composition (Svoboda and O'Shea 1987).

The OV is subsectioned into different regions, each containing specific RPCs. The specialized regions correspond to the presumptive neural retina, defined by the expression of *Vsx2*, the presumptive RPE, defined by the expression of *Mitf*, and lastly the presumptive optic stalk, which is defined by the expression of *Pax2* (I. S. C. Liu et. al 1994; Nornes et. al 1990).

After the formation of the OV, a second larger-scale morphological change occurs. Both, the lens placode and the OV coordinately invaginate, forming the lens vesicle and the bilayered OC (Figure 3.2). During this process, the central part of the OV, the presumptive neural retina, fold onto the peripheral parts, the presumptive RPE (Jackson 1981). It was a long held assumption that the lens placode is required for the invagination process (Hyer et. al 2003). However, *in vitro* studies with pluripotent stem cells presented evidence that Rx^+ domains are able to invaginate in the absence of other structures like the lens placode (Eiraku et. al 2011).

3.1.3 Splitting of RPE and Neural retina

Prior to OC formation, the retina is patterned into specific domains. During this patterning process, a neural retina domain and an RPE domain emerges. These domains are strictly exclusive and characteristic transcription factors are expressed. In the presumptive neural retina, expression of RPC-markers like *Vsx2, Ascl1* and *Pax6* are predominant (Wright et. al 2015). *Vsx2* is a key regulator of RPC proliferation and is also involved in mediating mitogen signaling, as it controls correct timing and magnitude of hedgehog signaling (Rowan and Cepko 2005; Sigulinsky et. al 2008). Reports also indicate an involvement of *Vsx2* in the proliferation of RPCs via the interaction with G1-phase cell cycle regulators (E. S. Green et. al 2003).

The RPE is characterized by the expression of transcription factors like *Mitf* and *Otx2*. Loss of *Mitf* expression also disrupts the RPE development (Capowski et. al 2014). The expression of *Mitf* is induced by surrounding extraocular mesenchyme, leading to the induction and maintenance of *Mitf* and *Wnt13*. Explant cultures in the absence of extraocular tissue did not show differentiation to RPE (Fuhrmann et. al 2000). Furthermore, a regulatory loop involving the retinal marker *Pax6* has been identified. Combined expression of *Mitf* and *Pax6* suppress the expression of *fibroblast growth factors 15 (Fgf15)* and *Dickkopf-3 (Dkk3)*. A combination of FGF

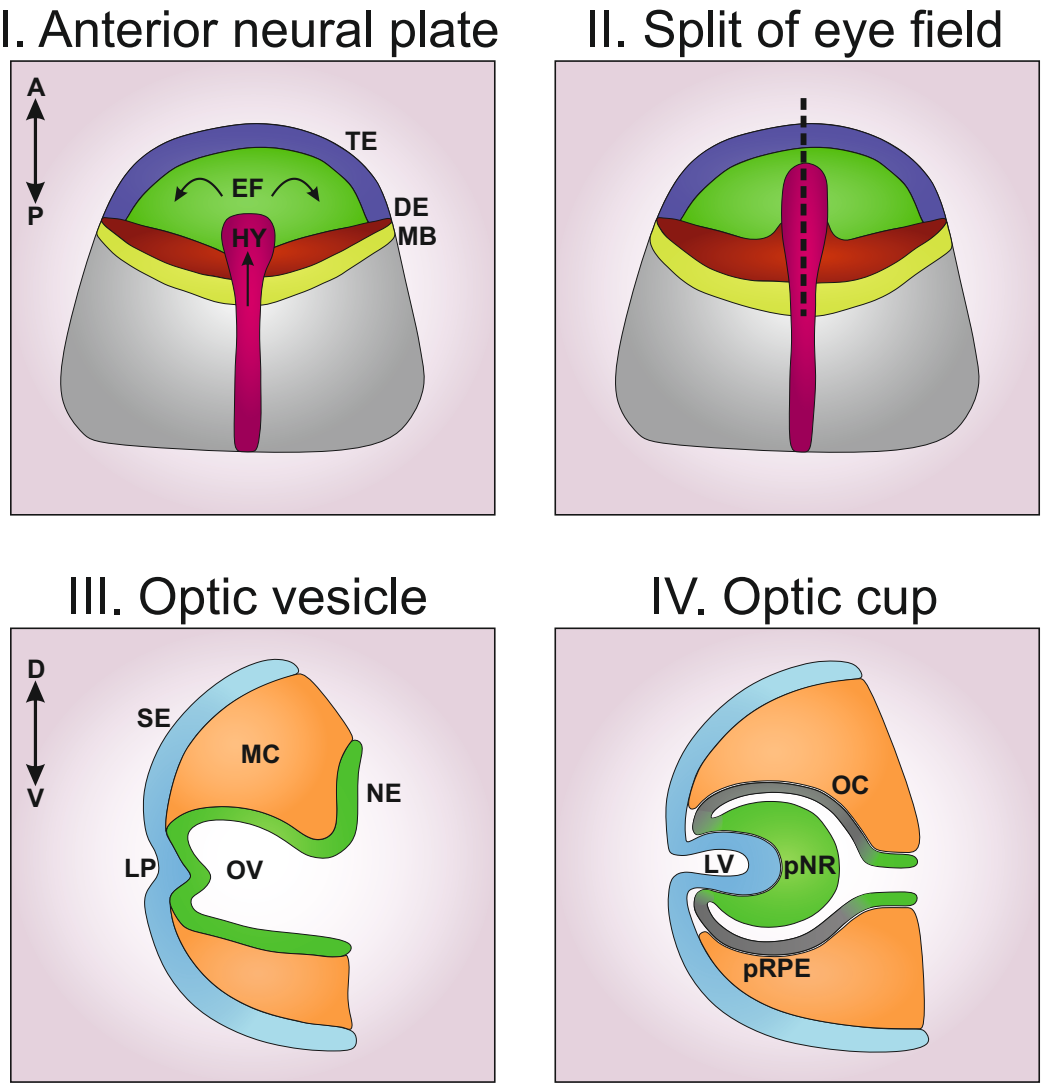

Figure 3.2: **Splitting of the eye field and formation of the optic cup.**
(I) The eye field (EF) is specified by a network of eye field transcription factors. (II) Axially moving prospective hypothalamic (HY) cells lead to the separation of the single eye field into two eye primordia. (III) The eye primordiums neuroepithelium (NE) evaginates, forming the optic vesicle (OV). Upon direct contact with the surface ectoderm (SE), the OV invaginates. The section of SE in apposition to the OV forms the lens placode (LP). (IV) Invagination of the OV and LP lead to the formation of the OC and lens veiscle (LV), giving rise to the lens later on. Secreted factors of the surrounding mesenchyme (M) lead to the specification of the presumptive retinal pigment epithelium (pRPE), while the central section of the OC faciliates the presumptive neural retina (pNR). TE, telencephalon; DE, diencephalon; MB, midbrain; A, anterior; P, posterior; D, dorsal; V, ventral

and DKK3 was shown to promote neural retina formation by inhibiting canonical WNT signaling and stimulating the expression of retinogenic genes like *Six6* and *Vsx2* (Bharti et. al 2012).

The expression domains of *Vsx2* and *Mitf* are exclusive and *Mitf* repression via *Vsx2* is required for the maintenance of neural retina identity in mammals (Horsford et. al 2005).

3.1.4 Signaling Cascades Involved in Development

The well coordinated and precise development of all retinal cell types is achieved by the interplay of transcription factors and signaling pathways, like those activated by bone morphogenetic proteins (BMP), fibroblast growth factors (FGF), hedgehog (HH) and WNT. These pathways adopt important functions during embryonic development by providing positional information to individual cells (Basson 2012; Clevers 2006).

In chick, *Bmps* are expressed in the surface ectoderm and BMP-coated beads were able to induce ectopic *Mitf* expression, thus leading to the differentiation towards RPE fate. However, OC morphogenesis is disturbed in BMP-treated eyes (Hyer et. al 2003; Müller et. al 2007). This is in contrast to studies in mammals, indicating the requirement of BMP signaling for correct patterning, growth and differentiation of the retina (Murali et. al 2005). *In vitro*, retinal fate could also be induced via the addition of BMP4 (Kuwahara et. al 2015).

Sonic hedgehog (Shh) is expressed along the entire axial mesoderm and is involved in the splitting process of the eye field into the future OVs. Mutations in *Shh* lead to malformations in which the forebrain hemispheres fuse, resulting in most severe cases in cyclopic embryos (Wallis and Muenke 1999). The neuroectodermal domain is sensitized by midline secreted FGF (M. Carl, F. Loosli and J. Wittbrodt 2002). During retinal development, *Shh* is expressed in retinal GCs, which themselves are also sensitive to SHH signaling. Additionally, SHH in combination with Notch stimulates RPCs to remain proliferative over time (Miesfeld and Brown 2019). SHH secreted from retinal GCs maintains the expression of *Pax2* in the optic stalk via expression of *Vax1* (Bertuzzi et. al 1999; Dakubo et. al 2003).

Canonical WNT signaling is required during the differentiation of RPE. This becomes apparent upon inactivation of WNT signaling, causing RPE to transdifferentiate to neural retina (Westenskow et. al 2009). In the neural retina, the canonical WNT pathway is suppressed by Rx, preventing the induction of posterior fates (Martinez-Morales and Wittbrodt 2009). In the absence of WNT, FGFs from the surface ectoderm are able to induce retinal fate via the expression of *Vsx2* (Horsford et. al 2005; M.-T. T. Nguyen and H. Arnheiter 2000).

3.1.5 RPE-PR Interface

PRs are a specialized cell type with high metabolic activity, requiring a complex polarized morphology and the presence of surrounding supportive structures (Brzezinski and Reh 2015). Even though RPE and PRs develop from two different sources, they form a functional unit in the adult retina. This is a key requirement for correct visual function of the retina. PRs have a modified primary cilium, the outer segment, where the light sensitive opsins reside in well-organized disc structures (Dowling 1965; Robertis and Lasansky 1958). The outer segments are also the point of contact to the RPE, where they are directly interacting with the ciliated apical side (Strauss 2005). The RPE adopts a number of important function:

Firstly, it facilitates the outer blood retinal barrier via the barrier function gained from tight junctions (Naylor et. al 2019). Thus, an environment with limited diffusion is created, which 1) allows passage of preferred solutes in an active or inactive manner, 2) also allows transcytosis, the invagination and budding of vesicles from either side of the cell in order to traverse the cell and release their content on the opposite side and, 3) functions as a barrier to solutes, leading to the degradation or transformation of solutes before they can cross the barrier (Rizzolo et. al 2011).

Secondly, the RPE facilitates transport of nutrients from the blood to the PRs, but also vice versa from the subretinal space to the blood (Gallemore et. al 1997).

Thirdly, as the retina is regularly exposed to light, photo-oxidation of lipids is a regular occurrence (Girotti and Kriska 2004). Furthermore, reactive oxygen species are accumulated, as the retina consumes high levels of oxygen (Country 2017; Cringle and Yu 2010; Cringle et. al 2006). The RPE works against these detrimental effects by absorbing light with the characteristic pigments and having a high number of antioxidants (Beatty et. al 2000; Frank et. al 1999).

Fourthly, the RPE phagocytoses spend PR outer segments and subsequently regenerates the used up light sensitive pigments of the disc membranes. Absorption of light changes the conformation of 11-*cis*-retinal into all-*trans*-retinal, which is metabolized to all-*trans*-retinol and transported to the RPE. The retinal pigment epithelium-specific protein 65 kDa (RPE65) is responsible for isomerization of all-*trans*-retinyl ester to 11-*cis*-retinol (Saari 2016).

Lastly, the RPE also adopts important secretory functions, secreting for example the pigment epithelium derived factor (PEDF) and vascular endothelial growth factor (VEGF) in a polarized manner. PEDF is secreted towards the retina, functioning as a neuroprotective and antiangiogenic factor (Adamis et. al 1993; Cao et. al 1999), while VEGF is secreted towards the choroid, maintaining the intact endothelium of choriocapillaries (Burns and Hartz 1992). The sum of these functions render the RPE a necessary supportive structure for PRs. This depen-

dency is further demonstrated in diseases like age related macular degeneration, where the RPE layer becomes dystrophic, leading to premature death of PRs as a secondary effect (Mitchell et. al 2018).

3.2 Two-dimensional *in Vitro* Cultivation Systems

It has been a long sought-after goal to reliably produce retinal tissue *in vitro*. As 2-dimensional (2D) cell culture has been the standard cultivation system for most cell cultures in the last decades, first attempts of achieving this goal were also conducted in a 2D-system. As the molecular processes underlying retinal differentiation have been elucidated to a quite high degree, this knowledge was transferred to an *in vitro* cultivation system. Using pluripotent stem cells and a combination of inducing factors, various protocols were established and tested.

3.2.1 Differentiation by Recreating Stimuli

Seminal work in this direction was done by Deepak Lamba and Thomas Reh. Forebrain development is induced *in vivo* by antagonizing BMP and WNT signaling (R. M. Anderson et. al 2002). This inhibition of BMP is achieved by factors like Noggin, while DKK1 is an antagonist of the WNT/β-catenin signaling pathway (Glinka et. al 1998). However, the combination of Noggin and DKK1 was thought to promote anterior neural instead of retinal identity. Thus, as injection of IGF-1 mRNA in *Xenopus* embryos promoted eye induction, insulin-like growth factor-1 (IGF-1) was tested in addition (Pera et. al 2001).

A mixture of these proteins was tested for its potency in inducing retinal fate in human embryonic stem cells (hESC). Indeed, after three weeks of cultivation, more than 80% of the cells stained positive for the retinal marker Pax6, and of these cells, 86% also stained positive for Vsx2, clearly indicating the RPC fate. The addition of IGF-1 also proved integral, as the level of retinal induction was markedly lower in the absence of IGF-1 (D. Lamba et. al 2006). Many cells in the hESC-derived cultures also stained positive for markers of GCs (Tuj-1), PRs (Crx, S-opsin, Rhodopsin, Nrl), bipolar cells (Pkcα) and horizontal cells (Prox-1).

In a follow-up study, the hESC-derived retinal cells were transfected with an adenovirus expressing eGFP and transplanted into the intra-vitreal or subretinal space of mice at birth or one day after birth. In these mice, migration of the transplanted cells into the retina was observed, which was absent in transplantation in older-stage mice (D. A. Lamba et. al 2009). However, later studies showed material transfer of donor and host cells, falsely suggesting a high level of correct integration in transplanted cells (Pearson et. al 2016). In order to prove the integration of human cells into the mouse retina, a staining for human-specific marker proteins would be required.

While the 2D cultivation system allows the differentiation of retinal cell types, a clear structure and organization, as would be the case *in vivo*, is lacking. In addition to neural retina cells, the 2D system is predestined to differentiate monolayers of RPE. This approach has been readily used in the last two decades, leading to the formation of well defined and pure monolayers of pigmented cells (Buchholz et. al 2013; Croze et. al 2014; Foltz and Clegg 2017; Meyer et. al 2009). Many of these protocols follow along similar lines, inducing retinal fate via the addition of Noggin and DKK1. However, retinal and especially RPE fate was further enforced via the addition of the transforming growth factor-β (TFG-β) superfamily ligand Activin A. The resulting monolayers showed the characteristic morphology, key marker expression verified via immunocytochemistry and qPCR.

3.2.2 Inducing Differentiation via Small Molecules

Purified proteins like Noggin, DKK1 and IGF-1 are sufficient to induce retinal fate, and similarly, the *in vivo* situation can also be transferred to other tissues in order to create viable *in vitro* protocols (Y. Kim et. al 2020). However, there are downsides to the use of purified proteins: they are expensive, the variety is limited, and they often function in a multitude of pathways. As an alternative, the use of synthesized small molecules as a source of stimulation is explored (Artero-Castro et. al 2019; Y. Kim et. al 2020; Qin et. al 2017). These small molecules are inexpensive, can be produced in large quantities, and the number of potential molecules is boundless. Additionally, when looking to translate protocols to a clinical application, non-animal derived substances are required. A number of protocols already demonstrate the usability of small molecules for retinal or RPE induction. One of the first protocols using small molecules to induce retinal fate in stem cells used the WNT inhibitor CKI-7 and the TGF-β 1 receptor activin receptor-like kinase 5 (ALK5) inhibitor SB431542. Upon stimulation, the expression of key retinal marker genes like *Rx* and *Six3* was significantly increased.

In another study, the Wnt/β-catenin inhibitor IWR-1, the BMP pathway inhibitor LDN193189, and ALK5 inhibitor SB431542 were used in combination with recombinant IGF-1 to induce retinal fate in induced pluripotent stem cells (iPSC) (Zhu and D. A. Lamba 2018; Zhu et. al 2018). This protocol was directly compared to the induction via Noggin, DKK1, and IGF-1 and proved a viable alternative while still following current good manufacturing practice regulations.

Also for the differentiation of RPE, the use of small molecules was successfully demonstrated. The addition of the neural inducer Nicotinamide and/or the anti-tumor agent Chetomin, which was identified as a potent inducer of RPE fate in stem cells, were tested (Maruotti et. al 2015). The resulting cells showed typical

morphology, strong pigmentation, and expression of key marker genes. Again underlining the usability of small molecules for the induction of retinal cell types *in vitro* cultivation systems.

3.3 Three-dimensional *in Vitro* Cultivation Systems

While 2D-systems offer a means of cultivating retinal cells, the complexity intrinsic to the tissue is lost. The application of 3-dimensional (3D) culture systems in the context of retinal cell culture will be further discussed.

3.3.1 Differentiation of Retinal Organoids

Attempts to introduce viable 3D culture systems were started in the 1980s. A cell suspension of dissociated day-6 embryonic chick retinae was reaggregated in a rotary culture system. The dissociated cells started to quickly reaggregate and an initial random alignment of retinal cells shifted towards a higher level of organization with the occurrence of primary rosettes (Vollmer 1984). These reaggregated retinae contained both neural retina and retinal pigmented epithelial cells. Further work with reaggregated chick retinae revealed a dependency on the specimens age and an organizing function of Müller glial cells and RPE (Layer and Willbold 1989; Vollmer and Layer 1986a; Willbold et. al 2000). While a stunning level of reaggregation and lamination can be achieved with the chick system, comparable levels of lamination of any brain part could not be achieved with any other animal system (Layer et. al 2002).

The reaggregation of chick retinae proved a viable method to follow tissue (re)organization *in vitro*, but more meaningful mammalian or even human *in vitro* 3D-systems were not possible. However, the isolation of embryonic stem cells and the advent of induced pluripotent stem cells offered a completely new tool-set to overcome this challenge (Martin 1981; Takahashi and Yamanaka 2006). Using murine embryonic stem cells, the developmental biologist Yoshiki Sasai conducted some seminal work that lead to the generation of stem cell-derived *in vitro* culture systems. Aggregating embryonic stem cells in the absence of serum led to the formation of embryoid bodies. Transition of these embryoid bodies from a GMEM/KSR based medium to DMEM/F12/N2 was sufficient to induce neuronal differentiation, resulting in apico-basally polarized cortical tissue (Eiraku et. al 2008). However, tissue derived from mESCs started to lose organization as the number of mitotic neuronal progenitor cells decreased. Still, early differentiation events could be replicated *in vitro*.

Inspirations for improving the system were obtained from work on the intestinal system. The epithelium of the small intestine is organized in crypts and microvilli. Even though the stem cells responsible for self-renewal of these crypts

were identified based on their Lgr5-expression, the crypt structure could not be maintained in long-term culture of isolated intestinal cells (G. S. Evans et. al 1992). This circumstance could be changed by the addition of Matrigel to the isolated cells, leading to the formation of crypt-like aggregates, which were able to be passaged and maintained in a floating culture for several months (Sato et. al 2009). Matrigel is a complex mixture of ECM, which was first isolated and characterized from Engelbreth-Holm-Swarm mouse sarcoma cells (Kleinman et. al 1982). The main components of Matrigel are laminin, type IV collagen, perlecan and entactin, among a large number of other components like growth factors (Kleinman and Martin 2005). As it is a biological product, concentrations of the single constituents of Matrigel tend to vary from batch to batch.

Combining the protocol for murine stem cell-derived cortical aggregates with Matrigel led to the formation of neural aggregates containing retinal tissue, thereafter termed retinal organoids (Eiraku and Sasai 2011; Eiraku et. al 2011). Remarkably, retinal organoids show morphological characteristics and processes similar to the development *in vivo*: by day 7, retinal domains (observable via a Rx-GFP knock-in) evaginate from the main aggregate, and according to Eiraku and colleagues, later on they again invaginate, forming an OC-like structure. As of now, the underlying developmental processes of the *in vitro* culture system are largely unknown.

Shortly after the first publication with mouse embryonic stem cells, the group of Yoshiki Sasai was able to also achieve retinal organoids with human embryonic stem cells. Slight adaptations of the protocol were sufficient to translate the protocol to these cells (Nakano et. al 2012).

3.3.2 Organoids Reliably Replicate Retinal Differentiation

Establishing a cultivation system to potentially obtain larger quantities of retinal cells has been a big feat, but the question arose if retinal organoids are able to also replicate the developmental steps observed during the formation of retinal tissue. Retinal development is temporally and spatially strictly organized and robust. Consequently, the emergence of all retinal cell types follows a determined temporal order and the localization is restricted to certain areas of the retina, which can be distinguished into three characteristic layers (Ewart and Thin 1874).

Strikingly, retinal organoids largely followed the same developmental characteristics observed *in vivo*. Eiraku and colleagues were able to show the presence of the main retinal cell types as well as the layered organization of retinal organoids. In most cases, organoids have distinguishable layers reminiscent of the outer and inner nuclear layer, as well as the GCL (Eiraku et. al 2011). Furthermore, they

were able to show a temporal progression in key marker gene expression. More detailed work showed similarities in organoids and *in vivo* generated tissue when comparing development of PRs (Kaewkhaw et. al 2015).

But not all features of a mature retina could be replicated in retinal organoids. A key feature of PRs are outer segments containing the light sensitive pigments (Dowling 1965). In early organoids, cells expressing PR markers were present, but they were lacking outer segments. However, adaptations of the protocol proved sufficient to generate inner segments, connecting cilia, outer segments, and presynaptic structures in organoid-derived cones and rods (Gonzalez-Cordero et. al 2017; West et. al 2012). Furthermore, Giorgia Quadrato and colleagues presented evidence for the presence of active neuronal networks in six-month-old retinal organoids (Quadrato et. al 2017).

Some publications also indicate an epigenetic memory intrinsic to reprogrammed cells. Thus, iPSCs derived from retinal cell types are more efficient in generating retinal organoids than iPSCs with a non-ocular source (Hiler et. al 2015; L. Wang et. al 2018). In general, differences in efficiency for generating retinal organoids can be attributed to the cell lines and differences in methodology, for example the addition of relevant growth factors like IGF-1 (Mellough et. al 2015, 2019).

By now, powerful next generation sequencing techniques and methods to characterize nuclear organization were also applied to analyse retinal development in more detail. These studies focused on regulatory elements and gene regulatory networks underlying retinal development (Brooks et. al 2019; Clark et. al 2019; Z. Cui et. al 2020; Sridhar et. al 2020; L. Wang et. al 2018; Welby et. al 2017).

3.3.3 Applications for Retinal Organoids

Organoids are a versatile system, faithfully replicating early retinal differentiation in an *in vitro* environment (Eiraku et. al 2011). As the required cell source – pluripotent stem cells - is virtually inexhaustible, the potential scale-up of organoids offers immense opportunities for various fields of basic and applied science. Chief among these fields are tissue engineering and regenerative medicine. Compared to traditional model systems like animal models, organoids can offer the advantage of a human system permissive to also be genetically modified. Furthermore, they hold the promise of a patient-specific model system for disease modeling and drug screening (Guo et. al 2019; Huch et. al 2017). Diseases leading to visual impairment and blinding are quite common, with an increased prevalence in aging societies (Pascolini and Mariotti 2012). However, the underlying molecular mechanisms can vary from humans to e.g. mice or rats, which are commonly used

as a model system (Ahmad et. al 2018; Grenier et. al 2020; Hoshino et. al 2017). Working with a human system allows a more faithful characterization of a given disease.

Prominent diseases leading to blindness in humans are age related macular degeneration or diabetic retinopathy (Araújo et. al 2018; Kaewkhaw et. al 2016; Kruczek and Swaroop 2020; Pascolini and Mariotti 2012; Ponnalagu et. al 2017). One characteristic of these diseases is the perpetual loss of PRs (Bharti 2019). PRs are metabolically heavily reliant on the supportive RPE, with which they are in close contact. In many degenerative diseases the RPE starts to degrade, resulting in the death of the RPE. As a secondary effect, PRs lack the necessary support, leading to insufficient nutrient supply and accumulation of waste products. Ultimately, this also leads to the death of the PRs. In the mammalian system, the loss of PRs is quite detrimental, as the pool of RPCs is depleted during development, rendering damage to the retina permanent.

Organoids offer a almost infinite source of transplantable PRs. Many studies focused on improving the quantity and quality of PRs obtained from organoids. Hence, a number of publications and protocols are available for transplanting PRs or progenitor cells in mouse and rat model systems (Gonzalez-Cordero et. al 2017; Santos-Ferreira et. al 2016; Zhu et. al 2018). The upsides of retinal organoids for basic research are immense. Access to retinal tissue in large quantities combined with the option of introducing mutations of interest in a human system offers new ways of analyzing the function of genes involved in retinal development and homeostasis.

3.3.4 Limitations of the Organoid System

Organoids offer incredible opportunities for research and medical applications, however, they are also inherently limited. As an *in vitro* system, organoids allow large-scale production of tissue-like cell constructs, which can be even generated from patient-derived cell sources (Clevers 2016; Deng et. al 2018; Drost and Clevers 2017; Dutta et. al 2017). The cultivation and differentiation process is often quite sophisticated and complex. Many protocols require additions of animal-derived products like Matrigel or recombinant proteins to succeed (Eiraku et. al 2011; Kuwahara et. al 2015). Even though coaxing the pluripotent cell source into the desired direction can be achieved for many tissues, it is an isolated system. *In vivo*, many different tissues and cell types are involved during the development of any given tissue. Consequently, the surrounding tissues create an individual niche via e.g. production and secretion of key growth factors, generation of a matrix for the tissue to attach to or limiting the expansion of the developing tissue. While these factors can be approximated *in vitro*, the complexity is lacking compared to the *in*

vivo system. Consequently, while the cells start to adopt the desired cell type, they might still be lacking important characteristics of the matured cell type (DiStefano et. al 2018; Kruczek and Swaroop 2020; Zhong et. al 2014).

Along the same line, the *in vivo* environment is complex and unique (Bonnans et. al 2014). To constantly keep a developing tissue supplied with oxygen, nutrients, minerals, and proteins, while at the same time removing waste products, an intact vasculature is of central importance (Country 2017; Cringle and Yu 2010). The vasculature is lacking in most *in vitro* system, but these functions can be replicated via a proper cultivation system to some extent (Cakir, B. Xiang, Yangfei et. al 2019; Pham et. al 2018). However, proper support and nutrient supply can only be maintained to a certain tissue dimension. With organoids, passive diffusion reaches a point of inefficiency, rendering more centrally located parts of the organoid undersupplied with nutrients. The undersupplied regions tend to become apoptotic with prolonged cultivation, leading to the occurrence of a so-called necrotic core (Lancaster et. al 2013; Nickels et. al 2020).

3.4 Improved Culture Systems for Organoids

Three-dimensional cultivation systems like organoids offer immense benefits as a cell cultivation system (Eiraku and Sasai 2011; Lancaster et. al 2013). Many cell types can also be differentiated in a 2D cultivation system with the addition of purified proteins or small molecules, but they lack the complex 3D structure. Probably, the complex 3D structure also adds to the reliability of the system, as this improves cell-cell interactions and also creates microenvironments similar to the *in vivo* situation (Amin and Paşca 2018).

While organoids are a very potent *in vitro* system, they also come with a number of downsides: growth and differentiation in organoids are limited, complex interactions with surrounding tissues are missing, and nutrient supply is lacking, which leads to the occurrence of necrotic cores in many protocols (Z. Cui et. al 2020; Lancaster et. al 2013; Nickels et. al 2020). In order to overcome these limitations, various optimisations to the organoid protocol have been attempted. These optimisations include the cultivation in bioreactors, the combination of multiple cell types, offering a bio-mimetic environment and combining organoid derived tissues with the complex environment of animals via transplantation (Achberger et. al 2019; Bagley et. al 2017; Cakir, B. Xiang, Yangfei et. al 2019; DiStefano et. al 2018; Mansour et. al 2018; Ovando-Roche et. al 2018; Pham et. al 2018).

Some of these optimisations were conducted in quite creative and sophisticated manners. For example, the group of Jürgen Knoblich created an organoid-based model system for the interaction of different brain regions by using organoids of dorsal and ventral fate. One organoid of each fate was fused in a droplet

of Matrigel, leading to the formation of a dorsal-ventral axis. This allowed for example the identification of directed neuronal migration within these organoids (Bagley et. al 2017).

To offer organoids another level of complexity, some groups also started to transplant organoids into animal models. For example, cerebral organoids were transplanted into mouse models, leading to vasculature-like structures and blood-brain-barrier-like functions (Cakir, B. Xiang, Yangfei et. al 2019).

3.4.1 Bioreactors

Organoids are an aggregate of large quantities of cells. The larger they grow in size, the higher their metabolic needs. Both, oxygen and nutrients, have to be offered via the culture medium. However, the occurrence of necrotic cores in organoid culture clearly indicates that nutrients and oxygen supplemented via the medium are not able to permeate the whole organoid (Lancaster et. al 2013; Nickels et. al 2020).

Bioreactors offer a means of increasing oxygen supply and distribution of nutrients, increasing survival and differentiation efficiency, and also enhancing the quality of 3D structures obtained (DiStefano et. al 2018; Ovando-Roche et. al 2018; Qian et. al 2016). Tyler DiStefano and colleagues cultivated murine retinal organoids in rotating-wall vessel bioreactors under normoxia. They could identify faster maturation in the bioreactors compared to organoids cultivated in static conditions. D25 organoids in bioreactors showed similar levels of maturation and transcriptome profile as those at D32 in static culture conditions. This indicates that bioreactors offer more suitable culture conditions (DiStefano et. al 2018). However, the authors also comment on a widespread downside of murine retinal organoids: retinal organoids were not able to differentiate further under any of the tested *in vitro* cultivation systems, suggesting that some other key factors are missing under current cultivation conditions.

3.4.2 Co-culture of Organoids

In vivo, tissue differentiation is not an isolated process, but many extrinsic factors are involved. These extrinsic factors include the bio-mechanical structure of the environment, the cell types present in the surroundings, stimulating factors secreted from nearby cells and their changes over time (Heavner and Pevny 2012). Organoids revealed an intrinsic program during development, which upon activation led to the reliable differentiation towards a certain cell fate (Eiraku and Sasai 2011; Lancaster et. al 2013). However, this intrinsic program and the resulting differentiation is often limited, probably stemming from a lack of the extrinsic factors. In order to emulate the *in vivo* situation, co-culture of organoids

was attempted by a number of groups (Achberger et. al 2019; Akhtar et. al 2019; Cattaneo et. al 2020; Dijkstra et. al 2018; Krencik et. al 2017; Nozaki et. al 2016). These examples include co-cultures of astrocytes and neurons, leading to the formation of a dynamic network, forming synapses. This system would allow improved studies of circuit function and disease modeling (Krencik et. al 2017). Co-culture systems were also employed in cancer research, combining T-cells with cancer organoids and examining their reaction towards the cancerous tissue (Cattaneo et. al 2020; Dijkstra et. al 2018).

For retinal systems, the co-culture of neural retina tissue with RPE was studied throughout the last decades (Layer and Willbold 1989; Sheedlo and J. E. Turner 1992). Experiments in chick indicated that retinal cells can differentiate and mature on their own *in vitro*, but the orientation was inverse. Only in the presence of RPE the retinal cells were correctly organized (Layer and Willbold 1989). Furthermore, as the support of the RPE is important for the neural retina, co-cultures of organoids and RPE were also attempted.

Seminal work in this field was done by Kevin Achberger and colleagues, who combined stem cell-derived retinal organoids and RPE with a microfluidic system. RPE was cultivated on a porous membrane and separate chambers were created by polydimethylsiloxane (PDMS). Upon maturation of the RPE, retinal organoids were cultured in close proximity of the RPE. Organoids were embedded in a hyaluronic acid-based hydrogel to prevent direct contact of these organoids and RPE, as this might lead to migration of cells. Underneath the porous membrane with the RPE cultured on top, a media channel allowed media to perfuse. Thus, an *in vitro* system of a neural retina-RPE construct with an active vasculature-like system was achieved (Achberger et. al 2019). In this system, an enhanced outer segment formation of PRs was evident and the RPE layer did show phagocytosis of bovine retinal outer segments. Phagocytosis could also be observed in the co-culture setup, where Rhodopsin^{+} particles were identified in the RPE layer.

Tasneem Akhtar and colleagues also reported a co-culture system of retinal organoids and stem cell-derived RPE. RPE was grown to confluency and organoids of the same age were added, leading to a direct contact co-culture. After two weeks of co-culturing, retinal organoids were analysed for marker expression, showing increased levels of PR marker gene expression (Akhtar et. al 2019). These examples clearly indicate that there are ways of improving the organoid system by adding more complexity via additional cell types, creating a system with conditions more similar to the *in vivo* situation.

3.5 Three-dimensional Substrates for Biological Systems

For the majority of the last few decades, 2D cell culture systems have been the predominant way of cultivating cells *in vitro* (Abbot 2003; Aoki et. al 2016;

Kendall 2015; Philippeos et. al 2012). However, this is in stark contrast to the *in vivo* situation, where cells are usually exposed to a 3D environment. This environment encompasses surrounding tissues, their secreted soluble factors, and cell-cell-interactions as well as the composition and mechanical properties of the surrounding ECM. This microenvironment is subject to constant changes, as the ECM is constantly remodeled, cellular composition might vary and levels of soluble factors might fluctuate. This remodeling is an important factor contributing to the tissue homeostasis and dysregulations of the ECM composition and structure can lead to severe diseases (Bonnans et. al 2014). The exact composition of the ECM is dependent on the specific cell type and also can change throughout development. A set of roughly 300 proteins makes up the variety of ECM components.

In order to offer cells a cultivation system closely approximating the conditions *in vivo*, the potential of various production techniques has been explored for creating a suitable cell culture environment. These techniques range from additive manufacturing techniques to methods employing biological substrates. As an example for the latter, biological tissues are decellularized and reused as a scaffold for the cultivation of new cells. This approach has been used for different tissues, including bone, tendon, liver and even the retina (G. Chen and Lv 2018; Kundu et. al 2016; S. Wang et. al 2017; Yang et. al 2018). After decellularization, only the ECM backbone and the attached growth factors remain, offering a suitable substrate for cell cultivation. For the decellularized retina system, bovine eyes were used as a source, the retina isolated and decellularized in sodium dodecyl sulfate. Thus, thin retinal films were created. These films were repopulated with RPC and analysed for the engraftment, viability and differentiation capability of seeded cells. Cells were able to adhere to the decellularized retina, survive for seven days and differentiate to retinal cell types (Kundu et. al 2016). However, this culture system was outperformed by fibronectin-coated tissue culture plates. Therefore, decellularized retinal films are a potential biocompatible scaffold, but even though the environment is quite similar to the *in vivo* situation, no beneficial effect was observed compared to standard culture conditions. Furthermore, these substrates have a limited availability and are an animal-derived product. Considering these points, decellularized retinae do not seem like a viable culture system. Additive manufacturing systems offer a means of generating custom 3D substrates, which can be additionally modified with ECM proteins to offer a more suitable environment to cells. There are a number of different manufacturing systems, like hydrogels, electrospinning, inkjet printing, and direct laser writing, which will be further discussed in the next sections.

3.5.1 Hydrogel-based 3D Culture

Hydrogels are a bulk of polymers or proteins with a high water content. They can be based on biological polymers like collagen, hyaluronic acid or Matrigel, but also on synthetic polymers like poly(ethyleneglycol), poly(vinyl alcohol) and poly(*N-iso*propylacralymide) (DeForest and Anseth 2012; Hughes et. al 2010; Masters et. al 2004; Rault et. al 1996). Because of their high water content, hydrogels often have a spongy structure, but depending on their composition, the stiffness can range for example from compliant (E 2.5 kPa) to stiff (E 110 kPa) (Huebsch et. al 2010).

A number of different hydrogels were applied in the field of retinal cell culture. Both, RPE and RPC were cultivated in hydrogels and successively transplanted (J. Park et. al 2019; Shin et. al 2019). For RPC, increased levels of proliferation were achieved in mussel-inspired hydrogels, as well as the promotion of retinal differentiation (Tang et. al 2019). Hydrogels were also used for applications not directly involving the cultivation of cells. A marine polysaccharide-based hydrogel was tested as a substitute for the vitreous, but long-term safety and efficacy has to be further assessed (Jiang et. al 2018).

3.5.2 Electrospinning

In electrospinning, a polymer solution is pumped through the tip of a needle. A high-voltage electric field is set up between the injection needle and the collecting surface. Upon reaching a critical value of the electric field, the repulsive electric force overcomes the surface tension of the polymer solution, leading to a jet of solution being ejected from the needle. The solvent then evaporates from the polymer solution and fine dry polymer fibers remain (Chun et. al 2018; Zadeh et. al 2019). The resulting fiber network is often spun randomly, but some groups also try to align the fibers (Sperling et. al 2017), which presents different stimuli to cells. While electrospun substrates show some level of topography, in most cases they are closer towards 2D than 3D.

Electrospun fibers were also applied for cell cultures with retinal cells (Chan et. al 2017). As a 2D culture system, electrospun fibers offer a perfect substrate for the cultivation and differentiation of RPE. When cultivated on such substrates, RPE cells adopted the typical honeycombed morphology and overall culture was improved compared to controls, which has been demonstrated on multiple accounts (Hotaling et. al 2016; Z. Liu et. al 2014). Additionally, electrospun substrates can be applied for the cultivation of retinal GCs, leading to a shortening of the differentiation process compared to 2D controls. The formation of functional axons and the occurrence of action potentials were also demonstrated (T.-C. Chen et. al 2019; K. Li et. al 2017).

3.5.3 *Inkjet (bio)printing*

Inkjet (bio)printing is a quite versatile field, with the technique having a common source with the printing techniques used for common paper printing. Instead of inks, other substances like polymers, proteins, DNA, and even cells are used to print (Derby 2010; Singh et. al 2010). For printing, the object is created virtually and its coordinates in space are used to guide a 3D-dispenser orifice. With these coordinates, the object is printed in a layer-by-layer deposition process. Thus, complex structures can be produced with feature sizes from low micro- to even centimetre (Ligon et. al 2017). Free-standing, complex structures can be generated which then can be used as a substrate for cell cultivation experiments.

Furthermore, inkjet printing can also be applied to directly deposit cells in an organized manner. To this end, a cell suspension with high cell density is prepared and used as bioink. Consequently, the suspended cells can be printed in a controlled manner. Among others, cells for cartilage and bone, cardiac and vascular, neural, and skin tissue have been successfully printed (X. Cui et. al 2012a,b; S. E. Kim et. al 2018; S. Y. Park et. al 2011; Xu et. al 2009; Yanez et. al 2015). Retinal GCs have also been printed (Lorber et. al 2014). While the authors could show that the printing process does not have any adverse effects on cell survival or morphology, a more complex application of this method regarding retinal cells is still missing. There are also other drawbacks to inkjet bioprinting: few materials can be used as bioinks, because inks have to fulfill certain criteria in regards to viscosity. In addition, toxicity of the materials also has to be taken into account (X. Li et. al 2020).

3.5.4 *Direct Laser Writing*

The direct laser writing (DLW) process is based on the simultaneous absorption of two photons (two photon polymerization, 2PP). First attempts at 2PP were already conducted in the 1960s, with limited success (Pao and Rentzepis 1965). One of the critical aspects was the lack of powerful lasers. Roughly thirty years later, more powerful lasers and more sensitive photoresists allowed successful realization of the 2PP principle (Maruo et. al 1997).

By now, easy to use commercial set-ups are available, with powerful lasers and well-developed photoresists offering a large variety of options. In principle, any conceivable free-standing structure can be 3D printed via a 2PP system. Similar to inkjet printing, the desired object is turned into a virtual object, yielding coordinates for a piezo stage mounted on a microscope to scan. Via the movement of the stage in x,y and z, the object's focal point is moved in a volume of photoresist. The simultaneous absorption of two photons is limited to the narrow focal volume of the laser, leading to focused polymerization of the photoresist. This polymeriza-

tion can be spatio-temporally well regulated, leading to the step-wise production of the 3D substrate. After all coordinates have been scanned with the piezo stage, the sample can be removed and cured by exposure to solvents. Depending on the photoresist employed, the characteristics of the resulting structure can vary heavily. For example, a photoresist based on poly(N-iso-propylacrylamide) generates substrates, which can be actuated via changes in temperature or exposure to light (Hippler et. al 2019).

Ultimately, the produced structure can then be used for further applications, for example the cultivation of cells. In the last decade, this application has peaked public interest, as DLW offers ways of generating substrates with custom design, which can later on be further modified via protein coatings (Richter et. al 2017). ECM proteins can be used as coating agent in order to enhance cell adhesion to the substrate. Thus, DLW-generated custom substrates offer modifiable 3D substrates for the cultivation of cells. Throughout the last decade, this avenue has been explored quite actively, showing the feasibility of this approach in mechanobiology (Autenrieth et. al 2016).

Other areas of biology have also been combined with DLW-generated 3D substrates. For example, 3D substrates were used for the cultivation and expansion of stem cells. Cage-like structures were generated and used for mesenchymal stem cells cultivation (Nava et. al 2017; Raimondi et. al 2013; Zandrini et. al 2019). Furthermore, stacked ring-like composite structures were used to differentiate mesenchymal stem cells in an osteogenic direction ("Osteogenic differentiation of human mesenchymal stem cells in 3-D Zr-Si organic-inorganic scaffolds produced by two-photon polymerization technique" 2015). Multiple groups also used 3D substrates for the cultivation of neurons. The respective substrate designs varied heavily, ranging from free-standing woodpile-like structures for colonization and cultivation of neuroblastoma cells, over free-standing tower-like structures which offer a substrate for long-term cultivation of pluripotent stem cell-derived neuronal cells, to sophisticated networks of microtowers and free-standing microtubes, facilitating a network-like structure. Cells cultivated in the latter structure are guided along defined paths, showing electrophysiological properties after ten days of cultivation (Accardo et. al 2017; Fendler et. al 2019; Turunen et. al 2017).

DLW-substrates were also used in combination with retinal cells. Many of these applications are aimed at a short-term cultivation platform and later usage as a cell-laden graft for transplantation (McUsic et. al 2012; Worthington et. al 2017). First work in this direction was done by Andrew McUsic and colleagues, using microchannel substrates made out of poly(lactic-co-glycolic acid). Dissociated neonatal mouse retina was seeded in the microchannel array, leading to engraftment and growth of the cells. Stainings of Otx2 as ONL and Pax6 as GCL markers indicated an organization in 3D, with a preferential localization of $Otx2^{+}$

cells to the bottom of the 3D substrate, while $Pax6^+$ cells were localized to the top. Stem cell-derived retinal cells showed similar trends, but the extent of separation was not as evident (McUsic et. al 2012).

The basic 3D substrate design was maintained by Kristan Worthington and colleagues, with slight changes. They included microchannels at the vertical faces of the substrate as well as walls surrounding the substrates. Stem cell-derived RPC were seeded in these substrates and demonstrated attachment to the substrate, migration into the microchannels, and the formation and extension of neuronal processes (Worthington et. al 2017). In later work they showed the feasibility of these 3D substrates as a cell graft for transplantation experiments. Cell-laden 3D substrates were transplanted in a porcine animal system, revealing no adverse effects of the 3D substrates and a favourable biocompatibility profile. In this publication, the photoresist was based on poly(caprolactone), a polymer with biodegradable properties (Thompson et. al 2019).

Overall, some work has been done combining DLW-generated 3D substrates with cell cultures, but little work has been done in regards to long-term cultivation of cell constructs in 3D substrates.

Chapter 4

4 Motivation and aim

Studies revolving around the eye and retina have been conducted in model animals for many decades, leading to a deep and detailed understanding about the morphology and functionality. From early studies characterizing the morphology of retinal cells, over studies identifying the generation and birth order of the various cell types to studies elucidating the molecular basis of the organization and functionality of the tissues, animal system have assumed an integral role (Cepko et. al 1996; Wade 2008). However, more extensive regulations and growing costs for animal models, as well as the wish for more flexible and scaleable systems called for *in vitro* systems to faithfully replicate tissue development.

One decade ago, this dream was realized with the advent of retinal organoids (Eiraku et. al 2011). Aggregation of pluripotent stem cells and their successive cultivation in a mixture of ECM proteins lead to the spontaneous generation of retinal tissue in a petri dish. This method was rapidly adopted by the community and a growing body of literature is available characterizing and applying retinal organoids for research. While they show the formation of a retina-like tissue containing all relevant neural retina cell types organized in separate layers, their differentiation potential is limited and starting from murine stem cells, organoids also lose their characteristic morphology with extended cultivation. Furthermore, while the neural retina is quite faithfully replicated, the supportive structure of the RPE is missing in most protocols.

In the last years and decades, various 3D manufacturing methods were developed and rapidly improved, leading to robust and reliable ways of fabricating 3D structures. These structures can be applied in cell culture to offer a defined 3D growth substrate.

In this thesis, establishing the differentiation and cultivation of retinal cells in *in vitro* culture as well as devising and starting the fabrication of 3D substrates were initial goals. When reaching these goals, a combination of retinal cells and 3D substrates would be the next step.

For differentiating mouse embryonic stem cells to retinal fate, the organoid protocol as well as induction via small molecules and inhibitors are viable options and would be examined. Fabrication methods for 3D substrates are manifold.

The system serving our needs best would be a 2-photon lithography setup. High spatio-temporal resolution and already established photoresists render this a perfect option for the present application. Thus, a new scaffold design would be drafted and its viability in the production process would be tested.

Upon succeeding with the retinal differentiation and fabrication of 3D growth substrates, the two constituents would be combined. This could be achieved via different approaches: directly placing retinal organoids on the 3D substrate or dissociating the organoids to a single cell suspension and successively seeding the cells on the substrate. While some publications show the combination of various tissues and cell types with 3D substrates, it remains to be seen how retinal cells perform during long-term cultivation in 3D substrates. Assessment of the viability, as well as the presence of all relevant retinal cell types and the spatial organization within the 3D substrates would be of interest.

Furthermore, in order to ultimately include all cell types in an organotypic cultivation system, separate differentiation of RPE should also be pursued. Combining both, RPE and neuroretina would lead to a more meaningful *in vitro* system and thus be a long-term goal.

5 Chapter 5
Materials and Methods

5.1 Devices

Table 5.1: **Devices**

Description	Company	Application
Nanoscribe Photonic Professional	Nanoscribe	Fabrication of 3D substrates
Leica CM3050 Cryostat	Leica	Cryosectioning of tissues

5.2 Microscopes

Table 5.2: **Microscopes**

Description	Company	Objective
Primovert	Zeiss	Plan-Achromat 4x/0.1 Plan-Achromat 10x/0.25
AxioObserver Z1	Zeiss	CP-Achromat 10x/0.25
LSM 510 meta	Zeiss	C-Apochromat 40x/1.2 Water
LSM 800	Zeiss	Plan-Neofluar 10x/0.3, Plan-Apochromat 40x/1.4 Oil, C-Apochromat 40x/1.2 Water
Supra 55 VP	Zeiss	N/A

5.3 Antibodies

Table 5.3: **Primary Antibodies**

Antigen	Concentration	Host	Supplier	Dilution
Calbindin	N/A	Mouse Mcl	Swant; Product # 300	1:2000
Calretinin	N/A	Rabbit	Swant; Product # 7697	1:2000
Islet 1	200 µg/ml	Goat Pcl	R&D Systems; AF1837	1:200
Laminin	N/A	Rabbit Pcl	Sigma-Aldrich; L9393	1:100
MiTF	N/A	Mouse Mcl	Exalpha; X2398M	1:200
Otx2	200 µg/ml	Goat Pcl	R&D Systems; AF-1979	1:500
Pax6 (AD2.35)	200 µg/ml	Mouse Mcl	Santa Cruz Biotechnology; sc-53108	1:100
Recoverin	N/A	Rabbit Pcl	Merck Millipore; AB5585	1:1000
Rhodopsin	N/A	Mouse Mcl	Merck Millipore; O4886	1:1000
RPE65	1 mg/ml	Mouse Mcl	Invitrogen; MA116578	1:100
Synaptophysin	N/A	Mouse Mcl	Merck Millipore; S5768	1:1000
Sox9	200 µg/ml	Goat Pcl	R&D Systems; AF3075	1:200
Vsx2	200 µg/ml	Mouse Mcl	Santa Cruz Biotechnology; sc-374151	1:100
ZO-1	200 µg/ml	Rat Mcl	Santa Cruz Biotechnology; sc-33725	1:100

Table 5.4: **Secondary Antibodies**

Antigen	Fluorophor	Host	Supplier	Concentration Dilution
Mouse IgG	Cy3	Donkey	Jackson Immunoresearch; 715-165-151	1:200
Mouse IgG	AF 647	Donkey	Invitrogen; A31571	2 mg/ml; 1:200
Rabbit IgG	AF 568	Donkey	Invitrogen; A10042	2 mg/ml; 1:200
Rabbit IgG	AF 647	Donkey	Jackson Immunoresearch; 711-175-152	1:200
Goat IgG	AF 568	Donkey	Jackson Immunoresearch; 711-175-152	1:200
Goat IgG	AF 647	Donkey	Invitrogen; A21447	2 mg/ml; 1:200
DAPI			Carl Roth; 6335.1	5 mg/ml; 1:1000
Phalloidin	AF 568		Molecular Probes; A12380	1:200
Phalloidin	AF 647		Molecular Probes; A22287	1:200

5.4 Materials

Table 5.5: **General Materials**

Product	Supplier	Comment
Accutase	Pan Biotech; P10-21100	For purification of RPE cells
Cell scraper	Falcon; 353085	To detach RPE cells from well plates

Table 5.5: **General Materials**

Product	Supplier	Comment
Cover slips 24x60 mm	Carl Roth; H878	Cover slips for cryosectioned samples
Dimethylsulfoxid (DMSO)	Sigma-Aldrich; D2650	For freezing cells and reconstituting small molecule agents
Gelatine Type A	Sigma-Aldrich; G6144	Surface coating for stem cell culture
High precision cover slips	Carl Roth; LH24.1	High precision cover slips for production of 3D substrates
Hoechst	Invitrogen; H1399	Nuclear stain compatible with living cells
Imaris image analysis software version 7.7.1	Oxford Instruments	For 3D-reconstruction of microscopy data
Latex beads	Sigma-Aldrich; L9654	Functional assay for RPE
Low adhesion well plates	ThermoFisher; 174925	For the formation of uniform aggregates
Methylisobutylketone (MIBK)	Carl Roth; 0338	For curing 3D substrates
Mowiol 4-88	Merck Millipore; 475904	Mounting medium
Pentaerythrit-triacrylat (PETA)	Sigma-Aldrich; 246794	Protein-adhesive photoresist
Photoinitiator	Sigma-Aldrich; 511447	Initiator of light-stimulated polymerization reaction
Silicone Elastomer Sylgard 184	Corning; 000105989377	PDMS for seeding and sample embedding
Superfrost Ultra Plus Slides	ThermoFisher; J4800AMNZ	Slides for cryosections
Surgipath FSC 22 Blue	Leica; 3801481	Mounting medium for cryosectioning
TPETA	Sigma-Aldrich; 412171	Protein-repellent photoresist
3-(Trimethoxysilyl)propylmethacrylate	Sigma-Aldrich; 440159	To interconnect 3D substrates and cover slips
Triton X-100	Carl Roth; 3051	For permeabilization of cells
Trypsin/EDTA	Gibco; 15400054	For detaching cells

Table 5.6: **Media and Supplements**

Product	Supplier	Comment
AGN193109	Sigma-Aldrich; SML2034	For enhanced retinal differentiation efficiency
All-trans retinoic acid	Sigma-Aldrich; R2625	To improve retinal differentiation in orgnaoids
Blasticidin	InvivoGen; Ant-bl-05	For selection of $Oct4^+$ mESC Rx-GFP
CHIR99021	Sigma-Aldrich; SML1046	Inhibits glycogen synthetase kinase 3, required during RPE differentiation
Dulbecco's Modified Eagle Medium (DMEM)	Pan Biotech; P04-03590	Base medium for mESC cultivation
DMEM/F12	Gibco; 10565018	Base medium for cultivation of retinal cells
Ethidium homodimer-1	Invitrogen; L-3224	Agent specifically staining dead cells
Glasgow's Minimum Essential Medium (GMEM)	Gibco; 11570576	Base medium for retinal differentiation
Glutaraldehyde (GA)	AppliChem; A3166	Fixation agent for REM samples
Hydrocortisone	Sigma-Aldrich; H0396	Supplement for RPE maturation
Knockout serum replacement (KSR)	Gibco; 10828010	Chemically defined serum substitute
Laminin	Sigma-Aldrich; L2020	ECM protein for surface functionalization
Leukemia inhibitory factor (LIF)	Merck Millipore; ESG1107	Supports maintenance of pluripotency in mESCs
Matrigel	Corning; 356230	Protein matrix inducing retinal differentiation
Minimum Essential Medium (MEM) Alpha	Gibco; 12509069	Base medium for RPE differentiation and cultivation
β-Mercaptoethanol	Sigma-Aldrich; M6250	Additive for culture media
Non essential amino acids (NEAA)	Sigma-Aldrich; M7145	Supplement for culture media
N1	Sigma-Aldrich; N6530	Supplement for RPE medium

Table 5.6: **Media and Supplements**

Product	Supplier	Comment
N2	Gibco; 17502048	Supplement for the cultivation of neural cells
PanseraES	Pan Biotech; P30-2602	Bovine serum tested for stem cell applications
Paraformaldehyde (PFA)	Merck Millipore; 104005	Fixation of cells
PD0325901	Sigma-Aldrich; PZ0162	Potent inhibitor of mitogen-activated protein kinase
Penicillin/Streptomycin (Pen/Strep)	ThermoFisher; 15140122	To prevent bacterial contamination
Phosphate Buffered Saline (PBS)	Pan-Biotech; P04-361000	Washing and reconstitution agent
Propidium Iodide	Molecular Probes; P3566	Agent specifically staining dead cells
Sodium pyruvate	Sigma-Aldrich; S8636	Additional carbon source in media
SU-5402	Sigma-Aldrich; SML0443	Inhibitor of fibroblast growth factor signaling
Sucrose	Carl Roth; 4621.1	For cryoprotection of tissues
Taurine	Sigma-Aldrich; T-8691	Supports growth of neural cell
Y27632	Sigma-Aldrich; Y0503	Supplement for RPE differentiation
3,3',5-Triiodo-L-thyronine sodium salt	Sigma-Aldrich; T5516	Maturation of RPE

5.5 Media Formulation

Table 5.7: Maintenance Medium (MM)

Component	Volume
DMEM	207.5 ml
Panserum ES	37.5 ml
NEAA	2.5 ml
Pen/Strep	2.5 ml
β-Mercaptoethanol (1M)	25 µl
Freshly added:	
LIF (10^5 Units/ml)	2 µl/ml

Table 5.8: Retinal Differentiation Medium (RDM)

Component	Volume
GMEM	93 ml
KSR	5 ml
NEAA	1 ml
Pyruvate	1 ml
β-Mercaptoethanol (1M)	10 µl

Table 5.9: Retinal Maintenance Medium 1 (RMM1)

Component	Volume
DMEM/F12	98 ml
N2	1 ml
Pen/Strep	1 ml

Table 5.10: Retinal Maintenance Medium 2 (RMM2)

Component	Volume
DMEM/F12	88 ml
Panserum ES	10 ml
N2	1 ml
Pen/Strep	1 ml

Table 5.11: RPE-Medium

Component	Volume
MEM alpha	240 ml
Panserum ES	2.5 ml
N1	2.5 ml
NEAA	2.5 ml

5.6 Cultivation of mESCs

The cultivation of mESCs is a well established procedure, which reliably maintains a pluripotent population of stem cells. The cells are kept in a 2D environment using standard tissue culture flasks. Addition of LIF ensures the pluripotency of the cultured cells.

Coating of Culture Flasks

To offer a suitable surface for stem cells, culture flasks have to be modified prior to culture. To this end, a 0.1% gelatin solution was prepared from a 1% stock solution and PBS. 5 ml of the 0.1% gelatin solution were added to each T25 culture flask. The flasks were coated for 30 min at RT. Afterwards, the gelatine solution was aspirated.

Cell Culture Routine

Unless otherwise indicated, cells were cultivated at 37°C and 5% CO_2 in a humidified incubator. The cells used in this work were kindly supplied by the RIKEN BioResource Research Center. It is a subline of the EB5 (129/Ola) mouse embryonic stem cell line, containing a GFP-knock in under the Retinal homeobox-promoter (*Rx*). This knock-in allows visual verification of onsetting retinal differentiation via the expression of the GFP construct.

Prior to passaging, the stem cells were visually inspected via a table-top microscope. The medium was aspirated and the cells were washed with 5 ml PBS. After aspirating the PBS, 300 µl of a 0.25% Trypsin solution was added and incubated for 1 minute at 37°C. The cells were released by gentle agitation and collected in 5 ml MM. The cell suspension was transferred to a 15 ml conical tube and centrifuged at 500 rpm for 5 minutes. The supernatant was aspirated and the pellet was released and resuspended in 5 ml MM. The cells were counted under a table-top microscope using a Neubauer chamber. 5 ml of MM + 2000 units LIF/ml medium was added to each flask and 4.2 * 10^5 cells or 1.5 * 10^5 were seeded for a two or three day interval, respectively.

5.7 Differentiation of Retinal Organoids

Seeding of mESC

Medium was aspirated from Rx-GFP mESCs, the cells were washed with PBS and released with 0.25% trypsin. Still adherent cells were detached with gentle agitation, collected in 5 ml MM and centrifuged in a 15 ml conical tube. The supernatant was aspirated and the cells resuspended in 5 ml MM. After assessing the number of cells, a cell suspension with 30.000 cells per milliliter was prepared using RDM. AGN193109, a pan-retinoic acid receptor antagonist, was added to the cell suspension with a concentration of 0.1 M. 100 µl of the cell suspension per well were transferred into a 96-well plate. The day of seeding is defined as Day0.

Addition of Matrigel

On Day1, Matrigel was slowly thawed on ice to prevent premature gellation. A 13.6% Matrigel-solution was prepared by mixing ice-cold RDM and Matrigel. 20 µl of this solution were added to each well, achieving a final concentration of 2% Matrigel per well.

Verification of Retinal Differentiation

With the GFP knock-in under the control of the promoter of the *Rx*-locus, tracking GFP fluorescence allowed direct verification of retinal fate adoption. In organoids, GFP expression started from Day5 onwards. On Day7, the 96-well plates were screened for GFP expression. GFP^+ aggregates were transferred to 60mm petri dishes containing 6.5 ml prewarmed RMM1. The following days, the general morphology and GFP-expression was closely monitored.

Dissection and Continued Cultivation

On Day10, the general morphology and GFP-expression of retinal organoids was assessed. If possible, GFP^- organoids were removed. An upright light microscope was sterilized with ethanol and placed under a sterile bench. Dumont #5 forceps were also sterilized with ethanol. Using a 4x objective, the GFP^+ organoids were dissected using two forceps. Depending on the morphology, single vesicles were separated. If no distinct vesicles were present, the organoids were randomly dissected into 3-4 similarly sized pieces (Figure 5.1 I). Roughly 30-40 pieces were transferred to a new petri dish containing 6.5 ml RMM2 supplemented with 0.5 µM all-trans retinoic acid and 1 mM L-taurine. A half-medium change was performed at D14, and from then on twice per week. Generally, at roughly Day25 the characteristic retinal vesicles started to lose their integrity and organoids were prepared for downstream applications.

Differentiation of RPE

To differentiate a separate monolayer of RPE cells, GFP^+ D7 retinal organoids were transferred to an Eppendorf cup and broken up with a syringe using a 23- and 26-gauge needle. The cell clumps were transferred to a 15 ml conical tube and centrifuged twice at 500 rpm and RT with low acceleration and deceleration. The supernatant was aspirated and the pellet resuspended in 2 ml RMM2 supplemented with 10 µM Y27632, 3 µM CHIR99021 and 5 µM SU5402. The fragmented organoids were seeded in a LN-coated 6-well plate (1 $\mu g/cm^2$, 2h at RT). A media change was performed at D8.

The culture medium and supplemented molecules induce a shift to RPE-fate, however, not all cells are undergoing this transition. To remove the non-RPE cells, a purification step was performed. To this end, at D11 the wells were washed with PBS and treated with 500 µl Accutase for 5 minutes at 37°C. To neutralize the reaction and remove less adhesive cells, fresh RMM2 was added and pipettet repeatedly. Excess medium and cell debris was removed and the still adherent cells were washed with PBS. A subsequent step with 3 minutes of trypsin treatment at 37°C removed the adherent RPE cells. The reaction was neutralized by addition of 3 ml RMM2 supplemented with 10 µM Y27632, 3 µM CHIR99021 and 5 µM SU5402. The remaining RPE-cells were ultimately released by repeated pipetting and 10^6 cells were seeded on LN-coated 12-wells.

The medium was changed at D12 with fresh RMM2 supplemented with 3 µM CHIR99021 and 5µM SU5402. Starting at D15, the RPE-cells were maintained in RPE-Medium supplemented with 250 mg/L Taurine, 20 µg/L Hydrocortisone and 0.013 µg/L triiodo-thyronine.

Viability Assay

To monitor the cultivated cells survival under different cultivation conditions, viability assays were conducted using Ethidium Homodimer-1 or Propidium Iodide. Both dyes are unable to pass the membrane of living cells, however, the membrane integrity of dead cells is compromised, allowing the dyes to enter the dead cells. They bind to and intercalate with DNA, leading to a substantial amplification of fluorescence with an emission maximum at 617 nm. Whole-mount organoids and dissociated retinal cells cultivated in 3D substrates were rinsed twice with PBS containing Mg^{2+}/Ca^{2+} and incubated with 4 µg/ml of the dye diluted in PBS with Mg^{2+}/Ca^{2+} for 30 minutes at 37°C. The staining solution was aspirated and fresh PBS with Mg^{2+}/Ca^{2+} was added. The samples were used for imaging in a pre-heated incubation chamber set to 37°C. After imaging, PBS was removed and the corresponding culture medium was added to the samples.

5.8 Three-dimensional Substrate Fabrication

To fabricate 3D structures, a method called direct laser writing was employed. A droplet of photoresist is put on a cover slip and placed onto a piezo stage mounted on a microscope. The photoresist is composed of a polymer (Pentaerythritoltriacrylate (PETA) or trimethylolpropane-ethoxylate-triacrylate (TPETA)) and a photoinitiator. One characteristic of the used photoresist is a threshold value for polymerization. Only upon exceeding the threshold, the local energy is sufficient to polymerize the photoresist. For this work, a commercial *Photonic Professional*-system by the company Nanoscribe was used, which is based on a two photon principle. Basically, exciting an atom or molecule can not only be achieved by exposure to the required energy, but also to two photons with half the energy. However, this is only the case in the very focus of the laser beam, leading to high spatio-temporal accuracy. The system is equipped with a femtosecond-pulsed laser to allow stimulation with half-energy photons in quick succession. To increase spatial resolution, the laser is focused into the sample via a high-NA objective.

Silanization

In order to increase the 3D structures adhesion to the cover slip, a pre-treatment with 3-methacryloxypropyltrimethoxysilane is required. High precision cover slips with a thickness of 170 µm were cleaned with isopropanol and blow-dried with nitrogen. To achieve an even coating with silane, the cover slips are plasma-cleaned for ten minutes. The plasma treatment leads to hydrophilization of the

surface. Afterwards, the cover slips were immersed in a solution of 1 mM 3-methacryloxypropyltrimethoxysilane and toluen for one hour. Finally, the cover slips were washed with ${}_{dd}H_2O$ and blow-dried with nitrogen.

Writing Procedure

To fabricate 3D structures, a blueprint ('job') directing the piezo stage in axial and lateral direction is required. Jobs were either devised on a text basis via DeScribe or via the 3D creation suite Blender (and later adjustments with DeScribe) with the support of Marc Hippler (Institute of Applied Physics, KIT). After generating the jobs, the Nanoscribe-setup was prepared. Up to ten cover slips were placed on a sample holder and a droplet of immersion oil and photoresist were placed on the corresponding sides. Upon insertion of the holder to the stage, the software allowed successive completion of the job on multiple cover slips in an automated fashion. Subsequently, the samples were developed in a 1:1 (v/v) mixture of methylisobutylketone (MIBK) and isopropanol to remove unpolymerized monomers. After development, cover slips were washed with isopropanol and blow-dried with nitrogen.

Typically, 3D structures were produced in a 2-step procedure. In the first step, the photoresist TPETA was used. This photoresist disallows adsorption of proteins, rendering the surface passivating. The passivation consisted of two types of structures 1) squares directly passivating the surface of the cover slip and 2) rectangular walls to contain cells within the 3D structure. After developing the structures in 1:1 MIBK and isopropanol (v/v) for at least ten minutes, the cover slips were blow-dried with nitrogen.

In the second step, the cover slips with TPETA-structures were placed into a sample holder and the photoresist PETA was used. The TPETA-structures were located and manually aligned. An array of pillars with a total of 28x28 pillars was written in the confines of the TPETA-walls. Afterwards, the cover slips were developed in 1:1 MIBK and isopropanol (v/v) at least over night.

Preparation of 3D Substrates

In some cases, we observed poor survival of cells on the 3D structures, which could be alleviated by washing the 3D structures with a 1:1 mixture of PBS and 70% ethanol (v/v) for at least three days. When preparing the 3D structures for experiments, the PBS-ethanol mixture was aspirated and rinsed with 70% ethanol. Afterwards, the 3D structures were left to air-dry.

5.9 Cultivation on 3D Pillar Arrays

For application of 3D structures in cell culture, modifications with ECM proteins typically are required in order to allow cells to attach to the surface. In order to restrict the available area, squares were devised from polydimehtylsiloxan (PDMS) Sylgard 184. Polymer and curing agent were mixed with a ratio of 9:1 in a petri dish and left to degas at RT for 30 minutes. The PDMS was cured over night at 60°C. After cooling to RT, squares were cut out of the bulk material with a scalpel (outside edge length of 2 cm and inside edge length of 1 cm) and sterilized with 70% ethanol. PDMS squares were placed on the cover slips centered around the 3D structures. LN is a prevalent protein of the ECM in neural tissues and the eye, rendering it a prime candidate for surface functionalization. To coat the 3D structures, a suspension with 20 µg/ml LN was prepared. 100 µl of this suspension were added to each 3D structure and incubated for 2 hours at 37°C.

D14 organoids were pre-selected under a table-top microscope. Organoids containing large areas of phase-bright epithelium were regarded as retinal organoids. The pre-selection was verified with a fluorescent microscope via the expression of the Rx-GFP construct in retinal tissues (Figure 5.1 II). To seed retinal cells on LN-coated 3D structures, a cell suspension was generated. To this end, GFP^+ retinal organoids were collected in an Eppendorf cup. Per cover slip, three organoids were dissociated and seeded. Remaining medium was carefully aspirated with a 1 ml pipette, washed with PBS to remove last remnants of the medium and incubated with 500 µl 0.25% trypsin solution at 37°C. After 10 minutes, excess trypsin was removed and RMM2 was added to the organoids. The pre-digested organoids were dissociated by repeated pipetting with a 1 ml pipette. Dissociation was continued until a homogeneous cell suspension without any larger clumps was obtained (Figure 5.1 III).

After 2 hours, the LN-solution was aspirated from 3D structures and 100 µl of cell suspension were added to each substrate and incubated at 37°C (Figure 5.1 IV). After 1 hour, seeded cells were checked for attachment under a table-top microscope. If cells started to attach to the substrate, excess cells were manually removed from the areas outside of the 3D structure. For this purpose, 2 ml of pre-warmed DMEM was added to each well and the PDMS-square was removed with sterilized forceps. A table-top microscope was surface-sterilized with ethanol and placed under a clean bench. Using a 2 µl pipette and 4x objective, cells beyond the scaffold were removed by scratching the surface. When all excess cells were removed, the medium was aspirated, washed once with PBS and 2.5 ml RMM2 + 25 µl Taurine were added per well. Dissociated retinal cells on 3D structures were cultivated under standard conditions for up to 50 days. Half-medium changes were performed once per week.

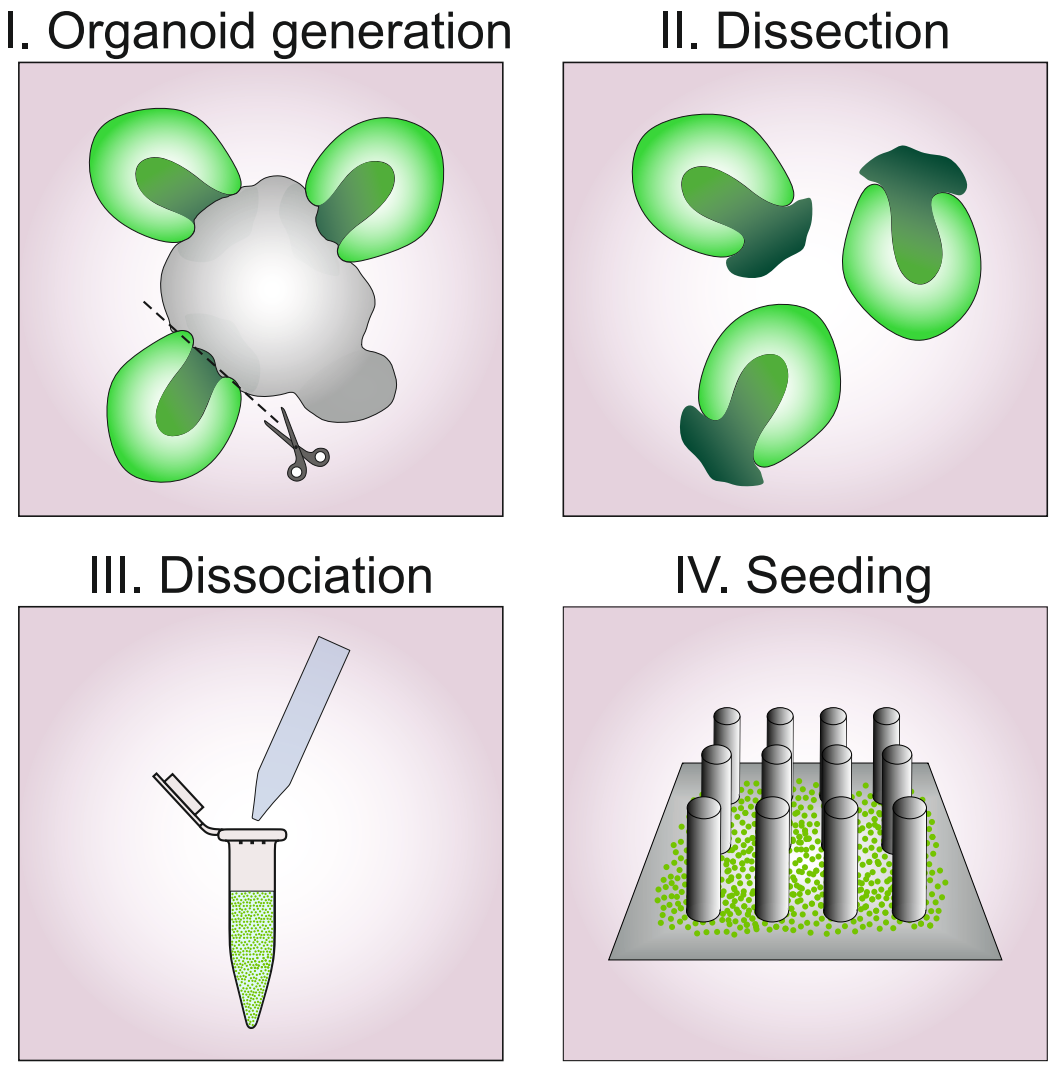

Figure 5.1: **Processing of retinal organoids and seeding in 3D substrates.**
(I) Retinal organoids are cultivated for ten days. In most cases, they consist of a main-aggregate and a number of Rx-GFP$^+$ retinal vesicles. (II) The Rx-GFP$^+$ vesicles are excised using two forceps under a table-top microscope and continued to be cultivated. (III) After fourteen days of cultivation, the retinal organoids are placed in an Eppendorf cup and get enzymatically and mechanically dissociated. (IV) The single cell suspension of retinal cells is then seeded on a LN-coated pillar array, offering a new substrate for continued cultivation.

5.10 Sample Preparation

Verification of correct tissue specification and the presence of the main cell types can be achieved through immunocytochemistry. This method employs fluorescently labeled antibodies and affinity probes to tag structures within or on the surface of cells. Immunocytochemistry can be done with a direct or indirect protocol. Shortly, a direct protocol utilizes fluorescently labeled antibodies raised against specific proteins of one or a number of target species. In contrast, in an indirect protocol, two cycles of antibody-exposure are combined. In a first cycle, a primary antibody raised against a specific protein is added to the cells or tissue. In a second cycle, fluorescently labeled secondary antibodies are used. An indirect staining procedure offers more flexibility in fluorophores and also amplifies the signal. In this work, only indirect immunocytochemistry was employed.

Cryoprotection and -sectioning

Compared to a monolayer of cells, organoids are large objects, leading to low efficiency of antibody penetration and imaging of areas deep within the organoid is challenging. Thus, samples were sectioned at a Leica CM3050 cryostat prior to staining. To avoid damage to the tissue from ice crystals forming during the freezing procedure, samples have to be cryoprotected with sucrose solutions of ascending concentration. Organoids were fixed with 4% PFA over night and washed with PBS. 15 and 30% sucrose solutions in $_{dd}H_2O$ were prepared. Upon removal of PBS, 0.5 ml of 15% sucrose solution were added. With addition of the sucrose solution, the organoids started to float to the surface as the sucrose solution has a higher density. if the organoids were soaked and sank to the bottom of the Eppendorf cup after one hour of incubation, sucrose solution was changed to 30% and incubated over night at RT. At this stage, cryoprotected organoids were either stored at -80°C or subjected to cryosectioning.

Organoids were embedded in Surgipath FSC 22 Blue with minimal transfer of sucrose solution. They were left to harden in the freezing chamber at -22°C. The frozen organoids were cut at the edge with a razor blade to reduce the amount of Surgipath FSC 22 Blue void of orgnaoids. They were fixed in the cutting head, the blade holder was set to a tilt of 5° and section thickness was set to 22 µm. The cutting head was moved towards the blade until cutting range was reached. One rotation of the hand wheel produced one section of 22 µm thickness. Sections were mounted on a Superfrost Ultra Plus slide and left to air-dry over night. To enhance the adhesion of sections to the object holder, a 20 minute fixation step with 4% PFA was performed.

Immunocytochemistry

Immunocytochemistry was usually performed on sectioned organoids mounted on an object holder, on dissociated organoids cultivated in 3D structures or on cells cultivated on a cover slip. The general protocol is described in Table 5.12. Depending on the type of sample, differences in the protocol occured. Antibodies used for immunocytochemistry were tested in P7 mouse retina beforehand, some samples are given in Figure 5.2. All stainings were conducted in a humidified chamber to reduce evaporation and volume of antibodies used. Additionally, sectioned orgnaoids on object holders were covered with a rectangular piece of parafilm. For 3D structures and cells on cover slips, a droplet of staining solution was placed in the center of the cover slip. Prior to mounting, samples were washed with $_{dd}H_2O$ and dried with a Kimtech wipe. Sectioned organoids were mounted with Mowiol by putting 3 droplets of Mowiol on the object holder and slowly placing a 24x60 mm cover slip on top. 3D structures were mounted on object holders modified with a PDMS-square fixed to the surface with PDMS for 30 min at 60°C. The cavity was filled with Mowiol and the cover slips with 3D structures were then placed upside down on the PDMS-square.

Table 5.12: **Staining Procedure**

Process	Solution	Duration
Fixation	4% PFA	o/n
Permeabilization	PBS + 0.1% Triton-X 100	1h
Primary Antibody	Antibody in 0.05% BSA + 0.05% Triton-X 100	o/n
Washing	PBS + 0.1% Triton-X 100	3x10 min
Secondary antibody and affinity probes	Antibody in 0.05% BSA in PBS + 0.05% Triton-X 100	o/n
Washing	PBS	3x10 min
Mounting	20% Mowiol	o/n

Sample Preparation for REM

Samples for analysis via REM were fixed with a mixture of 2% PFA/GA in PBS over night at 4°C. Dehydration of the tissue was achieved via incubation in acetone dilutions with ascending concentration (10, 30, 50, 70, 90 and 100 % acetone) for 10 minutes each. The last incubation step with 100 % acetone was done three times. Subsequently, critical point drying was achieved with a Leica EM CPD300

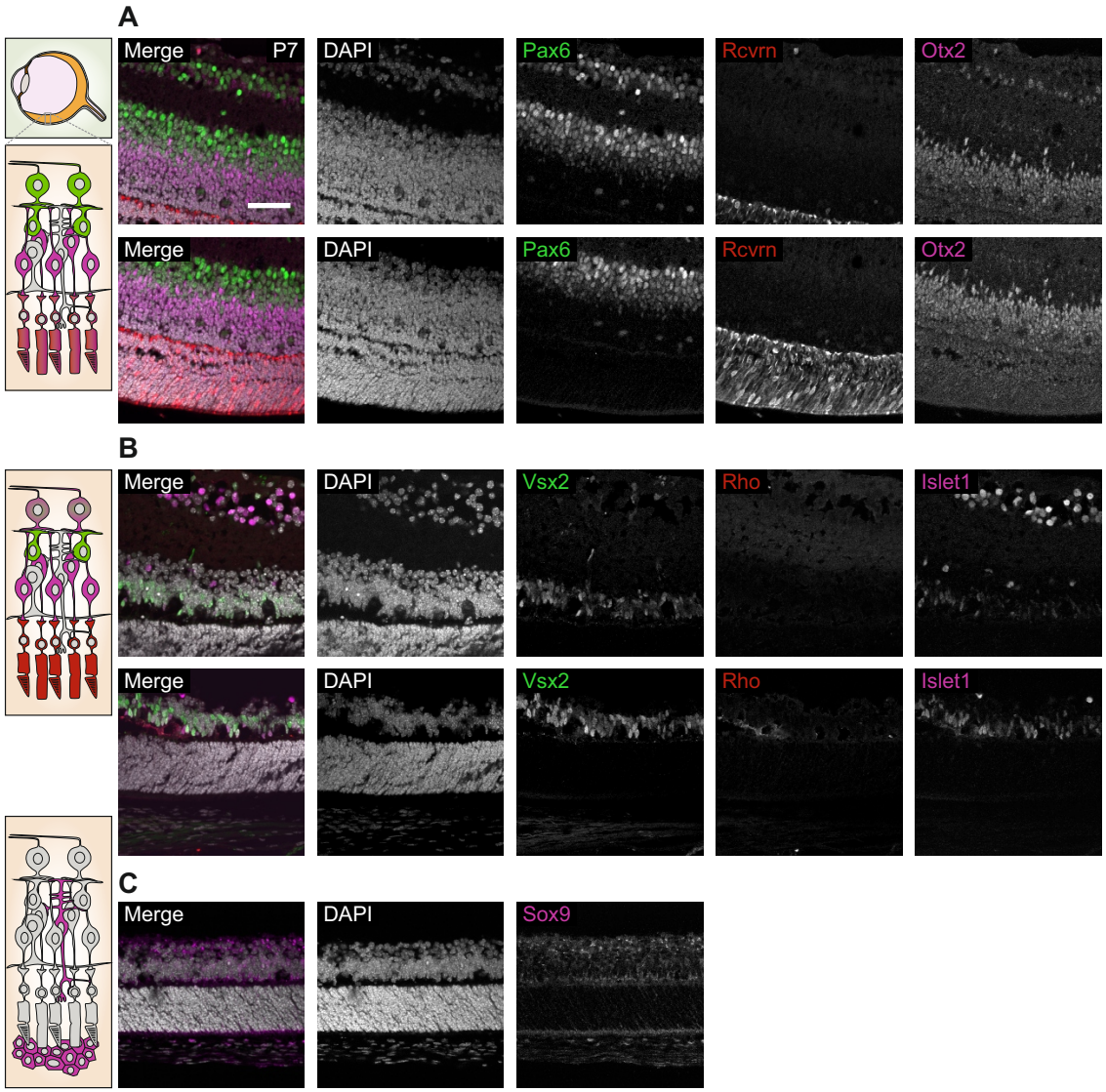

Figure 5.2: **Marker validation for immunocytochemistry.** (A) P7 mouse retina stained for Pax6 (green), Rcvrn (red), Otx2 (magenta) and DAPI (grey). The upper row of images reflects the central part of the retina with the INL and GCL (top part of images), while the bottom row of images reflects the basal part with the ONL (bottom part of images). (B) P7 mouse retina stained for Vsx2 (green), Rhodopsin (red), Islet1 (magenta) and DAPI (grey). Same orientation applies as in (A). (C) P7 mouse retina stained for Sox9 (magenta) and DAPI (grey) with the ONL and INL visible. Scale bar = 50 µm, applies to all images. The retinae were of a mOR37a-IRES-eGFP strain with a C57B1/6J background.

critical point dryer. Samples were washed with liquid CO_2 and dried at 40°C and pressure below 100 bar. The dried samples were fixed on a sample holder with a conductive silver paste and a 5 nm thick layer of gold particles was sputtered onto the sample. Imaging was performed by Vincent Hahn (Institute of Applied Physics, KIT) at a Zeiss SUPRA 55 VP.

Chapter 6
6 Results

For decades, *in vitro* studies were reliant on primary cell cultures. This changed with the cultivation and differentiation of embryonic stem cells and in recent times induced pluripotent stem cells. These cells can differentiate into all cell types of an organism. However, harnessing this potential in an organized and directed fashion is quite challenging. One widespread method for generating organized tissues is called organoids. Organoids turned out to be a promising approach to obtain organ-like tissue in a petri dish. While this is a great advance, there are still problems inherent to the organoid culture. These problems include challenging reproducibility, limited cultivation, and incomplete differentiation. In order to improve these problems, direct laser writing (DLW) produced substrates are employed to offer a suitable environment for retinal cells to grow in.

In this chapter, I present my results on combining retinal organoid-derived cells with 3D substrates. In the first section, I introduce the cultivation of retinal organoids and show some of the limitations connected to this system. Then, the 3D-produced substrates are introduced, including the cultivation of stem and retinal cells on these substrates. The cell composition of resulting tissue constructs is presented and characterized. The organization within the 3D substrates is also addressed, and lastly, the separate differentiation of RPE cells is demonstrated.

6.1 Generation of Retinal Organoids

The differentiation of mature cell types from pluripotent cells has been subject to a large amount of research. Complex interactions of a multitude of pathways render directed differentiation of cell types quite challenging. However, there are still some cell types that can be generated quite easily, as the underlying signaling pathways have been sufficiently elucidated. One of these cell types are retinal pigment epithelial cells (RPE), which can be induced by activating the WNT-signaling pathway and inhibiting fibroblast growth factor receptor and

vascular endothelial growth factor receptor via the addition of small molecules or purified proteins. This leads to the enhanced generation of RPE cells, which can be purified and expanded solely based on their characteristic pigmentation.

However, this is one of the exceptions to the rule, as many other protocols lead to the generation of an increased number of the target cell type, but in an inhomogeneous cell population. Cell sorting mechanisms have to be employed in order to purify the desired cell type.

In the case of organoids, the protocol seems rather simple. Depending on the various tissue fates, the complexity of the protocols vary. But overall, a key factor for the protocol's success is the addition of ECM, mostly in the form of Matrigel. The geometrical environment offered by Matrigel and the factors included in the mixture are sufficient to induce the differentiation of the desired cell types.

6.1.1 Increased Retinal Induction via Addition of a Retinoic Acid Receptor Antagonist

The first mention of retinal organoids in literature is from 2011 by Mototsugu Eiraku and Yoshiki Sasai (Eiraku et. al 2011). They combined free-floating mouse embryonic stem cell aggregates with Matrigel. After five days, the aggregates started to form vesicular structures which also expressed a Rx-GFP construct indicative of retinal differentiation. Upon further cultivation, these vesicular structures invaginated to form optic cup-like structures.

The group of Masayo Takahashi introduced an optimized protocol for retinal organoids (Assawachananont et. al 2014). They added the retinoic acid receptor antagonist AGN193109 (thereafter abbreviated as AGN) and increased the knockout serum replacement (KSR) concentration from 1.5% to 5%. This protocol demonstrates a higher percent yield of Rx-GFP$^+$ cells obtained in organoids.

In order to have sufficient retinal cells available for the cultivation in 3D substrates, an organoid protocol with a high outcome of Rx-GFP$^+$ cells is desired. Thus, we tested both protocols under our specific cultivation conditions.

Organoids started from the same passage of mESCs and cultivated under the same conditions were induced with both protocols (Figure 6.1 A). In the presence of AGN, the organoids show a strong fluorescence signal of the Rx-GFP construct. Furthermore, the formation of vesicular structures is observable. The phase-bright margin regions of the vesicle are positive for Rx-GFP. In contrast, in the absence of AGN but with addition of Matrigel, no or little Rx-GFP is present in the organoid. Morphologically, the organoids with and without AGN heavily differ. In the absence of AGN, barely any vesicles are present, but irregular growth on the surface as well as neuronal extensions can be observed. In the absence of both, Matrigel and AGN, the stem cell aggregate just grows in size but lacks the previously described vesicular structure and presence of Rx-GFP$^+$ cells. A

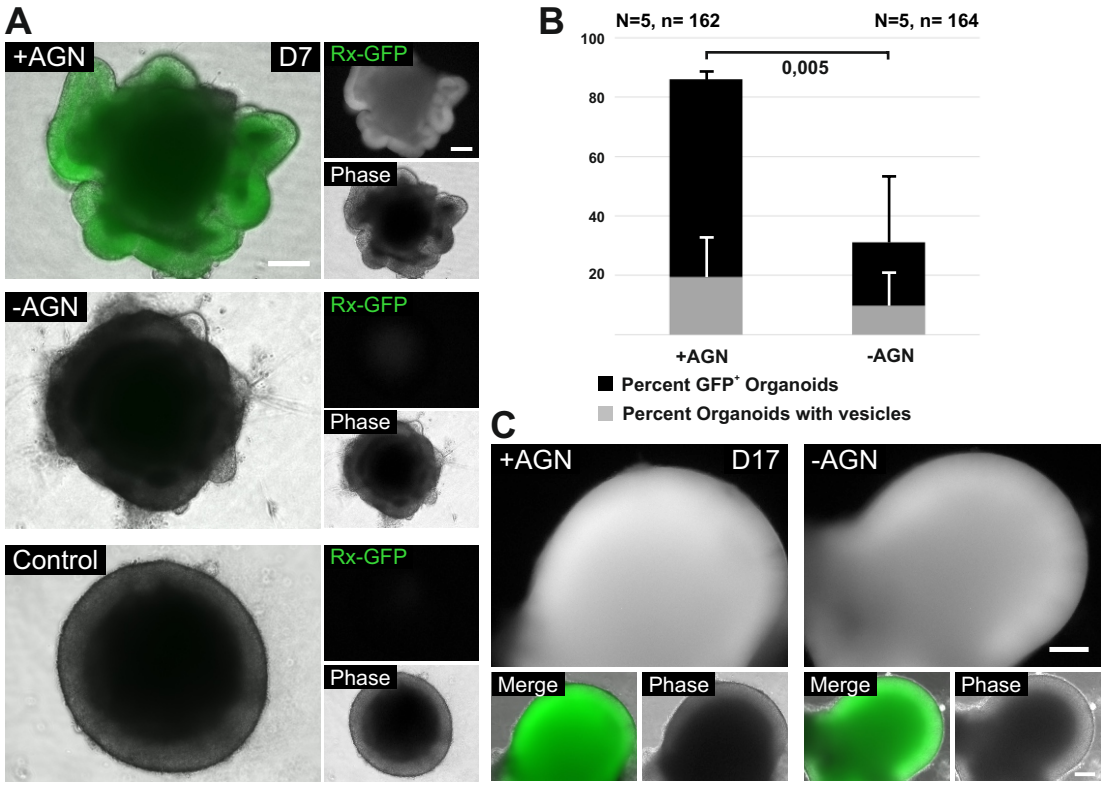

Figure 6.1: **Retinal organoid induction and early differentiation.**
(A) Representative images of organoids induced with Matrigel towards retinal fate, in the presence of AGN (top) and absence of AGN (center). The systems dependency on Matrigel as inducing factor is shown in the bottom image (control without Matrigel). (B) Quantification of retinal induction in organoids depending on the addition of AGN. The formation of vesicles was also assessed. N=5, n=162 for +AGN, n=164 for -AGN. Two-sided T-Test was applied. Error bars indicate standard deviation. (C) D17 organoids generated either in the presence or absence of AGN. single-channel images as well as merged images are given. Rx-GFP is depicted in green, phase contrast in gray. Scale bar = 100 µm, applies to all images in (A) and (C), respectively

quantification of five independent experiments (Figure 6.1 B) shows a markedly higher frequency of retinal induction and higher occurrence of vesicular structures in the presence of AGN. However, as indicated in Figure 6.1 C, in later stage organoids, morphology did not differ between the different protocols, indicating that the more frequent retinal induction does not come with drawbacks in later stage differentiation.

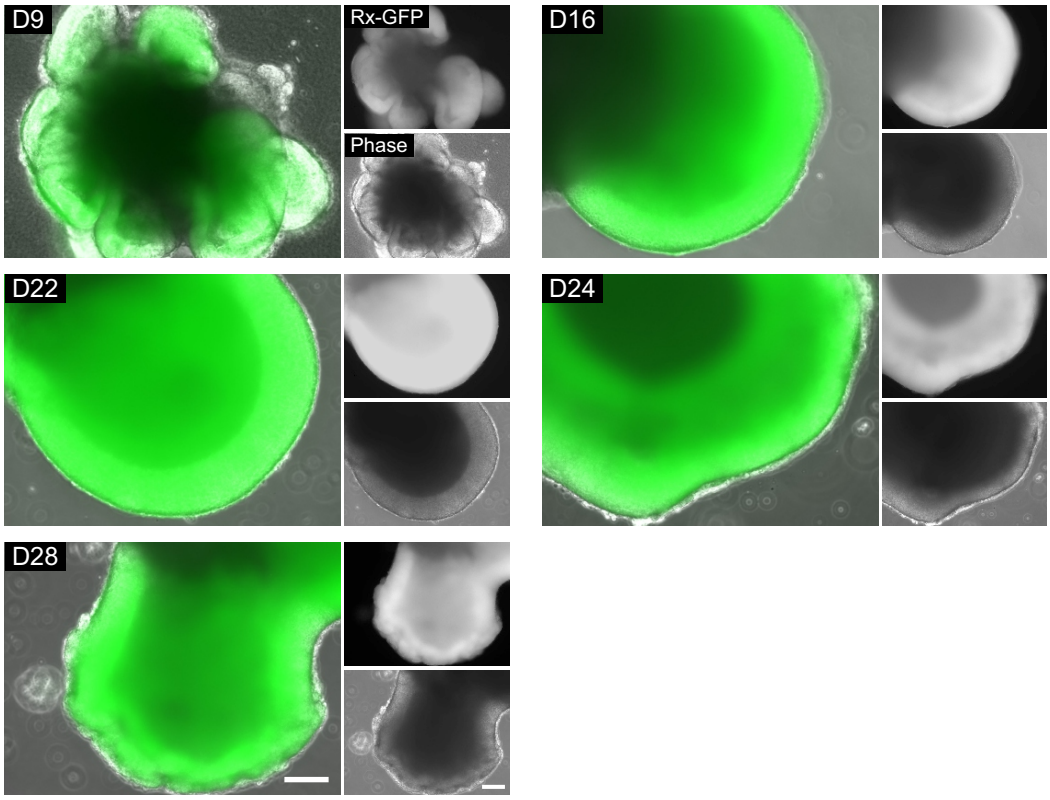

Figure 6.2: **Long-term cultivation of retinal organoids.**
Retinal organoids induced with Matrigel and AGN were monitored throughout their development. Examples are shown from D9 prior to dissection up until a matured stage at D28. Single-channel and merged images are shown. Rx-GFP is depicted in green, phase contrast in gray. Scale bar = 100 µm, applies to all images.

6.1.2 *Retinal Organoids Lose Organized Morphology with Extended Cultivation*

For long-term cultivation of retinal organoids, D7 organoids are transferred from ultra-low adhesion well plates used for induction to standard petri dishes. They are cultivated in a DMEM/F12 based medium with N2 supplement. Using a microscope and forceps, single vesicles are cut from the main aggregate. Dissected organoids are then cultivated in a DMEM/F12 based medium with N2 supplements and 10% FCS. Figure 6.2 shows representative images of organoids at different days of cultivation. At D16 and D22 a well defined and organized structure with a smooth outer margin is present. However, with continued cultivation this structure deteriorates, as can be appreciated on D24 and D28. The

formerly flat surface starts to be jagged. The effect is even more pronounced at D42, resulting in clumps of cells on the organoids surface and seemingly a loss of epithelial thickness and overall size.

As tissue organization and function are tightly linked, we raised the question if the loss of integrity and morphological deterioration corresponded to a reduction in cell viability. Thus, a time series of organoids treated with the apoptosis marker propidium iodide (PI) was obtained. PI is non permeant to live cells but can enter dead cells to intercalate with DNA. In the aqueous, non-bound state PI shows neglectable fluorescence, which is amplified 20-30 fold upon binding to DNA. Dissected organoids were incubated for 30 minutes with PI, washed and immediately imaged.

On earlier days of cultivation, retinal organoids show low levels of PI^+ cells. However, upon continued cultivation, retinal organoids show increased levels of PI^+ cells. On D31 and D35, PI^+ cells are most prevalent. The absolute number of PI^+ cells is declining after D35. Interestingly, apoptotic cells are enriched in Rx-GFP negative areas (see arrowheads in Figure 6.3). Furthermore, the morphological decline of retinal organoids can be followed during this experiment. At D24, the once flat surface of the organoid shows brighter and irregular spots in the Hoechst staining and Rx-GFP. On D31, the organoids structure is more jagged and this trend continues until D38. Additionally, while the organoids overall size decreases, larger Rx-GFP negative areas appear in the center of the organoid, which also appear to have a lower cell density.

Overall, long-term cultivation of organoids is possible, however, there are clear restrictions in cultivation time, as organoids lose integrity with prolonged culture, are shrinking in overall size and cells undergo apoptosis.

6.2 Three-dimensional Substrates for a Retinal Cell Culture System

The loss of morphology observed in long-term murine retinal organoid cultivation is detrimental for studies focused on problems in later-stage development of organoids. Thus, we attempted to combine retinal differentiation with tailor made 3D substrates in order to address some of the downsides of retinal organoids. To produce well defined 3D substrates in a micrometer-range, various techniques are available. We chose a two photon-based lithography setup because of its high level of spatio-temporal resolution and high flexibility in scaffold production and design. The first step was to compose a design for the DLW substrates. We assumed that cells in standard organoid culture might lack sufficient stability and support, as well as having low levels of nutrient supply and removal of waste products in central regions of the organoids. Thus, we wanted to formulate a design for

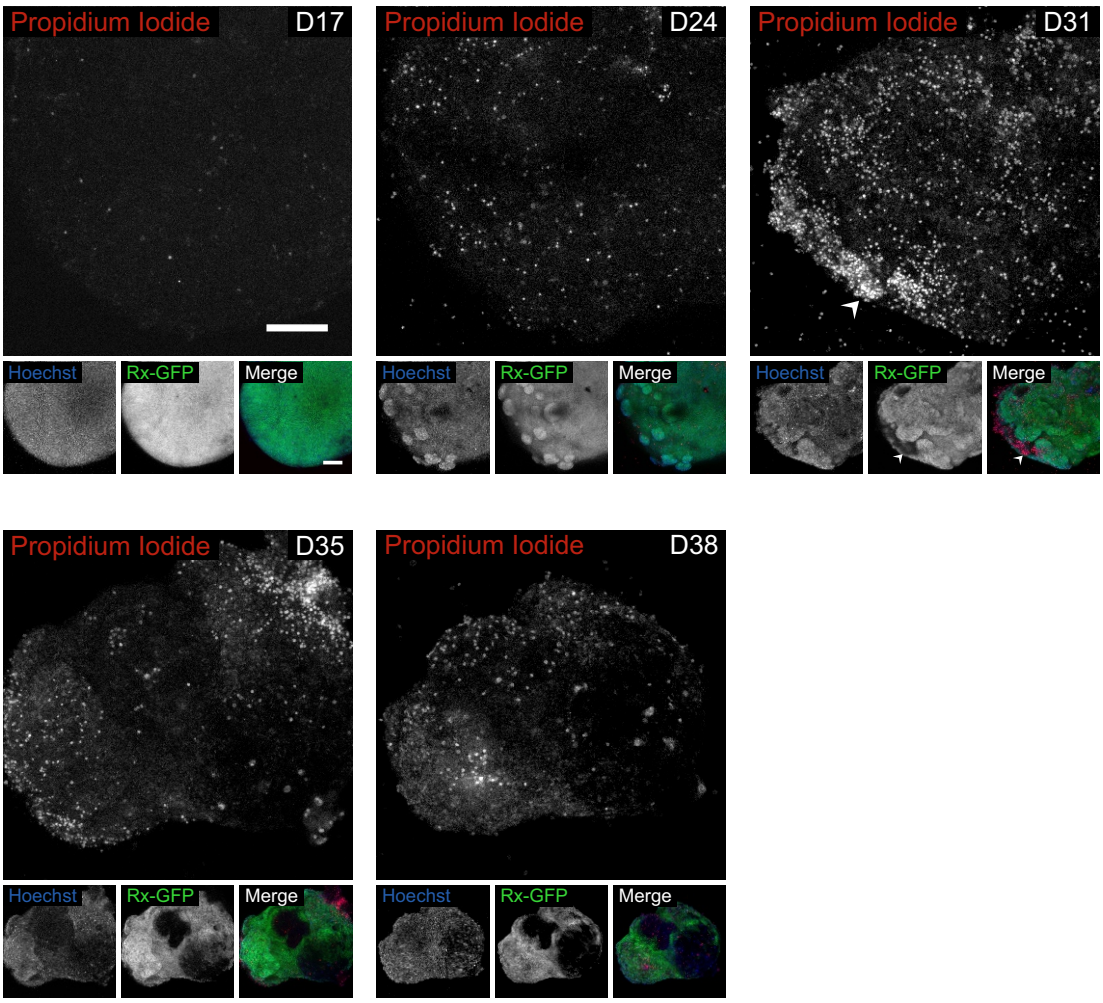

Figure 6.3: **Assessment of viability in developing retinal organoids.** Representative images of retinal organoids stained with Propidium Iodide at different stages of development. Organoids were counter-stained with Hoechst staining solution. Single-channel and merged images are shown. Propidium Iodide is depicted in red, Hoechst in blue and Rx-GFP in green. Scale bar = 100 µm, applies to all images of corresponding size. Experimental execution and image acquisition by Chiara Windsor.

substrates to offer sufficient stability for cells cultivated on the substrate, yet offering ample accessibility for regular exchange of nutrients and waste products. A cell type with central function in yielding structure and stability to the retina are Müller glial cells.

To emulate the function of Müller cells, we designed an array of pillars with a height of 70 µm, a diameter of 3.5 µm and an edge-to-edge distance between

pillars of 20 µm to be written with the protein-adhesive photoresist PETA. To prevent cells from migrating and completely overgrowing the substrate, walls with a height of 80 µm and flat squares with the passivating photoresist TPETA were written to surround the pillar array. This would disallow cells from adhering directly outside of the pillar array. Figure 6.4 A shows a top-view of a pillar array coated with LN, which was visualized by immunolabeling. Pillars and the glass surface in between the pillars show a high level of fluorescence signal, while the signal on the passivated squares is more spotty and overall lower in intensity (Figure 6.4 A). 3D reconstructions of z-stacks taken from these substrates allow an approximation of the substrates architecture (Figure 6.4 A′ and A″).

To clearly show the pillar arrays architecture, substrates were prepared for scanning electron microscopy (SEM). SEM micrographs in Figure 6.4 B-B″ show an overview of a whole pillar array with surrounding passivating walls and squares (B), an oblique-view of pillars and sections of surrounding walls (B′) and a top-view of pillars and walls. Here, a reduction in diameter and thickness of both, the pillars and walls can be observed (B′ and B″). The substrates are generated in a layer-by-layer method, starting at the plane of the cover slip. When writing higher structures, the laser beam has to be focused through layers of already polymerized photoresist in order to polymerize new photoresist, thereby experiencing reductions in laser power. This effect can be corrected by inverting the whole system, but this would require changes in writing mode, which would render automated writing of multiple samples impossible. Figure 6.4 (C) shows retinal cells cultivated in a pillar array for eight days. The cells form a thick sheet of cells, filling the array in *x-y* dimensions. Some shrinking effects from dehydrating the substrates can also be observed. Larger cell clumps are present on top of the cell sheet. As no pillars are visible, the height of the cell sheet has to be at least 70 µm, but as they are also surpassing the constraints of the walls, a height of more than 80 µm is likely. In the areas around the pillar array, sheets of cells are also present. These cells are undesired, as the 2D environment might lead to an unwanted shift in cell fate. Figure 6.4 (C′) allows a direct view of some clearly discernible cells in a pillar array. The cells differ in morphology and size, but are closely packed next to each other.

6.2.1 Cultivation of mESCs in Pillar Arrays

After characterization of the pillar arrays, they were used for cell culture experiments. To this end, we first attempted a direct conversion of the organoid protocol, meaning to seed stem cells into the pillar array and induce retinal fate within the 3D substrate. One day after seeding mESCs on LN coated pillar arrays, they formed a sheet-like structure (Figure 6.5 A). The cell sheets were encased

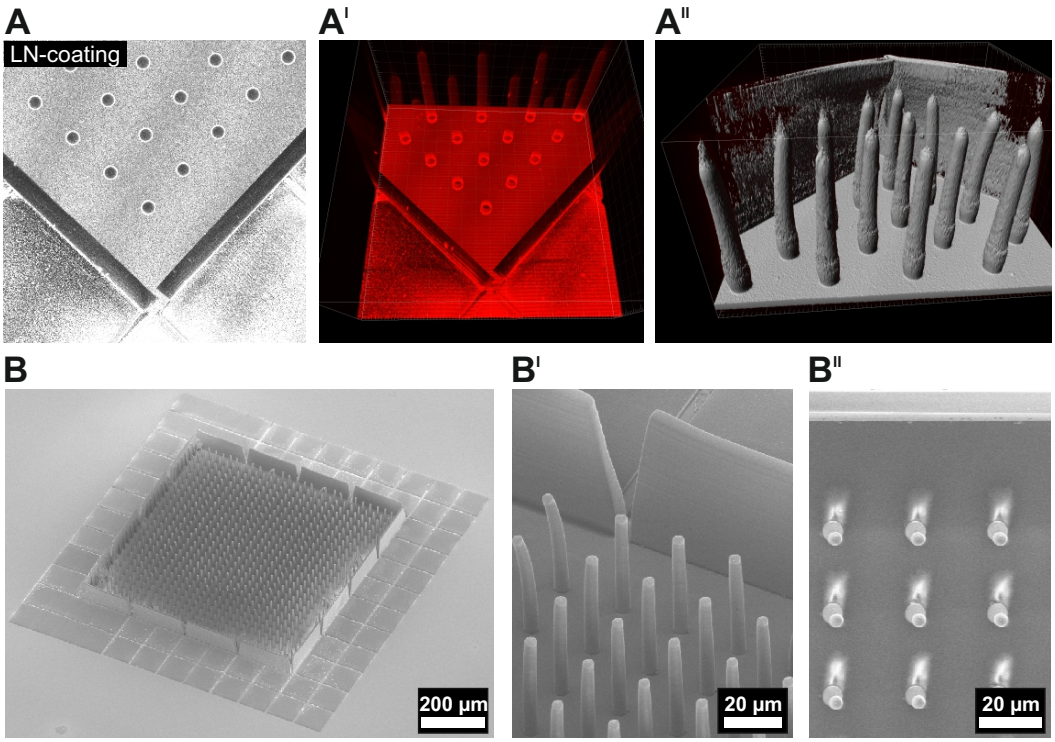

Figure 6.4: **Characterization of direct laser writing-produced pillar arrays for cell cultivation.**
(A) Single-plane image of a LN-coated pillar array. Pillars are fabricated from the PETA photoresist, while the surrounding walls and squares are fabricated from TPETA photoresist. (A') and (A") Simple 3D representation of LN-coated pillar array and a corresponding 3D reconstruction of the pillar array. (B) Scanning electron micrograph of one pillar array field, with a magnified side (B') and top (B") view of pillars. Scale bars are specified in the corresponding images.

in Matrigel and differentiation medium was added to the substrate. One day after addition of Matrigel, the cell sheet showed changes in morphology, as the previously flat sheet with some occasional cell clusters turned into a rather even sheet with a rippled surface structure. This rippled surface is quite reminiscent of stem cell aggregates after addition of Matrigel.

Upon continued cultivation of mESCs on pillar arrays with Matrigel, the cells heavily proliferated and outgrew the constraints presented by the TPETA walls. The cell sheet had a dark coloring in the phase contrast, reminiscent of stem cell aggregates which did not adopt retinal fate and died during cultivation (Figure 6.5 A"), a viability assay was conducted with ethidium homodimer, specifically staining apoptotic cells by intercalating with DNA. This dye is only able to enter dead cells since their cell membrane's integrity is lost. The viability assay turned out negative for the mESCs cultivated in pillar arrays, as can be observed in Figure 6.5

(A''). However, there was also no retinal induction observable, indicated by monitoring Rx-GFP expression. To verify the general functionality of the materials and protocol, same batch mESCs were cultivated and induced with the optimized organoid protocol, using Matrigel from the same LOT. Figure 6.5 (B) clearly shows that under free-floating conditions, retinal induction was achieved in organoids. Thus, apparently cultivation conditions in pillar arrays were not adequate to induce retinal fate in mESCs.

6.2.2 Cultivation of Dissociated Retinal Organoids in Pillar Arrays

As a plain transfer of the protocol from a free-floating stem cell aggregate to a pillar array could not be realized, we had to explore other avenues of combining retinal cells with tailor-made 3D substrates. As retinal organoids were established in the scope of this work, we chose to use organoids as a reservoir for retinal cells. We chose to use D14 organoids to be seeded in pillar arrays, as they should be on the verge of switching from a progenitor-like state to terminal differentiation and giving rise to the various cell types. Accordingly, they should be able to arrange in 3D and maybe even self-organize. To indicate that dissociated organoids in pillar arrays are discussed, the nomenclature will be D14+X, while X is the corresponding cultivation time in the pillar arrays.

In order to offer a suitable environment, pillar arrays were also surface coated with LN. On average, 3 dissociated organoids were seeded per pillar array as a single cell suspension. After an initial adhesion phase, cells beyond the pillar array were removed manually with a pipette tip. The cells were cultivated in the same medium as same-age organoids. Figure 6.6 (A) shows representative images of dissociated organoids cultivated in a pillar array. After seeding, small aggregates of retinal cells were present in between the pillars. Within the next week, these aggregates continued proliferation and visibly grew in size. At D14+8, sufficient proliferation occurred that single aggregates merged into a cohesive sheet. With the exception of a few small sections, most of the seeded cells are GFP+. By D14+17, the pillar array seemed well colonized by retinal cells, which largely remain within the constraints of the walls. However, with continued cultivation, cells occasionally also overgrew the pillar array. These cells were GFP^- in most cases. At this stage of cultivation, manual cleaning is quite challenging, as cells are interconnected in sheets, so they can not easily be isolated and removed. Additionally, the pillar arrays integrity can also be compromised with prolonged cultivation. Sometimes, pillars were removed by the cell sheet and walls displaced. However, the GFP signal within the pillar array was still quite strong. When comparing standard cultivation conditions (Figure 6.6 B) and the dissociated

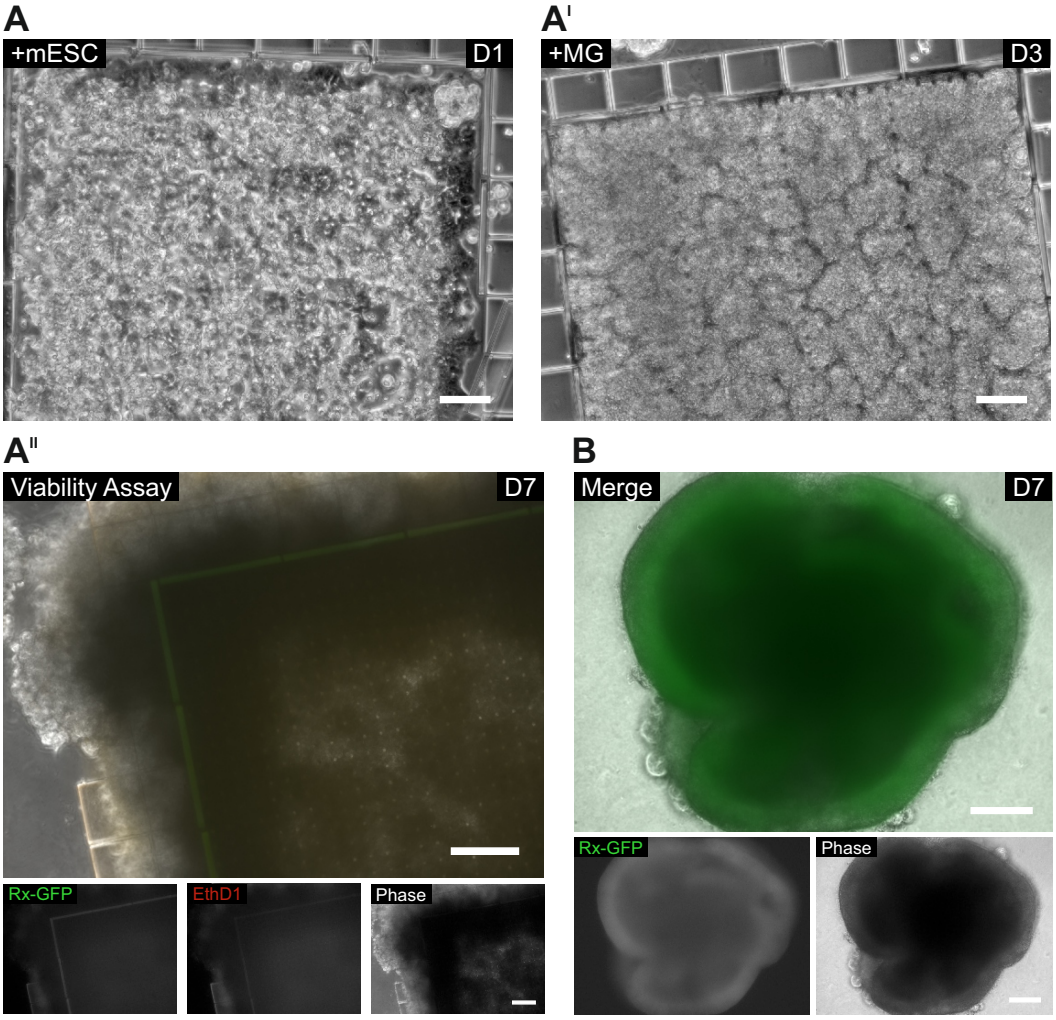

Figure 6.5: **Retinal induction of mESCs in pillar arrays.**
(A) Pillar arrays with mESCs. (A‘) Matrigel was added to the cells on D1 and further cultivated. (A“) mESCs cultivated in pillar arrays for seven days in the presence of Matrigel do not show any GFP-signal. Dead staining with ethidium homodimer (EthD1) was also negative. (B) Same passage mESCs induced with standard cultivation methods and same batch Matrigel showed marked GFP signal at D7. Rx-GFP depicted in green, EthD1 based dead staining in red and phase contrast in gray. Scale bar = 100 µm.

organoids in pillar arrays, organoids did not appear to proliferate to a similar level both in quantity and time scale, and also showed signs of morphological deterioration, which could not be observed to that extend in the pillar arrays.

Thus, the cultivation of organoid-derived retinal progenitor-like cells in direct laser writing produced pillar arrays appeared to be feasible. Additionally, they seemed to maintain their structure for a longer time than free-floating organoids. To assess the cellular composition of the cultivated tissues, immunocytochemical stainings of both, dissociated progenitor-like cells in pillar arrays and retinal organoids were conducted.

6.2.3 Assessment of Viability in the in Vitro Cultivation System

We were able to cultivate the retinal cells for up to 50 days, while maintaining a more defined morphology. In order to have a better understanding of how the pillar arrays influence the cells, Chiara Windsor, a master student under my supervision, performed viability assays with dissociated organoids cultivated in pillar arrays.

Figure 6.7 is a time series of one pillar array that has been repeatedly treated with PI for staining dead cells and subsequently imaged. To prevent too much additional stress for the cells after dissociation and seeding on the pillar array, the viability assay was started after 8 days of cultivation on the pillar array. At this stage, the amount of cells stained positive with PI was rather low. However, the amount of PI^+ cells increased up until 18 days in culture. From that point on the presence of clearly PI^+ cells was declining, coming to a very low level at 32 days in culture. However, in contrast to earlier phases of cultivation, a weaker background-level staining becomes more apparent.

6.3 Cellular Composition in the Retinal *in Vitro* Culture System

The retina is a well-characterized tissue of neuronal origin. It comprises one glial and six neural cell types, which are organized in an ordered, laminar manner *in vivo*. To assess the cellular composition of our *in vitro* systems, we chose to analyse the individual cell types via immunocytochemistry. However, while some cell types like PRs have a number of markers clearly identifying them as PR, for other cells such as interneurons, most markers are present in a number of cell types. Additionally, identification and characterization of certain cell types can be even more challenging, as many markers are expressed differentially throughout development. Thus, while some stainings clearly identify the presence of a certain

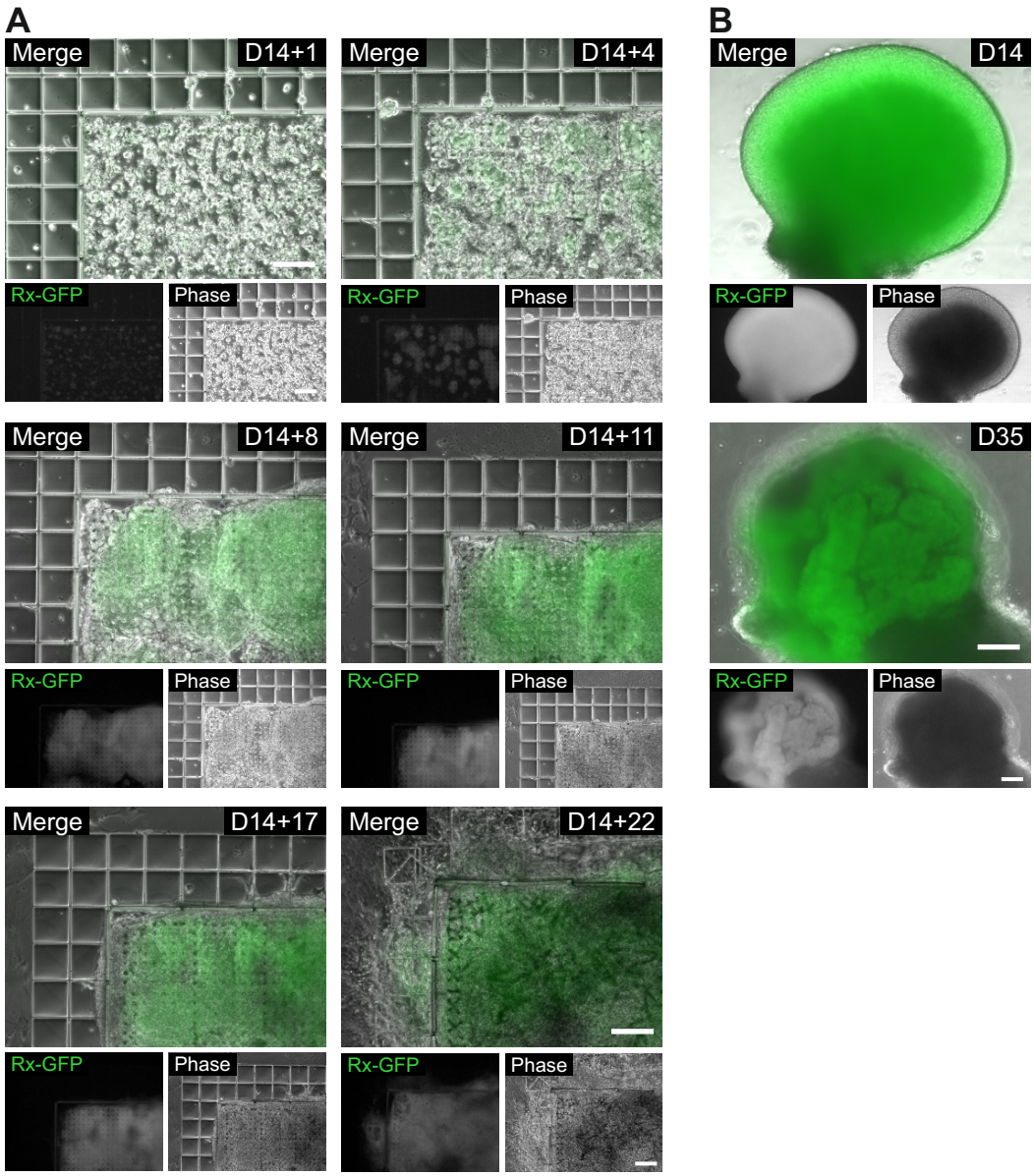

Figure 6.6: **Long-term cultivation of retinal progenitor-like cells in pillar arrays.** (A) Dissociated retinal organoids seeded in LN coated pillar arrays and cultivated for up to 22 days in the pillar arrays. (B) Same batch organoid control cultivated under standard conditions. Single-channel and merged images are shown. Rx-GFP depicted in green, phase contrast in gray. Scale bars = 100 µm, applies to all images.

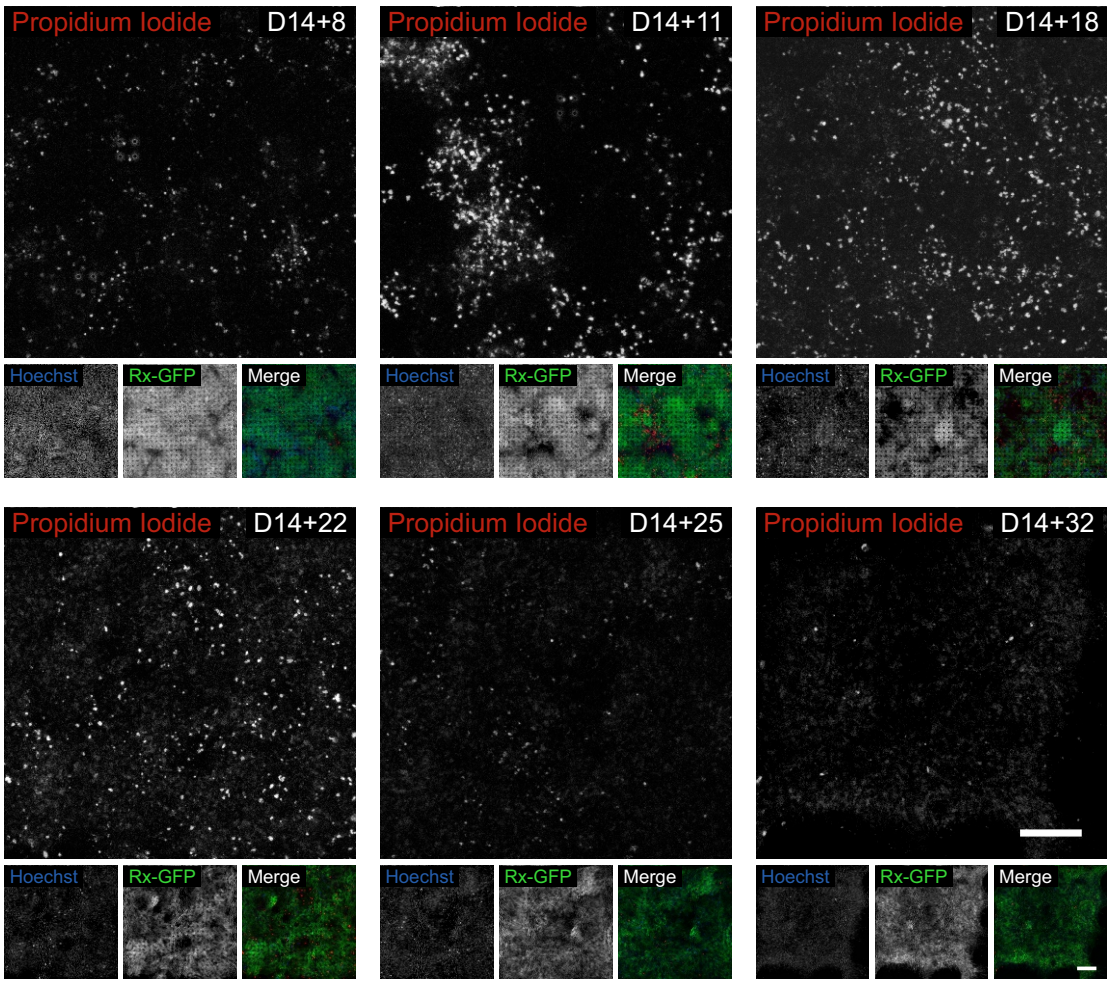

Figure 6.7: **Assessment of viability in retinal cells cultivated in pillar arrays.** Representative images of dissociated retinal organoids seeded in pillar arrays and stained with Propidium Iodide at different stages of cultivation. Cells were counter-stained with Hoechst staining solution. Single-channel and merged images are shown. Propidium Iodide is depicted in red, Hoechst in blue and Rx-GFP in green. Scale bar = 100 µm. Experimental execution by Chiara Windsor.

cell type, other stainings only indicate the presence of different cell types. In the latter case, combinations of multiple markers can consolidate the evidence. In the following section, immunocytochemical stainings of progenitor-like cells cultivated in pillar arrays and organoids are presented.

6.3.1 Occurrence of Photoreceptors in an in Vitro Cultivation System

Photoreceptors are a very specialized cell type central to the detection of visual stimuli. Rods and cones are the two PR classes present in the retina. Rods are more numerous than cones, rather located in the periphery and involved in peripheral and night vision. Cones, on the other hand, are located mostly centrally and are responsible for high acuity and color vision. To characterize PRs, we employed two markers: Recoverin (Rcvrn) and Rhodopsin. Among others, Rcvrn regulates phototransduction in rod and cone cells. Thus, it is a pan-PR marker, which is already present in PR progenitor cells. Additionally, a subpopulation of bipolar cells does also express Rcvrn. Rhodopsin, on the other hand, is a marker specific to rod PR.

Immunocytochemical stainings were conducted with dissociated D14 organoids cultivated for an additional 35 days on the pillar arrays. Figure 6.8 (A) shows a single-plane image of a z-stack taken from the pillar array. A quite clear and specific signal for Rcvrn$^+$ cells can be observed and a few single cells are also positive for Rhodopsin. Figure 6.8 (A') shows a zoom-in of Rcvrn$^+$ cells and two Rhodopsin$^+$ cells. The signals for Rcvrn and Rhodopsin are colocalized. As a comparison, both markers were also stained in D38 organoids. Rcvrn shows an apical staining in the supposed ONL. However, the signal is not as pronounced as in Figure 6.8 (A) and the strongest signal is directly on the surface of the organoid (see arrowheads), while it would be expected to be more within the constraints of the organoid itself. The D38 organoid shows a strong staining for Rhodopsin (Figure 6.8 C), with a number of cells in the supposed ONL stained positive. However, there is also a larger number of cells stained positive for Rhodopsin located in more central areas. Some Rhodopsin$^+$ cells located in the supposed GCL are highlighted with arrowheads in Figure 6.8 (C). Overall, cells stained positively for PR markers are present in both cultivation systems. In the pillar arrays, some of the Rcvrn$^+$ cells show neurite outgrowth, which might indicate rather a bipolar fate. However, the colocalization with Rhodopsin$^+$ cells clearly validates the presence of PR cells. While in organoids both markers could be detected, the localization of the stained cells does not necessarily match the expectations, indicating some irregularities in cell distribution and layer formation.

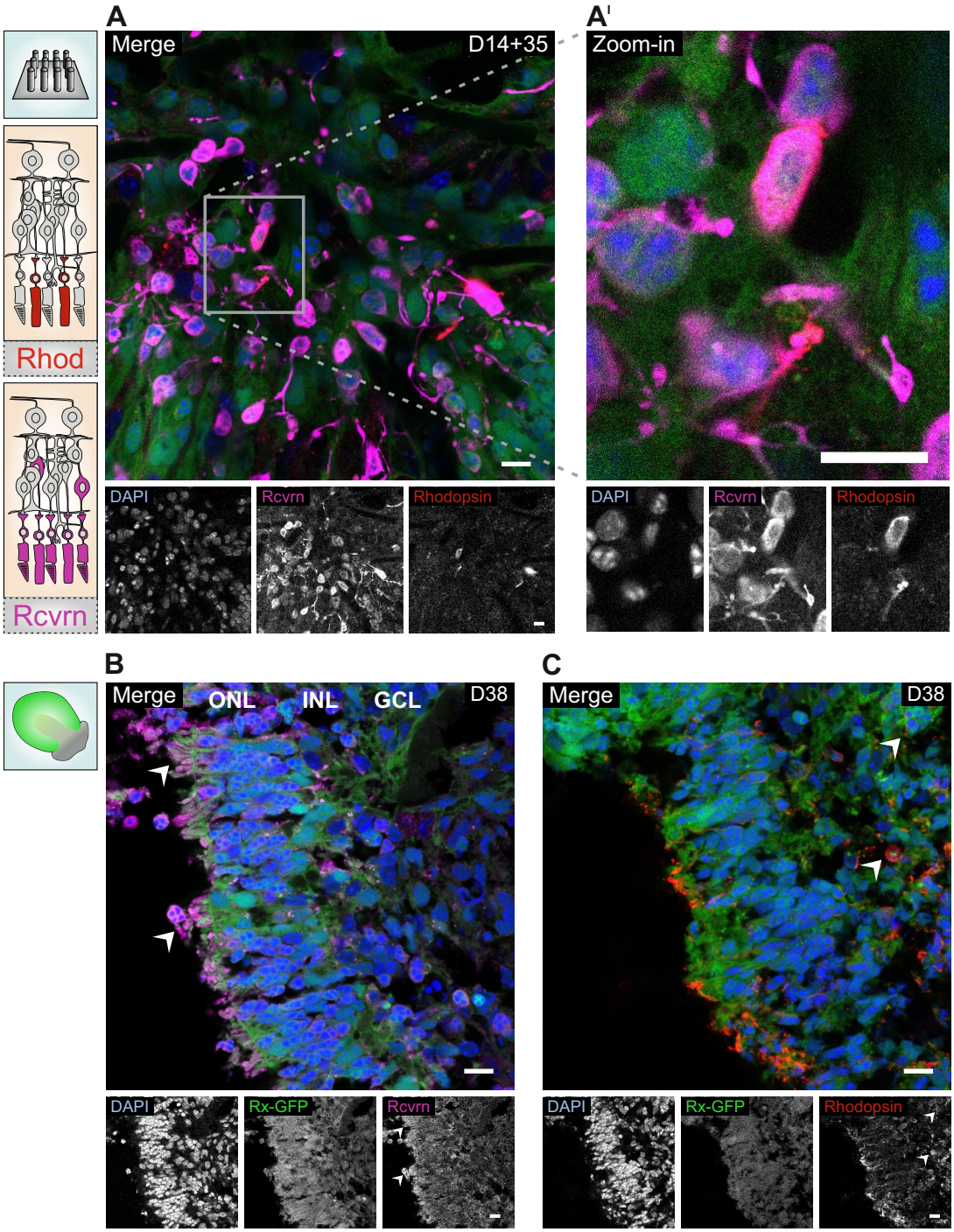
A
Merge
D14+35
A'
Zoom-in
Rhod
Rcvrn
DAPI
Rcvrn
Rhodopsin
DAPI
Rcvrn
Rhodopsin
B
Merge
ONL
INL
GCL
D38
C
Merge
D38
DAPI
Rx-GFP
Rcvrn
DAPI
Rx-GFP
Rhodopsin

Figure 6.8: **Differentiation of photoreceptors in retinal cultures.**
(A) Single-plane image of dissociated retinal organoids cultivated in pillar array for a total of 49 days. PR markers Rcvrn and Rhodopsin are stained. Single-channel and merged images are shown. (A') Zoom-in of Rcvrn$^+$ cells. Two of the cells are also positive for the rod marker Rhodopsin. D38 sectioned organoid stained for Rcvrn (B) and Rhodopsin (C). Rx-GFP depicted in green, DAPI blue, Rcvrn magenta and Rhodopsin red. Scale bars = 10 µm.

6.3.2 *Occurrence of Ganglion Cells and Synapse-like Structures in an in Vitro Cultivation System*

Ganglion cells (GC) are the cell type responsible for relaying visual information to the brain. In the retina, GCs form a separate layer, the ganglion cell layer. Their axons coalesce to form the optic nerve. During retinal differentiation, GCs are the first cell type to arise. However, culture conditions in organoids are not quite favoring GC maintenance, partially leading to their premature death. Islet1 is a transcriptional activator with a central role in gene regulation during RGC differentiation. Vsx2 is also a transcription factor involved in GC development, but also functions as a marker for bipolar cells in the mature retina. Synaptophysin (Syn) is a component of synaptic vesicles and functions as an indicator of synaptic structures.

For dissociated organoids cultivated for an additional 30 days in pillar arrays, *Islet1* expressing cells could readily be identified. Also, positive stainings for Syn could be obtained, but the spot-like signal is dispersed throughout the whole sample Figure 6.9 (A). In D38 organoids, most of the Islet1$^+$ cells were located in the central part of the organoid, in the supposed GCL. This was also true for the Syn staining, showing most prevalent staining in the supposed transition of INL and GCL, the inner plexiform layer (Figure 6.9 B). However, at the apical side of the organoid a larger cluster of cells was extruded from the organoids surface. This cluster of cells was also positive for Islet1 and Syn (Figure 6.9 (B), arrowheads), again underlining the morphological and organizational problems inherent to later-stage organoids. In D42 organoids, stainings for both Islet1 and Vsx2 were positive. Some of the stained cells were positive for both GC-markers and localized in the supposed GCL, clearly indicating the presence of GCs in these organoids. As Vsx2 is a marker linked to earlier stages of GC development, it seems likely that - given the prominent staining - most of the GCs are not yet fully matured.

6.3.3 Occurrence of Interneurons in an in Vitro Cultivation System

Interneurons are involved in relaying visual information gathered by PRs to the GCs. They have also functions in modulating and pre-processing the information. Interneurons are a collective term, which includes bipolar, amacrine and horizontal cells. Bipolar cells are involved in transmitting signals from PRs to ganglion cells. Amacrine cells have a coordinative and regulative function in the signals relayed from bipolar cells to ganglion cells. Lastly, horizontal cells regulate signals emerging from multiple rods and cones.

Most markers for interneurons are not specific to a certain cell type, but present in a number of cell types or sub-classes. We chose to use Calbindin, Calretinin, Pax6 and Otx2 as markers. Calbindin is a protein involved in buffering cytosolic calcium and is present in horizontal and amacrine cells. Calretinin is a calcium-binding protein which is present in some amacrine cell sub-types and ganglion cells. Pax6 is a prominent transcription factor involved in eye and central nervous system development. During retinal development, Pax6 plays a central role in progenitor cell development, but in later stages is restricted to the developing interneurons. Otx2 also has central roles in the early retinal development, where it is involved in the development of RPE, PRs and bipolar cells.

Figure 6.10 (A) shows dissociated retinal organoids cultivated for 35 days in a pillar array and subsequently stained for Calretinin and Calbindin. The cells stained positive for both markers show prominent neuronal extensions. In many cases, the signal for Calbindin and Calretinin colocalizes (Figure 6.10 (A'), see *), but there are also cases where only one of the markers is present (Figure 6.10 (A'), see **). For retinal organoids cultivated under standard conditions, Calbindin$^+$ cells can be identified. They mostly localize in the presumptive INL or GCL. However, Calretinin$^+$ cells could barely be detected.

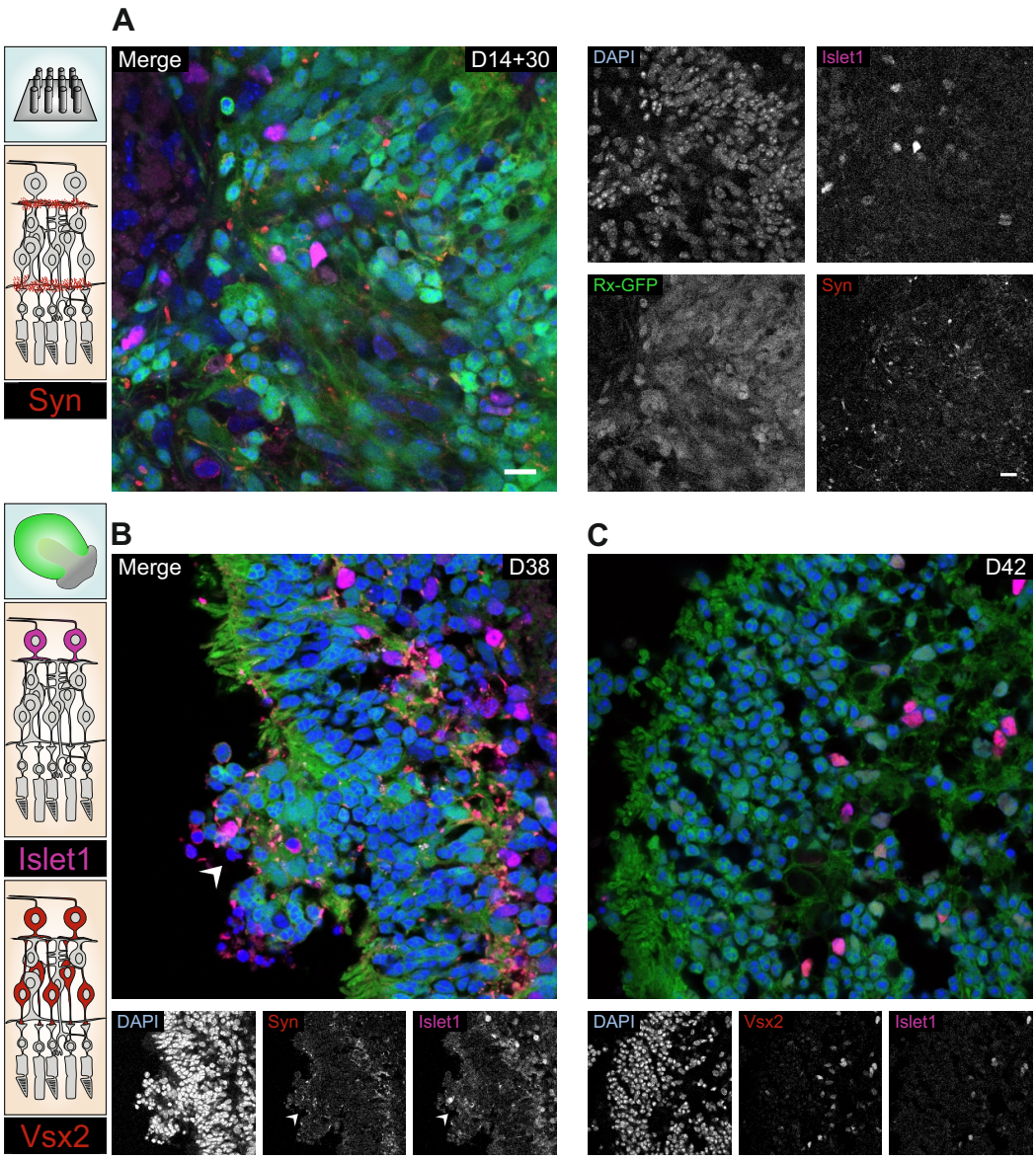

Figure 6.9: **Differentiation of ganglion cells and synapses in retinal cultures.** (A) Single-plane image of dissociated retinal organoids cultivated in a pillar array for a total of 44 days. GC marker Islet1 and synaptic vesicle marker Synaptophysin are stained. D38 sectioned organoid stained for Synaptophysin and Islet1 (B) as well as for Vsx2 and Islet 1 (C). Single-channel and merged images are shown. Rx-GFP depicted in green, DAPI blue, Islet1 magenta, Synaptophysin and Vsx2 red. Scale bar = 10 µm, applies to all images of corresponding size.

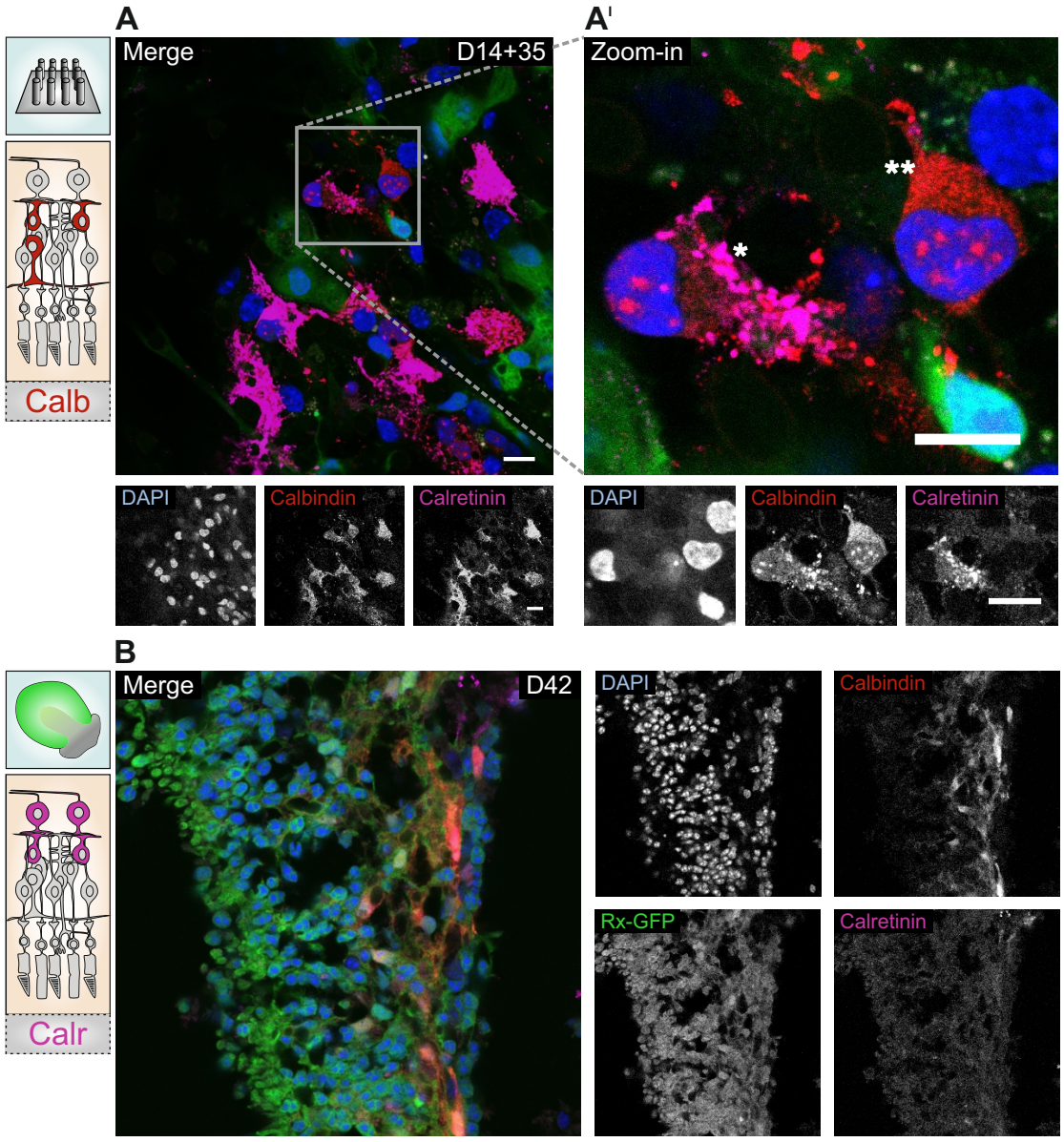

Figure 6.10: **Differentiation of interneurons in retinal cultures.**
(A) Single-plane image of dissociated retinal organoids cultivated in a pillar array for a total of 49 days. Interneuron cell markers Calbindin and Calretinin are stained. A' Zoom-in of a Calbindin$^+$ cell (**) and a cell positive for both markers (*). (B) D42 sectioned organoid stained for Calbindin and Calretinin. Single-channel and merged images are shown. Rx-GFP depicted in green, DAPI blue, Calretinin magenta and Calbindin red. Scale bar = 10 µm.

In figure 6.11, dissociated retinal organoids cultivated for 30 days in a pillar array and D42 organoids cultivated with the standard organoid protocol were processed for immunocytochemistry. Both markers are present in the dissociated

organoids, with most of the stained cells showing mutually exclusive stainings (Figure 6.11 A). The same was also the case for the D42 organoids, with $Pax6^+$ cells localizing to the border of supposed ONL and INL. Some $Pax6^+$ cells also localized in the GCL and ONL close to the apical border. Most $Otx2^+$ cells were present in the INL and showed a mutually exclusive staining towards $Pax6^+$ cells in most cases. Also, notice the organization of the D42 organoid. While there appears to be a semi-distinguishable layering, many cells are also localized beyond the border of the organoids apical side. This once more highlights the morphological changes occurring in later-stage organoids.

The combination of various markers identified via immunocytochemistry indicates the presence of all types of interneurons.

6.3.4 Occurrence of Müller Glial-like Cells in an in Vitro Cultivation System

Müller glial cells adopt important functions in maintaining homeostasis, supplying neurons with sufficient nutrients and clearing waste products. They are also partially involved in the visual cycle and function as a scaffold, yielding stability to the retina. With our pillar arrays we aimed at offering additional stability to the developing cells. However, all the other functions Müller glial cells carry out in the retina also need to be taken care of in the *in vitro* system. Thus, the presence of functional Müller glial cells is of utmost importance. Additionally, Müller glial cells are the last cell type to differentiate during retinal development. Obtaining Müller glial cells in an *in vitro* system might also indicate that the system robustly follows along the *in vivo*-like differentiation.

We chose to analyse two known markers for Müller glial cells, Sox9 and glial fibrillary acidic protein (GFAP). GFAP is a functional protein present in matured Müller glial cells, involved in forming filament-like structures. Sox9 is a transcription factor present in a subset of multipotent retinal progenitor cells, which is involved in Müller glial cell development. Figure 6.12 (A) shows dissociated retinal organoids cultivated for 35 days in a pillar array stained for GFAP. Filament-like structures can be identified throughout the whole section of the pillar array. This is also the case in D38 organoids, but to a smaller extend (Figure 6.12 C). In D50 organoids, a much more prominent signal for GFAP can be observed (Figure 6.12 E).

Also, Sox9 positive cells can be detected in dissociated organoids cultivated on a pillar array for 22 days (Figure 6.12 B). There are also some clearly $Sox9^+$ cells in D38 organoids (Figure 6.12 D) and D49 organoids (Figure 6.12 F). It should be noted that the localization of Müller glial-like cells would be expected to be in

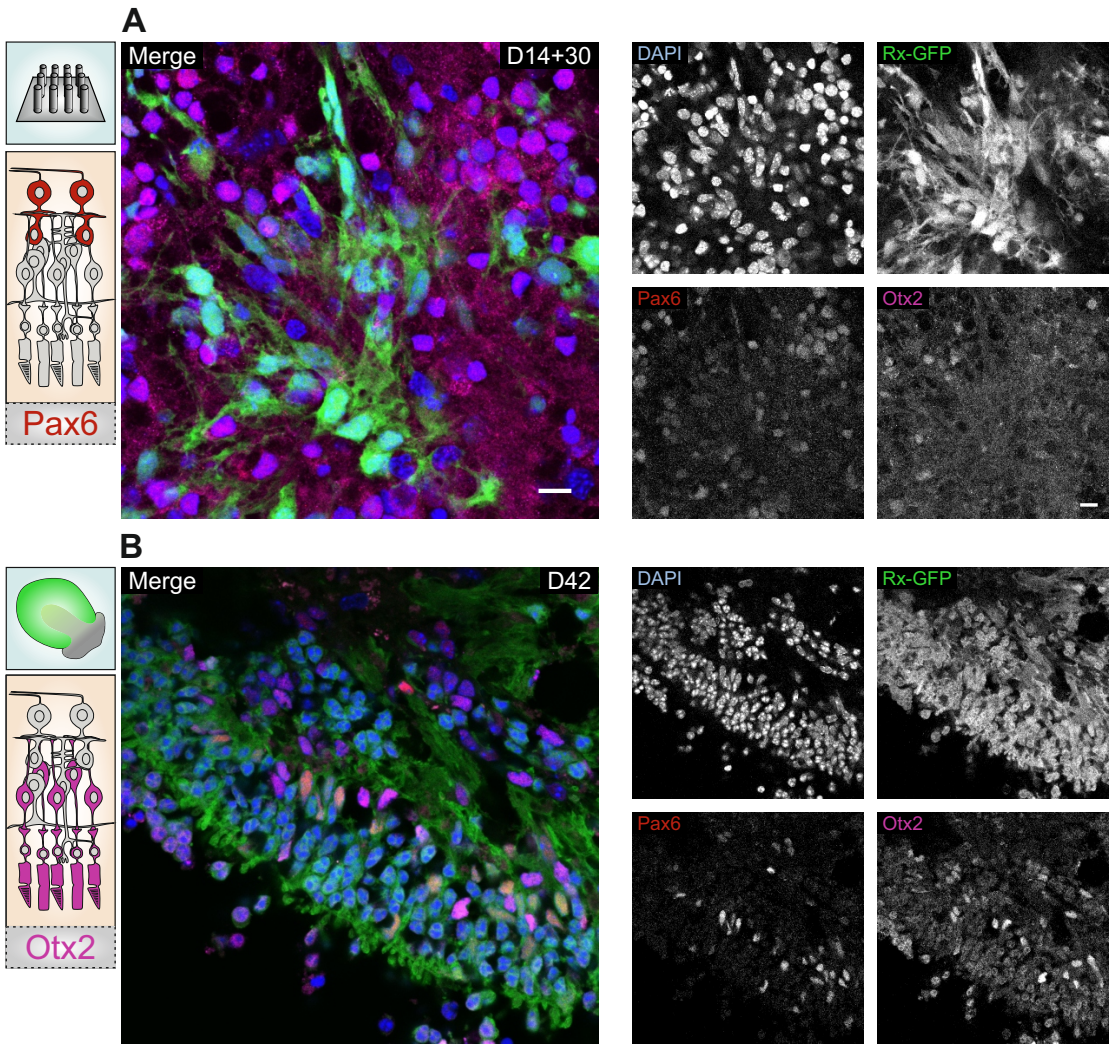

Figure 6.11: **Differentiation of interneurons in retinal cultures.**
(A) Single-plane image of dissociated retinal organoids cultivated in a pillar array for a total of 44 days. Interneuron cell marker Pax6 and bipolar and PR progenitor marker Otx2 are stained. (B) D42 sectioned organoid stained for Pax6 and Otx2. Single-channel and merged images are shown. Rx-GFP depicted in green, DAPI blue, Otx2 magenta and Pax6 red. Scale bar = 10 µm, applies to all images.

the INL, but in the stained organoids most $Sox9^+$ cells are located in the ONL. The combination of both markers, however, hints towards the presence of Müller glial-like cells in both *in vitro* cultivation systems.

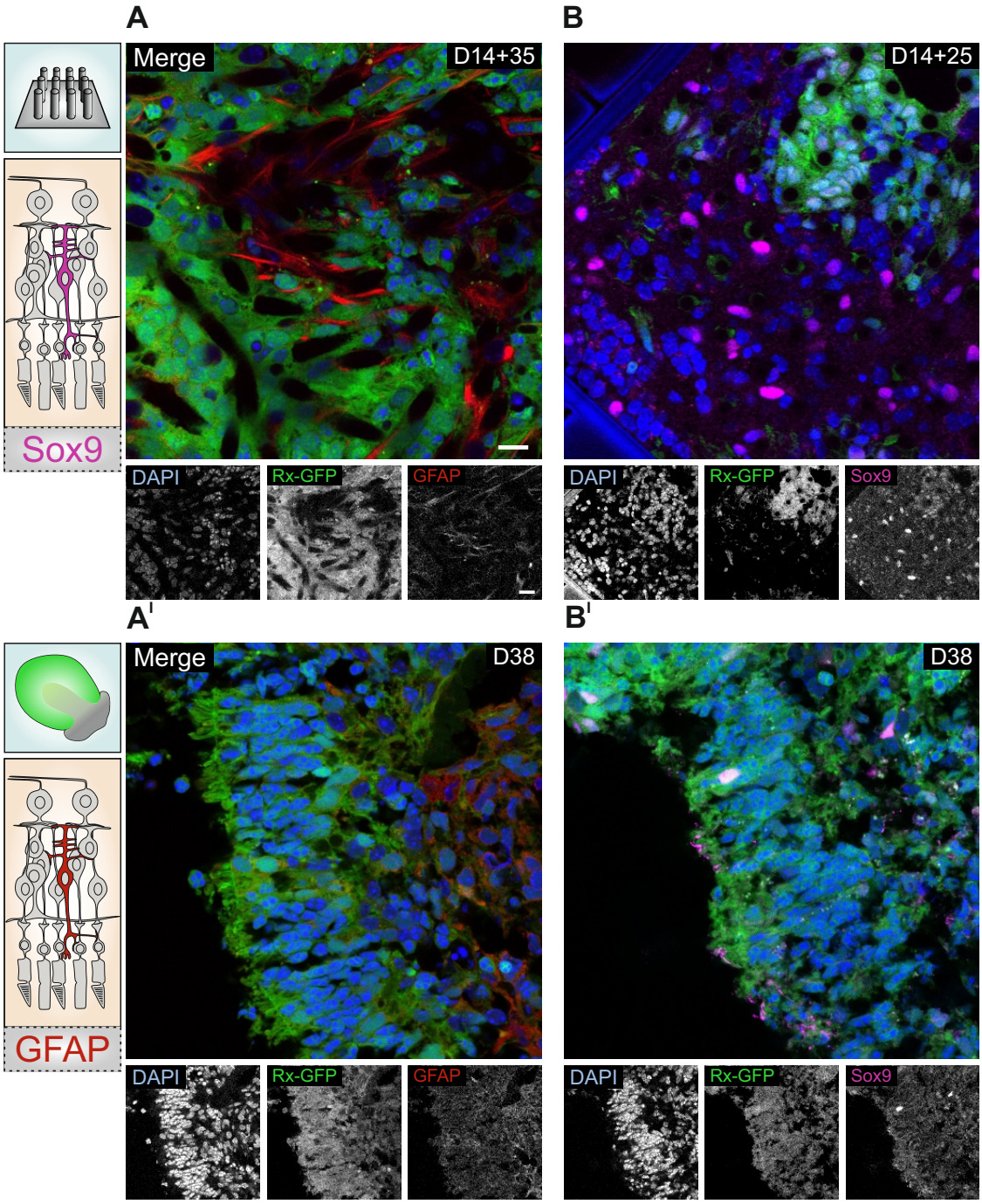

Figure 6.12: **Differentiation of Müller glial-like cells in retinal cultures.**
(A, B) Single-plane image of dissociated retinal organoids cultivated in a pillar array for a total of 49 days. Müller glial cell marker GFAP (A) and Sox9 (B) are stained. D38 sectioned organoid stained for GFAP (C) and Sox9 (D). (E) D50 sectioned organoid stained for GFAP and (F) D49 sectioned organoid stained for Sox9. Single-channel and merged images are shown. Rx-GFP depicted in green, DAPI blue, Sox9 magenta and GFAP red. Scale bar = 10 µm, applies to all images.

6.4 Organization of Retinal Cells in Pillar Arrays

Cells show a high degree of specialization. For example, PRs are specialized to detect and process visual stimuli. In turn, they out-sourced many of the metabolic and regenerative duties to the RPE and Müller glial cells. Thus, as interactions of certain cell types are required for maintaining the tissues functionality, they are also in most cases located in close proximity. In many neuronal tissues, this leads to a strictly layered organization, with each layer adopting different functions. This is also the case in the retina, where a clear layering from the apical side with the RPE to the central side with the GCL can be observed.

In retinal organoids, this layering is also largely present, leading to the presence of three semi-distinguishable layers, the ONL, INL and GCL. As retinal organoids show morphological deterioration with extended cultivation time, the organized layering is also lost during cultivation. As the dissociated organoids cultivated in pillar arrays can be maintained for a longer time without apparent morphological downsides, we also wanted to see if there is a certain level of self-organization or layering in the pillar arrays. To this end, we analysed z-stacks of cells cultivated in pillar arrays and checked for preferential localization of certain markers in some areas of the pillar arrays.

6.4.1 Similarly Distributed Markers in Pillar Arrays

When analyzing retinal cell cultures in DLW pillar arrays, not all markers show an organized or preferential distribution. Yet, the examples presented in this section do also show some level of colocalization, which renders these markers interdependent to some extend. The first example is a pillar array cultivated for 22 days and then fixed and stained for Calbindin and Calretinin. As can be appreciated in Figure 6.13 (A), Calretinin$^+$ and Calbindin$^+$ cells largely colocalize in the bottom-plane images, with the exception of a few cells only positive for Calretinin in the upper part of the image. The same trend continues for the center- and top-section images, where both signals largely colocalize, with the exception of some Calretinin$^+$ sections. The 3D reconstruction verifies the general impression of the single-plane images: in many cases, Calretinin and Calbindin are colocalized. Thus, as Calbindin$^+$ and Calretinin$^+$ cells are often colocalized and otherwise in close proximity and additionally distributed throughout the whole z-stack in z-direction, there is no clear organization or layering observable.

Furthermore, the localization and distribution of retinal cells cultivated in pillar arrays and stained for Islet1 and Vsx2 were assessed (Figure 6.13 B). The amount of Vsx2$^+$ cells was greater than of Islet1$^+$ cells. This holds true for the exemplary image from the bottom, center and top of the pillar array. In many cases, the Islet1$^+$ cells were also positive for Vsx2, while many Vsx2$^+$ cells were only stained

for this marker. The 3D reconstruction also verifies the impression from the single-plane images, as Vsx2^{+} cells are more prevalent and both cell types appear to be equally distributed throughout the sample. However, co-localization of both markers can not be well discerned in the 3D reconstruction.

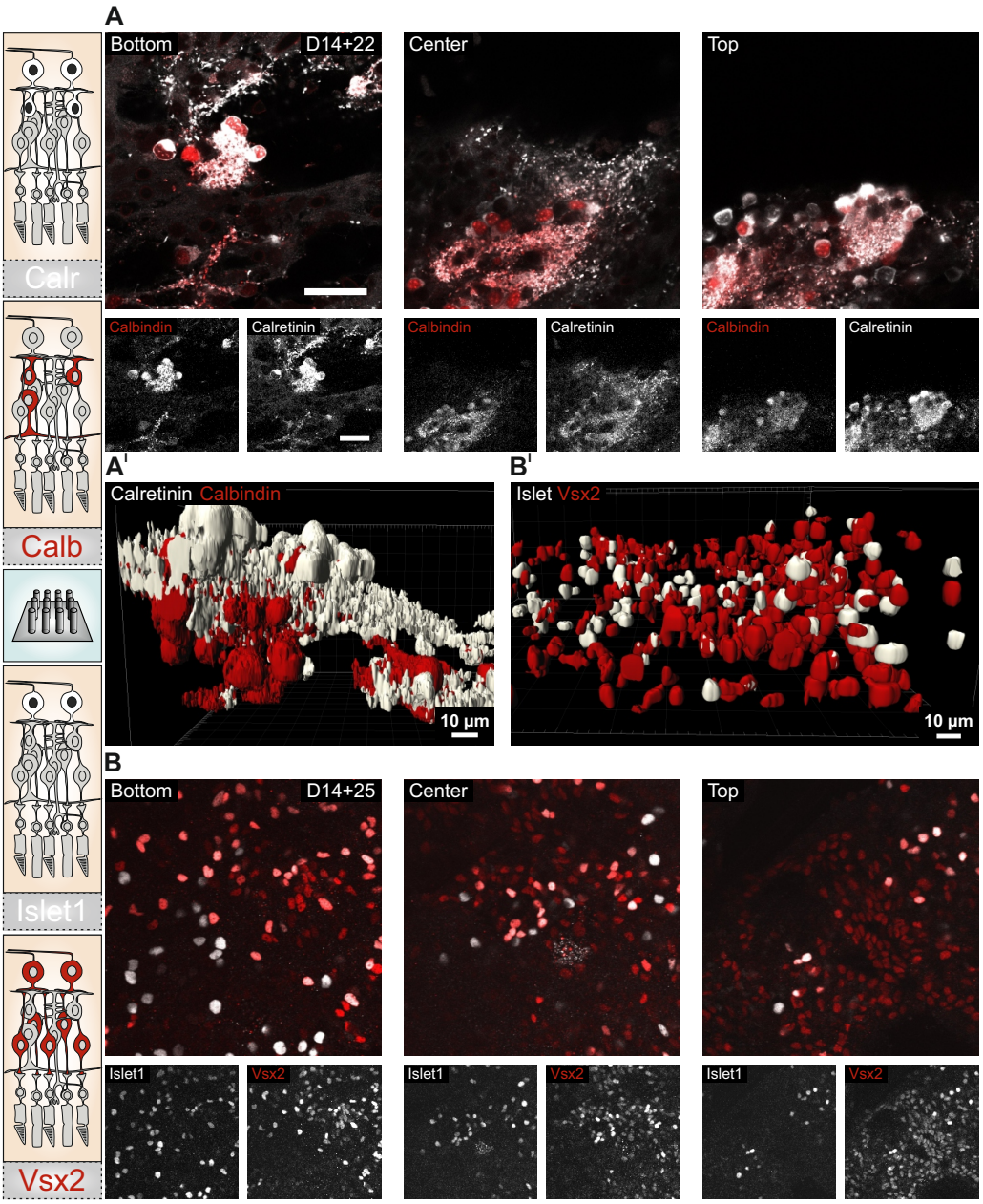

Figure 6.13: **Organization of retinal cells in pillar arrays.**
(A) Representative single-plane images of dissociated retinal organoids seeded in pillar arrays and cultivated for a total of 36 days. Images were taken at the bottom, center and top of the cultured cells relative to the glass slide. (A') Three-dimensional reconstruction of the z-stack used in (A). Interneuron marker Calbindin and Calretinin are stained. (B) Representative single-plane images of dissociated retinal organoids seeded in pillar arrays and cultivated for a total of 36 days. Images were taken at the bottom, center and top of the cultured cells relative to the glass slide. (B') Three-dimensional reconstruction of the z-stack used for (B). GC marker Islet1 and GC and interneuron marker Vsx2 are stained. Single-channel and merged images are shown. Calretinin and Islet1 depicted in white, Calbindin and Vsx2 in red. Scale bar = 50 µm, corresponds to all images in A and B, scale bar in A' and B' specified in corresponding images.

6.4.2 Basic Self-organization of Retinal Cells in Pillar Arrays

We could identify a number of substrates and marker combinations, which indicated some level of self-organization or layering. Some of these examples are shown in Figure 6.14. Single-plane images of retinal cells cultivated for 25 days in a pillar array at different levels in *z*-axis are depicted in Figure 6.14 (A). When comparing the bottom and top layers in the pillar array cultivation system, it can be observed that the bottom plane is enriched in Otx2 positive cells when compared to the upper plane. In contrast Pax6 positive cells are enriched in the upper plane compared to the lower plane. Thus, establishing an opposing gradient with a balanced occurrence of Otx2 and Pax6 positive cells in the middle plane.

This effect is clearly illustrated in the 3D reconstruction which was generated to get a better understanding of the distribution of the various cell types in *z*-axis (Figure 6.14 A'). Most of the $Pax6^+$ cells are rather localized at the bottom or center, with some exceptions also at the top. In the case of $Otx2^+$ cells, most show a localization to the center or top-part of the pillar array, as the single-plane images suggested.

The same trend was also observed in a pillar array cultivated for 25 days and stained for Sox9 and Rcvrn (Figure 6.14 B). On the pillar arrays bottom planes, a large amount of cells was stained positive for Sox9, while a few $Rcvrn^+$ cells were also present. Towards the center, the amount of $Sox9^+$ cells remained on a similar level, while the number of $Rcvrn^+$ cells heavily increased. At the top layers, almost no cells were positive for Sox9, but still many cells were positive for Rvcrn. The 3D reconstruction of this z-stack clearly shows a preferential distribution of $Sox9^+$ cells towards the bottom and center of the pillar array, while $Rcvrn^+$ cells are preferentially in the center or at the top of the pillar array (Figure 6.14 B').

These examples clearly indicate that there is a potential for retinal progenitor-like cells and their progeny to arrange and self-organize in the pillar arrays. How robust and reliable this self-organization is, remains to be established.

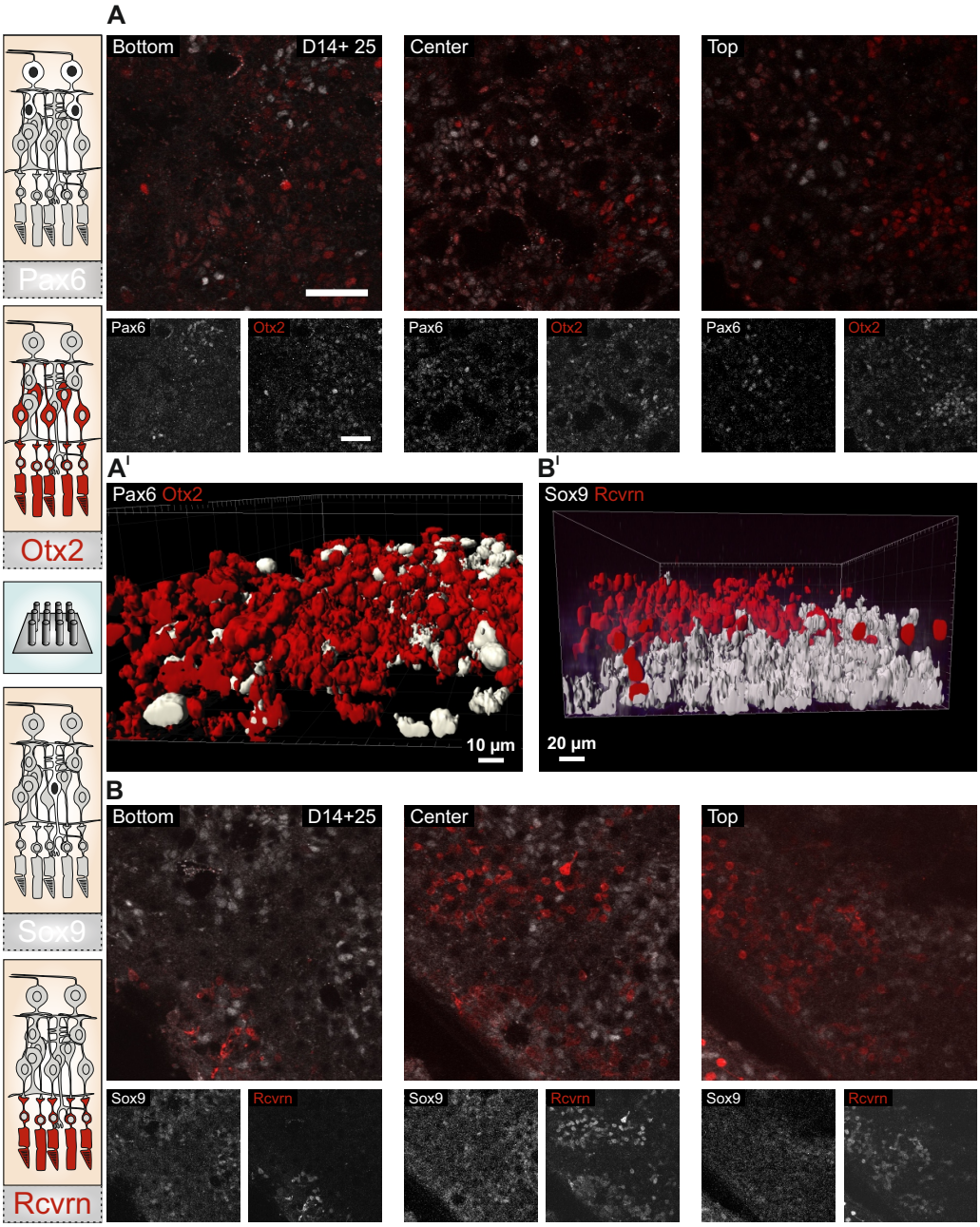

Figure 6.14: **Preferential localization of retinal cells in pillar arrays.**
(A) Representative single-plane images of dissociated retinal organoids seeded in pillar arrays and cultivated for a total of 39 days. Images were taken at the bottom, center and top of the cultured cells relative to the glass slide. (A') Three-dimensional reconstruction of the z-stack used in (A). Interneuron marker Pax6 and GC and PR marker Otx2 are stained. (B) Representative single-plane images of dissociated retinal organoids seeded in pillar arrays and cultivated for a total of 39 days. Images were taken at the bottom, center and top of the cultured cells relative to the glass slide. (B') Three-dimensional reconstruction of the z-stack used for (B). Müller glial cell marker Sox9 and pan-PR marker Rcvrn are stained. Single-channel and merged images are shown. Pax6 and Sox9 depicted in white, Otx2 and Rcvrn in red. Scale bar = 50 µm, corresponds to all images in A and B, scale bar in A' and B' specified in corresponding images.

6.5 Differentiation of mESCs to Retinal Pigment Epithelium

Organoids are a promising system for larger-scale generation of retinal tissue *in vitro*. However, they have some inherent downsides, among them the fact that they mostly comprise neural retina cells. This also means that most organoid approaches lack the supportive RPE layer. While at first glance this system seems sufficient to study neural retina development and function, the RPE massively influences and contributes towards the differentiation and maintenance of specifically PRs, but also to the neural retina in general. It would be highly desirable to combine both, the RPE and neural retina in one culture system.

The differentiation of RPE cells from mESCs and their characterization were conducted in a master thesis by Kai Richler within the scope of this dissertation (Richler 2019). While for human stem cells numerous protocols for differentiation of RPE cells are available, there was only one protocol available for murine stem cells. Thus, we chose to test this protocol. An overview of the protocol is given in Figure 6.15 (A). By starting from retinal organoids, cells with retinal fate were obtained. Instead of further cultivation in a free-floating system, the organoids were broken down into smaller pieces, which were replated on LN-coated plates and cultivated in the presence of the glycogen synthase kinase 3 (GSK3) inhibitor CHIR99021 and the fibroblast and vascular endothelial growth factor receptor inhibitor SU5402, which are both involved in the RPE fate decision. After four days of cultivation, the fate-shifted RPE progenitor cells are purified and replated.

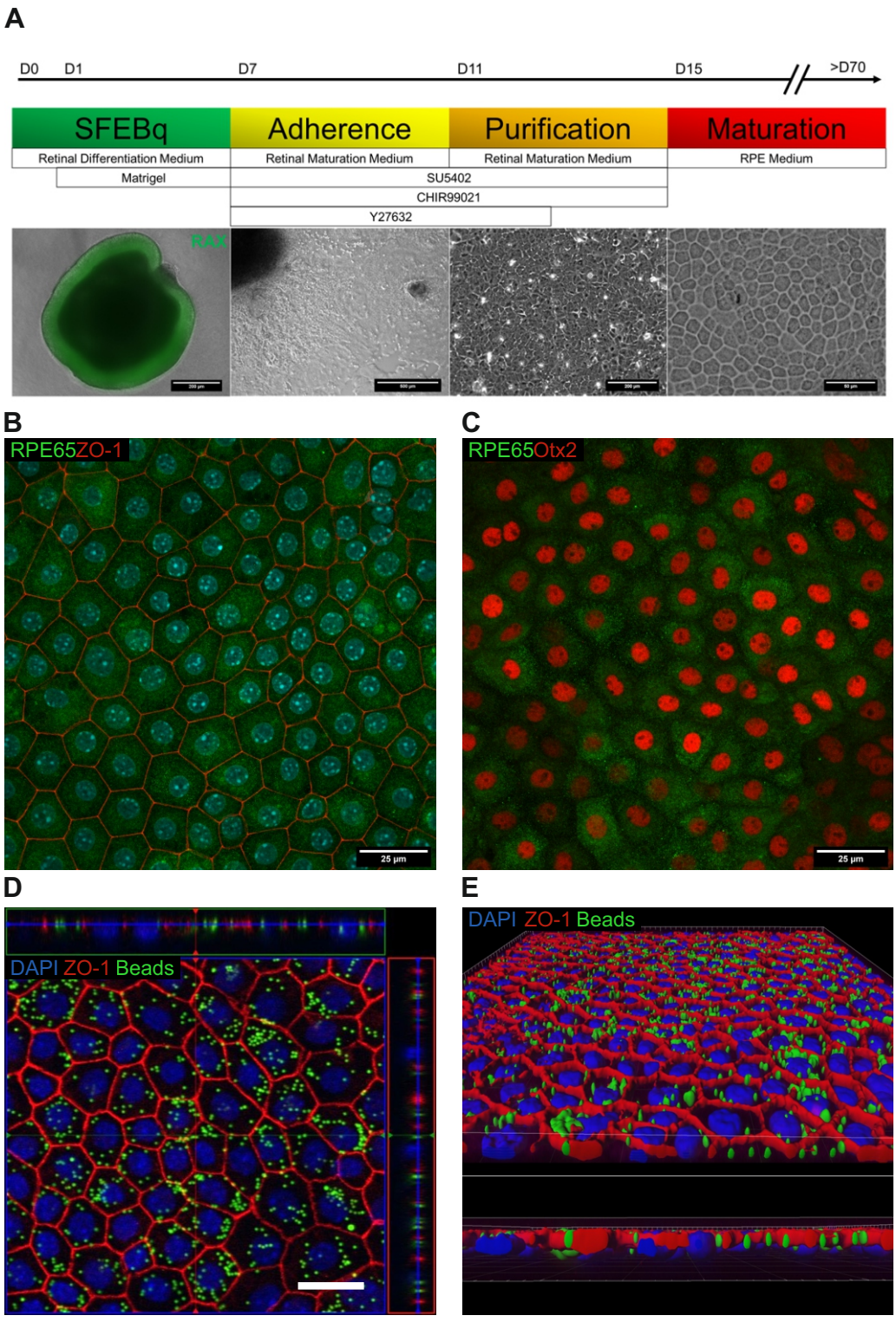
A
D0
D1
D7
D11
D15
>D70
SFEBq
Adherence
Purification
Maturation
Retinal Differentiation Medium
Retinal Maturation Medium
Retinal Maturation Medium
RPE Medium
Matrigel
SU5402
CHIR99021
Y27632
RAX
B
RPE65ZO-1
25 µm
C
RPE65Otx2
25 µm
D
DAPI ZO-1 Beads
E
DAPI ZO-1 Beads

Figure 6.15: **Differentiation of retinal pigment epithelium.**
(A) Overview of the protocol employed to differentiate stem cells into RPE cells. A timeline is given with the corresponding experimental steps. Used media and factors added to the medium are also listed. Additionally, representative images of every major step are presented. Scale bars from left to right: 200 µm, 500 µm, 200 µm, 50 µm (B) Image of fully matured RPE cells stained for retinoid isomerohydrolase RPE65 and tight junction protein ZO-1. (C) Mature RPE stained for RPE65 and the transcription factor Otx2, centrally involved in the differentiation of RPE cells. (D) RPE cells were incubated with fluorescently labeled beads. Internalization of beads shows functionality of RPE cells. Scale bar = 20 µm. (E) Three-dimensional reconstruction of z-stack shown in (D). Experimental execution and image acquisition by Kai Richler

After continued cultivation, the cells adopted the honeycombed morphology characteristic to RPE cells. As additional verification to the general morphology, immunocytochemical stainings were conducted. They showed the presence of the matured RPE marker retinoid isomerohydolase RPE65 and the tight junction marker ZO-1 (Figure 6.15 B), as well as the transcription factor Otx2, which plays a central regulatory role in the fate decision between RPE and neural retina (Figure 6.15 C).

In order to not only show the character of the differentiated cells, but also show some functionality, an internalization assay was conducted. One central role of RPE is the internalization of spend rod outer segments. Fluorescently labeled latex beads were used as a replacement for outer segments. After incubation of RPE cells with fluorescently labeled beads, internalization of beads was clearly visible (Figure 6.15 D). Orthogonal views (Figure 6.15 D) and 3D reconstructions (Figure 6.15 E) of the RPE layer show that the beads were actually internalized and are within the borders of the cells, as they are below the ZO-1 signal. Thus, the generated RPE cells show on the one hand presence of key markers and on the other hand functional maturity.

Chapter 7
7 Discussion

In the previous chapter, I presented the data obtained within the scope of this thesis. The new cultivation system of retinal organoids was established and the induction efficiency improved via the addition of a retinoic acid receptor antagonist. The previously established method of DLW was employed to generate a new design for 3D substrates. Retinal cells obtained from organoids were combined with these 3D substrates, indicating no adverse effect on the viability of the cells, instead allowing an extended cultivation within these substrates for up to 50 days. Furthermore, all major retinal cell types are present in the combined *in vitro* cultivation system. These retinal cells even show a preferential localization within the substrates in some cases. A separate protocol was realized to generate RPE, which is usually lacking in the organoid protocol.

These results will be put into perspective with regards to the literature. The organoid system will be discussed in general, showing its' up- and downsides also in regards to long-term cultivation. The impact of the 3D substrates on the cultivated retinal cells will also be addressed, with a special focus on the organization of the cells within axial and lateral direction. General patterning mechanisms will be discussed, which might also be applicable and directly inducible in the 3D substrates. Lastly, the role of the RPE and potential combinations with neural retinal tissue will be discussed.

7.1 Differentiation of Retinal Organoids

The differentiation of retinal organoids seems quite straightforward: seeding of pluripotent stem cells, formation of embryoid body-like aggregates, addition of ECM, usually in the form of Matrigel and then the differentiation will happen autonomously (Eiraku and Sasai 2011; Eiraku et. al 2011). However, the described protocols are unexpectedly challenging to establish. Some of the challenges led to low levels of retinal induction, which could be traced back to components of the media as well as sub-par Matrigel lots (data not shown). Mototsugu Eiraku and colleagues hint towards the concentration and efficiency variability in commercial

Matrigel products, suggesting to use Matrigel lots with a protein concentration of 9.5 mg/ml and above (Eiraku and Sasai 2011). Even though this suggestion was carefully followed, drastic differences in induction efficiency were observed, which could not be rectified by changes in cell number or media composition (data not shown).

Hence, we screened literature on murine retinal organoids for alterations to the Eiraku-protocol. Work by the group of Masayo Takahashi offered a promising option for improving retinal induction, the retinoic acid receptor (RAR) antagonist AGN193109 (Assawachananont et. al 2014; Iwasaki et. al 2016; Johnson et. al 1999). RA signaling plays a crucial role during development of various neural structures like the hindbrain, where it is implicated in regulating the expression of anterior-posterior and DV patterning genes like the hox genes (Gale et. al 1996; Grapin-Botton et. al 1995). Signaling is achieved via the RAR α, β and γ, which are expressed in overlapping regions and show high levels of functional redundancy (Duester 2009; Glover et. al 2006; Ruberte et. al 1991, 1990). Upon ligand binding, RARs form heterodimers with the rexinoid receptors (RXR) (Chambon 1996; Mangelsdorf and R. M. Evans 1995). In our hands, supplying the culture media with the RAR-antagonist AGN193109 in early retinal organoid differentiation enhanced the level of retinal induction, while also increasing the number of available vesicles (see chapter 6.1). This matches the results obtained by Juthaporn Assawachananont and colleagues (Assawachananont et. al 2014).

RA signaling is also important in the retina. Initially, similar functions in patterning were also assumed for the eye. However, it was shown that the function in patterning is not prevalent in the retina. Instead, RA is involved in regulating and guiding morphogenetic cellular movements during the OC stages (Fan et. al 2003; Molotkov et. al 2006). In later stages of retinal development, RA is also involved in the expression of DV topographic guidance molecules (Sen et. al 2005).

In addition to its function in early retinal development, RA is also involved in later stages of development. It was shown that RA signaling influences the fate decision of uncommitted progenitor cells, shifting the progeny from amacrine to PR fate (Kelley et. al 1994). Thus, for the differentiation of retinal organoids, RA is also supplemented at day 10, a stage when mostly retinal progenitor cells are present (Eiraku et. al 2011).

Based on the different actions of RA depending on the various tissues, inhibition of RA signaling in early steps of the organoid protocol seems to be a reasonable adaptation. This is also demonstrated in our experiments, as with the addition of AGN193109 neural outgrowth is reduced and retinal induction is enhanced (see chapter 6.1).

The variability of the organoids protocol was also demonstrated in publications of other groups (Cowan et. al 2020; Hiler et. al 2015; Mellough et. al 2019; Völkner et. al 2016). Daniel Hiler and colleagues demonstrated that depending on the

pluripotent cell line the outcomes of the differentiation protocol heavily varies. Compared to established cell lines like the EB5 Rx-GFP line, iPSCs generated from rod PRs showed a higher level of retinal induction and OC-like structure formation (Aldiri et. al 2017; Hiler et. al 2015). However, no examples of the OC-like structures are given. Carla Mellough and colleagues examined the production of retinal organoids derived from human pluripotent stem cells. They identified differences in retinal differentiation depending on the method employed and mode of culture maintenance as well as differences in induction level depending on various cell lines used (Mellough et. al 2019). Interestingly, they report maintenance under stationary culture conditions to be the most efficient approach for generating laminated retinal organoids. However, they examined organoids until week five, but when aggregates grow larger in size in later stages of the protocol, the beneficial effect of shaking resulting in higher supply with nutrients and oxygen might be required (DiStefano et. al 2018; Ovando-Roche et. al 2018). Similar results were also obtained by Cameron Cowan and colleagues, identifying different levels of induction efficiency depending on the human pluripotent stem cell line used. Most interestingly, not only differentiation efficiency varied, but also the degree of lamination (Cowan et. al 2020).

The variability in retinal organoid induction and differentiation also becomes apparent in the work of Manuela Völkner and colleagues. Using hPax6-GFP mESCs, they also derived retinal organoids using the Eiraku-protocol. Lacking widespread retinal induction and in many cases clear vesicle formation, they non-selectively dissected retinal organoids on day 10 by cutting the aggregate into three equally sized pieces, which they named the trisection protocol (Völkner et. al 2016). Further cultivation led to the formation of stratified retinal organoids in quite high quantity. They did not observe any invagination events of the OVs to form OC-like structures as demonstrated by Mototsugu Eiraku (Eiraku et. al 2011). This event was only observed in retinal organoids not subject to a dissection step on day 10, but these organoids showed incomplete stratification and an inverse polarity (Völkner et. al 2016). However, the lack of complete retinal induction of stem cell aggregates as well as the low amount of vesicle formation clearly demonstrates the sensitivity of the system and the challenges of reproducing the retinal differentiation reliably.

One critical factor for the protocol's success is the quality of the Matrigel lot used. Matrigel is a complex mixture of ECM, composed of hundreds of different proteins and peptides (Hughes et. al 2010; Talbot and Caperna 2015). Although Matrigel provides ECM molecules, growth factors and biophysical stimulation via the stiff matrix, its use for retinal differentiation of organoids underlies limitations (Hughes et. al 2010; Soofi et. al 2009; Talbot and Caperna 2015). These limitations restult from varying composition and changes in concentration. It was reportet that these limitations of Matrigel result in low reproducibility of experiments (Vukicevic et. al 1992).

To circumvent the limitations of Matrigel, various synthetic alternatives have been explored. Such synthetic alternatives were tested in intestinal organoid differentiation, indicating robust and highly reproducible generation of organoids in a maleimide-terminated poly(ethylene glycol)macromer-based gel (Cruz-Acuña et. al 2017). In a different approach, a non-synthetic hydrogel based on ECM derived from decellularized intestinal tissues also supported the growth of endoderm-derived organoids (Giobbe et. al 2019). Cerebral organoids were also induced and cultured in hydrogels based on sodium hyaluronan and chitosan, or in hydrogels based on gelatin methacrylate (Lindborg et. al 2016; Tomaskovic-Crook and Crook 2019). The resulting organoids successfully generated neural rosette and neural tube-like structures as well as responses towards glutamate and depolarization in many cells, indicating basic neural behavior.

In a different study, the vitronectin-mimicking oligopeptide Synthemax was used for retinal induction (Perepelkina et. al 2019). The authors were able to also induce Rx-GFP mESCs to retinal fate with the synthetic product. But the aggregates under Synthemax and Matrigel conditions did not show a pronounced bright neuroepithelium at the rim, vesicular structures were largely missing and GFP expression was disperse throughout the aggregate. While these examples indicate that viable options for replacing Matrigel based on synthetic substrates are available, more work is still required in order to also have a robust and reliable system for retinal induction in mESCs.

While organoids are a powerful *in vitro* method, they still lack reproducibility and lead to quite heterogeneous results. More robust induction methods not relying on inconsistent animal products would be required to make organoids a widespread and comparable method.

7.2 Long-term Cultivation of Retinal Organoids

Mototsugu Eiraku and colleagues established and convincingly showed that a long-term cultivation of retinal organoids is possible, obtaining well-stratified tissue after 24 days of cultivation (Eiraku et. al 2011). Later publications demonstrated an increased cultivation time to the early/mid-30 day range (Brooks et. al 2019; H. Y. Chen et. al 2016; Ueda et. al 2018). This increase in cultivation time was mainly linked to a change in cultivation medium, shifting from the regularly used DMEM/F12 based medium supplemented with N2 and 10% FBS to supplementation with N2 and 1% FBS. Kaori Ueda and colleagues attributed the increased cultivation time to the lower levels of FBS and the accompanying reduction of proliferation in undifferentiated retinal neurons. However, they also mention that even under these conditions, the retinal morphology was only maintained up

until day 27 (Ueda et. al 2018). To this date, protocols for differentiating murine pluripotent stem cells to retinal organoids while also maintaining the morphology at later stages are missing.

Interestingly, human-derived retinal organoids are much more robust in regards to long-term cultivation. Cultivation times of 200 days, even exceeding 300 days have been reported (K. C. Eldred et. al 2018; Gonzalez-Cordero et. al 2017; Kaya et. al 2019; S. Kim et. al 2019; Lukovic et. al 2020; Nakano et. al 2012; Quadrato et. al 2017; Reichman et. al 2017; Zhong et. al 2014). In addition to the extended cultivation time, human retinal organoids also maintain their structure throughout cultivation, leading to well-stratified tissues (Cowan et. al 2020; Zhong et. al 2014). Human retinal organoids also showed responsiveness to light stimuli, indicating not only morphological maturity, but also partial functionality (Cowan et. al 2020; Quadrato et. al 2017).

A number of sequencing studies tried to shed more light on the exact cellular composition and differentiation speed in organoids compared to *in vivo* retinae (Collin et. al 2019; Cowan et. al 2020; S. Kim et. al 2019; Mao et. al 2019; Quadrato et. al 2017; Sridhar et. al 2020). They could identify similar differentiation time lines in organoids, but with extended cultivation the differentiation speed in organoids slightly dropped off. Fully matured murine organoids correspond to P6-P10 retinae (Brooks et. al 2019). The same was true for human organoids, where week 24 organoids showed quite high correlation to week 20 retinae (Cowan et. al 2020). Analysis of cellular composition showed a higher ratio of RPCs in early human organoids, while early human retinae showed a higher amount of GCs. At later stages of development, cellular composition of human retinal organoids and fetal retinae were quite similar (Sridhar et. al 2020). Overall, matured human retinal organoids were more similar to peripheral retina samples than to foveal ones (Cowan et. al 2020).

But what is the difference in murine and human systems? Why do seemingly similar methods lead to different outcomes in the long run, with the only significant difference being the cell source? Given that both sources are pluripotent stem cells, the differences should be minimal. Zekai Cui and colleagues addressed these questions in a recent publication (Z. Cui et. al 2020). Using bioinformatic transcriptome analysis of published RNA sequencing data (Brooks et. al 2019; K. C. Eldred et. al 2018; Hoshino et. al 2017), they could identify close similarities throughout development of retinal organoids and retinae. Additionally, the developmental timeline of various cell types in organoids and retinae was quite similar, confirming results of other studies (Cowan et. al 2020; Sridhar et. al 2020).

Analysis of differentially regulated genes in human and murine organoids revealed that for both systems genes involved in cell division were downregulated, while genes involved in neurogenesis and PR development were upregulated. For genes with opposite regulation patterns, human organoids showed upregulation in glutathione metabolic processes, fatty acid metabolic processes, hydrogen per-

oxide metabolic processes, mitochondrial matrix and exosomal secretion. Genes upregulated in murine organoids are involved in glycogen catabolic processes, histone deubiquitination, Wnt signaling pathway, response to TGF-β and Ras protein signaling transduction. Thus, the main difference between murine and human organoids appears to be energy metabolism revolving around mitochondria. A more focused look at mitochondria development in retinal organoids and retinae revealed that in developing murine and human retinae, expression of mitochondrial components peaks twice: once during early differentiation and a second peak at later stages (P0-P14 in mouse, D111-D250 in human). However, in retinal organoids, the first peak of expression was present in both systems, whereas, the second peak of mitochondrial component expression was only present in human organoids. The authors also attribute mitochondria an important role in retinal development, as retinal mitochondrial development time showed high correlation with PR development (Z. Cui et. al 2020).

The cellular composition of the retina might also favour differences in retinal organoids between human and murine systems. As nocturnal animals, murine retinae are dominated by rods (ratio rods:cones approximately 30:1), while humans are diurnal animals, showing a lower prevalence in rods with only 18:1 to 20:1 rods to cones (Cangiano et. al 2012; Mustafi et. al 2009). Cones are implicated with a higher density of mitochondria, estimated ca. 26.4 times higher than in rods (Z. Cui et. al 2020). The naturally cone-rich human retina might be favoured in this regard. Published protocols for human organoids also aimed at increasing the number of cones (S. Kim et. al 2019; Zerti et. al 2020). This was achieved by the addition of γ-secretase inhibitor DAPT ((2S)-N-[(3,5-Difluorophenyl)acetyl]-L-alanyl-2-phenyl]glycine 1,1-dimethylethyl ester), a potent inhibitor of Notch signaling. In murine organoids, the function of DAPT was also tested, leading to a shift of retinal progenitor cells towards cone fate at the loss of other cell types (Kaufman et. al 2019; Völkner et. al 2016). However, DAPT-treatment can also result in the loss of laminar organization (Kruczek et. al 2017). It would be interesting to see if these organoids show different expression patterns of mitochondria related genes and if increased cultivation times would be possible.

In our cultivation system largely following the Eiraku-protocol, morphology is maintained until approximately day 25. However, even if an organized morphology is lost, the amount of dead cells is only moderate, often restricted to GFP^- areas (see chapter 6.1). Given that developmental speed declines in retinal organoids with prolonged cultivation, potentially the maintenance of structure and tissue integrity is also an important stimulus for further development (Brooks et. al 2019; Cowan et. al 2020; Z. Cui et. al 2020). One way of potentially addressing this issue is by offering a defined 3D substrate for retinal progenitor cells, leading to the formation of a tissue showing some level of organization and improved access to nutrients and oxygen. The implementation of such a system will be discussed in the following chapters.

7.3 Three-dimensional Pillar Arrays for Cultivating Retinal Cells

As cells typically face a 3D environment *in vivo*, modern cultivation systems aim at resembling the corresponding 3D niches. These niches vary in composition and complexity, depending on the various cell types and tissues parencite (Murphy et. al 2017; Quarta et. al 2016). As discussed before, organoids are a promising cultivation system, with the induction of stem cells leading to the formation of a complex tissue *in vitro*, often in a free-floating system. In the case of organoids, the niche environment is resembled via the addition of soluble factors or the embedding in a mixture of ECM. However, the free-floating cultivation of organoids does not replicate the presence of tissues or structures like blood vessels, larger deposits of ECM or bone. Consequently, efforts are made to combine cell culture with more complex and defined substrates (Shafiee and Atala 2017). The available methods for producing defined substrates are numerous. Some fabrication methods are highlighted in chapter 3.5. Among these methods, we chose to employ direct laser writing to fabricate defined culture substrates.

While some publications describe the use of DLW-produced 3D substrates as substrates for retinal cell culture, these substrates were conceived as a short-term cultivation system for the transplantation of cell sheets or tissue-like constructs (McUsic et. al 2012; Shrestha et. al 2020; Thompson et. al 2019; Worthington et. al 2017). However, our focus is on the long-term cultivation of cellular constructs in DLW-produced 3D substrates. The types of substrates used in these publications are usually a block of photoresist interspersed with microchannels. Retinal cells seeded in those substrates colonized the microchannels. However, as the microchannels are separate from each other, unless the cells overgrew the confines of the substrates, only small cell consortia can form (McUsic et. al 2012; Worthington et. al 2017).

As cell-cell interactions are integral to the formation of a tissue-like construct, we aimed at designing a 3D substrate more permissive in this regard. One cell type important for structuring and stabilizing the retina are Müller glial cells, which are regularly spaced in *x-y* axis and span the whole length of the retina (J. Wang et. al 2017). Thus, we devised a pillar array adopting a stablizing function like the Müller glial cells, consisting of 28x28 pillars. For the height of the pillars we tried to take the thickness of a mouse retina into account, which is approximately 200 µm, or the thickness of a murine organoid, which is approximately 120-150 µm (Eiraku et. al 2011). But the production mode used with the DLW only allows a maximum height of 100 µm. This maximum height is dictated by the objectives distance to the cover slip. Additionally, the procedure is limited by the feature size at larger distances from the cover slip, as the laser beam has to be focused through the whole sample, leading to refraction. Hence, at larger distances, substrates

tend to show aberrations caused by refraction, leading to reduction in feature size. Furthermore, the larger the substrates, the more unstable they get. This can be countered by reducing the feature size, but too bulky pillars were also unwanted. Taking all these factors into account, we decided on using pillars of 70 µm height, distanced 20 µm in x and y with a radius of 3.5 µm. This pillar array is surrounded by a combination of flat squares and walls with a height of 80 µm. While the pillars are written in a protein-permissive photoresist, surrounding walls and squares are written in a protein-prohibitive photoresist.

The ultimate goal is to generate a stratified retinal tissue containing all relevant cell types with basic levels of functionality. To examine the general feasibility of this project, the long-term cultivation of retinal cells was tested in this work. If this should prove possible, more complex 3D substrate designs can be explored.

7.3.1 Retinal Induction in 3D Pillar Arrays

Generating retinal cells was the first important task to achieve a more complex *in vitro* cultivation system. There are different protocols available to induce retinal fate in pluripotent stem cells. The most promising of these protocols in regards to induction efficiency and the resulting cells and tissue-like constructs are organoids. Thus, we tried to transfer the organoid protocol to embroynic stem cells cultivated in 3D pillar arrays (see chapter 6.2). After addition of Matrigel, seeded mESCs proliferated throughout the following days, but they did not obtain retinal fate. We observed on multiple accounts that the formation of a uniform aggregate is necessary to induce retinal fate in floating culture (data not shown). If the aggregate formation was lacking, we mostly observed no retinal or only neural induction. In aggregates, only the outer layers of cells are directly in contact with Matrigel, potentially leading to a subregionalization of the aggregate. However, in the pillar array only a thin layer of cells was present. All of these cells were in direct contact with the Matrigel, which might change the specific influence of the ECM mixture on the mESCs differentiation program. Furthermore, one upside of the floating system is the potential for cells to move throughout the aggregate and for the tissue to perform larger-scale morphological changes, like the evagination of vesicular structures (Eiraku et. al 2011). While single cell migration is still possible in 3D substrates, larger scale movements are limited in the pillar arrays, which might explain the lack of retinal induction in this environment.

We also explored the induction via small molecules in a floating system, in order to replace Matrigel as inducing agent, leading to a more reliable and reproduceable retinal induction. To this end, IGF-1, Wnt-inhibitor CKI-7, Nodal-inhibitor SB-431542, BMP-inhibitor LDN193189 and bFGF were tested in different combinations. As one of the original publications introducing small molecules was done using hiPSC, we adapted the concentrations to better suite the mouse system

(Osakada et. al 2009). However, none of the tested combinations led to retinal induction (data not shown). This might be caused by insufficient function of the small molecules or insufficient concentration of the molecules. Deepak Lamba and colleagues reported the generation of retinal cells via the addition of purified proteins IGF-1, BMP-signaling inhibitor noggin and WNT/β-catenin signaling pathway antagonist DKK1. 82% of the hESCs expressed Pax6 after three weeks of cultivation, and of these, 86% coexpressed Vsx2. Initial stages of the protocol were conducted with embryoid bodies, but most of the protocol was done in 2D culture. This might be a more suitable system for retinal induction in pillar arrays than the adaptation of the organoid protocol. However, the fact that not all cells are induced to retinal fate can be quite detrimental, as terminally differentiated retinal cells are limited in their proliferation capacity, while the non-retinal cells might maintain this function for an extended period of time and overgrow the substrate (Kassen et. al 2008).

Another method for generating retinal cells from hESCs *in vitro* was presented by Atsushi Kuwahara and colleagues. They tested a number of BMP, WNT and FGF agonists/antagonists and among the screened substances identified low concentrations of BMP4 at day 6 to be the most effective way of inducing retinal fate (Kuwahara et. al 2015). We also adapted this protocol to the mouse system, changing concentrations and time of addition correspondingly. However, no retinal fate could be induced with any of the tested alterations (data not shown). BMP4 was also used in murine organoid culture, but it was supplemented from day 9 onward for a period of four days in combination with triiodothyronin and DAPT in order to increase the amount of cone PRs (Ueda et. al 2018). BMP4 signaling has been implicated with lens and retina formation in mice as well as suppressing RPE differentiation. In mice with conditional deletion of *Bmp4*, lens induction and OC formation was prevented (Huang et. al 2015). However, in these mice, genes known to be important during eye development showed only moderate or no changes in expression. This might also mean that there are differences in the human and mouse systems response towards stimulating factors like BMP4.

While various methods exist to differentiate stem cells to retinal fate, most of these methods were established with human pluripotent stem cells. Transfer and adaptation of these protocols to our culture system did not show any retinal induction. Not only can mouse stem cells show different reactions towards stimuli compared to the human system, but they also behave differently in a cell culture environment. For example, some protocols require a confluent cell sheet, which for human stem cells is apparently feasible, but as soon as the mESCs grew to confluency, they started to round up and larger patches of cells detached from the surface (data not shown). Consequently, some aspects of protocols established in hPSCs can not be replicated in mESC culture.

Furthermore, instead of attempting to replace Matrigel, it might also be worthwhile to enhance the outcome of the standard protocol by supplementing the culture system with additional morphogens, growth factors and important inhibitors at comparable stages to the *in vivo* retina development. As was demonstrated with the addition of AGN193109, such factors can massively influence the outcome of the induction protocol (Assawachananont et. al 2014).

7.3.2 Pillar Arrays as a Viable Substrate for Organoid-derived RPCs

As seeding of mESCs in 3D substrates and successive differentiation to retinal fate did not succeed, we decided to explore other options. With the retinal organoid protocol we already were able to differentiate mESCs to retinal fate *in vitro*. However, free-floating aggregates are hard to combine with pillar arrays attached to a cover slip, or with most complex 3D substrate designs. Occasionally, organoids attach to the culture surface in routine culture, leading to a flattening of the organoid and outgrowth of cells in 2D (data not shown, also compare (Iwasaki et. al 2016)). A similar fate would also be expected for direct cultivation of organoids on pillar arrays. Hence, we attempted to dissociate retinal organoids and seeded the obtained cell suspension in pillar arrays. Dissociation and re-seeding of organoids has been reported on various accounts for dentin-pulp-like, cerebral and intestinal organoids (Jeong et. al 2020; Kar et. al 2020; Mussard et. al 2020; H. Sakaguchi et. al 2019). Small intestinal organoids were dissociated and seeded in a 2D monolayer. This monolayer did show presence of cell lineages of the small intestine. After dissociation and re-seeding of our retinal organoids, they adhered to the pillar array and formed small GFP^+ cell clusters. With continued cultivation, these clusters proliferated and grew in size. In comparison to free-floating organoids, cultivation of dissociated organoid cells in pillar arrays did not have any adverse effect on their survival or maintenance (see chapter 6.2), validating the feasibility of long-term cultivation of retinal cells in 3D pillar arrays.

One critical aspect of long-term cultivation is nutrient and oxygen supply. Increased media exchange was achieved by cultivating organoids in bioreactors (DiStefano et. al 2018; Lancaster et. al 2013; Ovando-Roche et. al 2018; Qian et. al 2016). These bioreactors lead to constant agitation, redistributing the culture media regularly. Thus, local accumulation of waste products and zones of nutrient deprivation can be avoided, leading to the formation of larger and more mature tissues (DiStefano et. al 2018; Selden and Fuller 2018). However, even though bioreactors have a positive effect on cultivated cells, they can not help to maintain the culture for an extended period of time. Tyler DiStefano and colleagues reported that neural retina structures in their rotating wall bioreactors started to degenerate from day 25 onward, while they maintained structure to some extend until day 30

in static culture. Still, in the bioreactor setup, organoids displayed similar or better morphology and differentiation of major cell types than in the static cultivation system (DiStefano et. al 2018).

Similar to our dissociated retinal organoids, Hideya Sakaguchi and colleagues dissociated human cerebral organoids between day 70 and 100. Upon re-seeding, the cells started to cluster and migrate. After a few days, networks between clusters formed tightly and glial-like shaped cells were generated. A vast network was formed after roughly four weeks in culture, connecting each cluster by thick neurite bundles. After prolonged cultivation, these self-organized neuronal networks contained mature glutamatergic and GABAergic neurons and showed synapse formation. Interestingly, these neuronal networks could be maintained *in vitro* for more than one year. In contrast to cerebral organoids, the dissociated and re-seeded neuronal networks showed synchronized burst activity (H. Sakaguchi et. al 2019).

When looking at long-term cultivation, dissociated retinal organoids in pillar arrays also could be maintained for a longer time, up to 50 days. Similar to other reports, retinal organoids in our hands started to degenerate at the latest after 25 days. As the retina is a well-stratified and organized tissue, the morphology is inevitably also linked to function and correct differentiation (Hoon et. al 2014). The laminar organization of the retina, retinal organoids and retinal cells cultivated in pillar arrays will be addressed in the next chapter.

7.4 Cellular Organization in 3D

Neuronal tissues often show an ordered architecture closely linked to the specific cellular function. Cells of the same type are organized laterally in the same laminar structure and axially in a functional and gradual manner. Thus, nuclear layers with the corresponding cell bodies and plexiform layers with the synaptic connections form. This general blueprint holds also true for the retina, which consists of three nuclear and two plexiform layers. How does this dazzling organization occur *in vivo* and to some extend *in vitro*? What are the underlying mechanisms, and how can this process be modified and improved upon? Might defined 3D substrates play an integral role in this pursuit?

7.4.1 Induction of Retinal Fate and Laminar Organization in Vivo

For decades, basic research was conducted on how retinal induction is initiated and moves forward in various vertebrate animal models. To this end, much work was done in mouse and chick, but also in *Xenopus* and zebrafish (Ail and Perron 2017; F. E. Anderson and C. B. Green 2000; Dalke and Graw 2005; Glass and Dahm 2004; Seabra and Bhogal 2010; Vancamp and Darras 2017). In early neurulation,

retinal fate is induced by a combination of TGF-β, FGFs and members of the Shh family, which emanate from the underlying axial mesoderm and lead to the activation of key retinal gene circuitry. A network of key marker genes has been identified, which concomitantly define the eye field (Zuber et. al 2003). Retinal differentiation is interlinked with morphological changes, namely the OV and OC formation. During these events, retinal fate is specified and differentiation is taking place.

Upon evagination of the OV, the presumptive neural retina cells of the vesicle are in close proximity to the surface ectoderm and later to the lens placode, which are BMP and FGF signaling nodes (Hyer et. al 2003; J. Hyer, T. Mima and T. Mikawa 1998; Pandit et. al 2015). While BMP4 during the blastula stage has a repressive effect on the emergence of eye-field cells, during the OV stage the relation changes. Concomitantly, the surface ectoderm gives rise to the lens placode. BMP4 from the lens placode is required and sufficient to maintain eye-field identity, block telencephalic character and specify neural retinal cells in zebrafish (Pandit et. al 2015). In mouse, BMP4 is expressed in the distal tip of the OV and is also required for the specification of the neural retina domain (Huang et. al 2015). However, in chick the function of BMP4 seems to be rather in the specification and maintenance of RPE cells (Müller et. al 2007). FGF8 has also been implicated as a central inducer of retinal fate, however, it appears to be downstream of BMP4 signaling, as inhibition of BMP4 signaling also leads to loss of FGF8 signaling. FGF8 is not required or sufficient to specify neural retina identity (Pandit.2015).

After specification of retinal character, the differentiation of retinal cells is induced by HH signaling. The first cell type to arise are the RGCs, which are induced by HH signaling (Neumann and Nuesslein-Volhard 2000; Shkumatava et. al 2004). In turn, RGCs themselves adopt a HH-signaling role (Dakubo and Wallace 2004). Hence, a central-to-peripheral combined wave of RGC development and HH signaling sweeps over the retina, which induces the differentiation of neighboring cell (Neumann and Nuesslein-Volhard 2000). Temporally overlapping, a second wave of differentiation sweeps over the retina, specifying amacrine cells in the INL. This second wave is independent of the first, as it also occurs in the absence of RGCs (Shkumatava et. al 2004).

The morphogens and factors listed here are only the key players for neural retina specification. There is still a large number of other factors involved to a lesser extend. Amongst these is FGF3, which adopts similar functions as FGF8. They are functionally redundant, as inactivation of either did not show any significant effect, but upon inactivation of both, retinal induction was blocked (Martinez-Morales et. al 2005). Various WNT ligands are also involved in retinal specification and differentiation. A regulatory network of WNTs and Sox2 is required for maintaining proliferation in RPC (Agathocleous et. al 2009). Additionally, Wnt/β-

catenin signaling is required for the expression of *Mitf* and *Otx2* in RPE cells (Westenskow et. al 2009). These early specification events are the basis of the later retinal lamination.

7.4.2 Processes Underlying Lamination

Overall, there are a number of cellular processes required for the establishment of correct laminar organization. Chief amongst them are I) establishment and selective recognition of guidance cues II) adhesive and migratory behaviour of cells.

A combination of various attractive and repellent guidance cues are used to guide cells and their processes to the correct laminar layer (Diao et. al 2018; Robles and Baier 2012). In order for cells and their processes to find their correct destination, cell signaling molecules are employed to define and locate certain cellular subgroups. Prominent examples are the semaphorin guidance cues and their corresponding plexin receptors (Matsuoka et. al 2011; Zhang et. al 2017). Sema5A and Sema5B constrain neurites from multiple retinal neuron subtypes within the IPL. Null mutants of both proteins show mistargeting in RGCs, ACs and BPCs into the outer portion of the retina (Matsuoka et. al 2011). Null mutations of Sema6A have also been shown to lead to targeting and lamination defects, in this case of HCs in the OPL (Matsuoka et. al 2012).

Other non-signaling molecules have also been implicated with a role in lamination. For example, loss of the atypical protein kinase C α leads to morphological defects in PRs, their inability to form ribbon synapses and severe laminar disorganization (Koike et. al 2005). The leucine-rich repeat-containing protein netrin-G ligand 2 has also been implicated in lamination. In null mutation mice, many HC axons fail to stratify in the OPL, instead invading the ONL. In these animals, fewer synapses of HCs and rods were observed (Soto et. al 2013).

Lamination is also tightly linked to migration of cells and how they arrange relative to each other. A prominent example of proteins related to this process are the calcium dependent homophilic adhesion receptors N-cadherin (Pokutta and Weis 2007; Takeichi 1995). N-cadherin is differentially expressed throughout development and while it is localized to the optic nerve fiber, inner nuclear layer, plexiform layers and outer limiting membrane in earlier stages, at later stages localization is restricted to the outer limiting membrane and inner nuclear layer (Honjo et. al 2000; Matsunaga et. al 1988). When interfering with the N-cadherin activity in chicken retinogenesis via addition of Fab fragments of a polyclonal antibody, retinae dissociated and could not be maintained. This indicates that N-cadherins play an important role during retinal development in maintaining the overall structure of the undifferentiated retina (Matsunaga et. al 1988). In zebrafish,

knock-out of N-cadherin leads to disorganization of retinal cells. However, all cell types are present in these retinae, which indicates that the lamination defects are not caused by general defects in development (Masai et. al 2003).

Another adhesion receptor family involved in retinal lamination are integrins. While cadherins mediate cell-cell interactions, integrins are known as cell-matrix contacts, binding to the conserved RGD sequence (Hynes 1992). They have been implicated to play an important role in retinal development (M. Li and D. S. Sakaguchi 2004). Adding the RGD-containing disintegrin echistatin or function blocking antibodies to the embryonic *Xenopus* retina lead to disruption in retinal lamination and the formation of rosette structures. This study highlights the important function of integrins during migration and retinal morphogenesis. Some reports also implicate integrins in the survival of RGCs during development (Kanamoto et. al 2009; Leu et. al 2004).

As retinal cells cultivated *in vitro* as organoids or dissociated in pillar arrays show some level of preferential localization, the question arises how this phenomenon occurs and is mediated. As previously established, the *in vivo* development relies on morphogens to pattern the developing retina in sub-domains throughout 3D space. In many cases, these morphogens are secreted by the surrounding (Huang et. al 2015). In the *in vitro* systems, positional information is lacking, meaning that the cellular organization must be based on other processes. To some extend, the relative positional information could be obtained via cell-cell or cell-matrix interactions. The homogeneous coating with LN renders cell-matrix interactions via integrins an unlikely candidate, as under these circumstances a differentiated positional information would not be expected. Cell-matrix interactions might still be of importance in regards to the tissue integrity and for promoting survival of the cells (Kanamoto et. al 2009; Leu et. al 2004). Along these lines, different surface coatings using other ECM proteins could be investigated, potentially influencing cellular behaviour to large effects. However, the protein coating should also be chosen in respect to the retinal ECM (Dorgau et. al 2018; Felemban et. al 2018; Hausman 2007; Taylor et. al 2015).

Cell-cell interactions on the other hand might be of integral importance for the positional arrangement of retinal cells in 3D *in vitro* systems. N-cadherin is involved in the cortical organization in the mouse brain (Kadowaki et. al 2007; Rasin et. al 2007), however, N-cadherins involvement could be traced back to the maintenance of adherens junctions. Furthermore, N-cadherin is involved in the laminar targeting of thalamocortical axons and also of PRs (Lee et. al 2001; Poskanzler et. al 2003; Yonekura et. al 2007). These examples offer a basis for the assumption, that organization of retinal tissues *in vitro* might in parts be mediated by N-cadherins. Interfering with the N-cadherin mediated cell-cell interactions in both, retinal organoids and dissociated retinal organoids cultivated on 3D

substrates, could prove quite interesting. This could potentially have a significant effect on the cellular organization and relative orientation, revealing important insights on the mechanics of laminar organization.

Another explanation for the preferential localization of some cell types in 3D pillar arrays might be slight changes in nutrient and oxygen accessibility. PR-marker positive cells often localized to the upper region of the pillar arrays. PRs are regarded as the cell type with the highest oxygen demand in the retina, while INL cells are thought to have a lower oxygen consumption (Cringle and Yu 2010; Cringle et. al 2006). Thus, PR-like cells might preferentially localize to the areas of highest oxygen concentration and accessibility. As the overall energy demand of PRs is quite high, not only the supply with oxygen, but of nutrients in general might be decisive. The effect of oxygen supply has also been assessed in retinal organoid culture. Both, for murine and human stem cell derived organoids a positive effect of changes in oxygen level has been demonstrated (H. Y. Chen et. al 2016; Eiraku et. al 2011; Gao et. al 2016). However, there are substantial differences to the various protocols. Mototsugu Eiraku and colleagues continuously cultivate retinal organoids at 40% oxygen after the dissection step, while Holly Chen and colleagues cultivated the early aggregates until the dissection step in hypoxia (5%) and switched afterwards to normoxia. Overall, given the important role of oxygen and nutrient supply during development, it probably also impacts the cultivation and maintenance of *in vitro* cultivated retinal cells. Compared to retinal organoids, the cultivation of retinal cells on pillar arrays might allow more efficient nutrient and oxygen supply because of the thinner tissue morphology achieved. This might allow nutrient transport more easily to the cells and waste products to be removed more efficiently. Thus, the individual response and reaction of a pillar array based *in vitro* cultivation system towards different levels of oxygen would be of interest and might change the experimental outcomes.

7.4.3 Pattern Formation in Vivo and in Vitro

Retinal development is a well-orchestrated and organized series of events that robustly results in the same structure. This level of developmental precision is achieved by characteristic and reliable patterning events during development. Under the control of different morphogens, DV and naso-temporal (NT) cell fate is specified. Patterning events occur during OV and OC stages and NT axis is determined by FGFs, while DV patterning is achieved by BMP signaling (Cardozo et. al 2019; Pandit et. al 2015; Picker and Brand 2005; Picker et. al 2009). SHH is also involved in all of these patterning events: in combination with FGFs it is involved in proximal-distal patterning and SHH restricts BMP to the distal domain of the OC, leading to the DV specification via the expression of *Tbx5* (Cardozo et. al 2019; Veien et. al 2008).

In fast-developing animals like zebrafish, the patterning events are happening concomitantly to the morphological event of OC formation, while in slower developing animals like chick and mouse, patterning events and morphological events are temporally separate (Cardozo et. al 2019; Eckert et. al 2019). In addition to the DV and NT patterning, the OC is also patterned in central to peripheral direction. Peripheral identity is established via WNT-signaling. It is both required for the maintenance of proliferative cells in the ciliary margin as well as the differentiation of RPE cells (Borday et. al 2012; Kubo and Nakagawa 2008). WNT-dependent differentiation of RPE is also a key requirement for the OC folding, which is mediated by the hinge region between NR and RPE (Carpenter et. al 2015). Disruption of the normal patterning leads to morphological perturbations, ranging from mislocalization of some cells to complete disorganization of the tissue (J. Hyer, T. Mima and T. Mikawa 1998; Martinez-Morales et. al 2005).

Regarding organoids and pattern formation, the question arises if pattern formation can be observed. Missing the characteristic stimuli, patterning would not be expected. Yet, organoids are still able to form tissues containing the relevant cell types and even show varying levels of lamination.

Already, some interesting work has been conducted regarding pattern formation in retinal organoids. Yuiko Hasegawa and colleagues analysed if there are some pattern formation events observable. Indeed, they identified selective marker expression of dorsal (Tbx5) and ventral (Vax2) markers. Expression of these markers appears to be regulated by endogenous BMP signaling. The authors hypothesize that this BMP-signaling in turn is regulated by canonical WNT-signaling. However, only 21% of the mESC-derived OCs did show the characteristic domains as *in vivo* (Hasegawa et. al 2016). The role of WNT-signaling for the formation of OCs was also examined in retinal organoids. Co-culture of organoids with *Wnt3a*-expressing cell aggregates lead to a substantial increase in RPE differentiation and NR invagination (Eiraku et. al 2011). Furthermore, modifications to the WNT-signaling cascade lead to changes in retinal induction in organoids. Using the standard approach leads to $Axin2^{+}$ retinal tissue with dorsal characteristics. Addition of the WNT antagonist IWP-2 leads to aggregates with low *Axin2* expression and also low levels of Rx-GFP, while addition of the WNT agonist CHIR99021 leads to the emergence of posterior central nervous system-like aggregates (Sakakura et. al 2016).

Another recent and prominent example of axis formation and organization within *in vitro* cultivation systems are the so-called gastruloids, stem cell aggregates which show characteristic organization events resembling the early stages of gastrula and primitive streak development (Martyn et. al 2019; Minn et. al 2020; Moris et. al 2020). The resulting patterning can be modified via changes to central morphogen signaling cascades (Chhabra et. al 2019). Combination of gastruloids with microwell-substrates also allows for 4D tracking of the cultivated cells (Samal et. al 2020).

Even though the *in vitro* system lacks the surrounding tissues and the corresponding morphogens and stimuli, some level of pattern formation can still be achieved. This fact is surprising, as the *in vivo* system is quite susceptible to changes and disturbances (J. Hyer, T. Mima and T. Mikawa 1998; Martinez-Morales et. al 2005). Cells cultivated in our pillar arrays showed some level of preferential distribution in z-axis, it would also be interesting to examine the arrangement in x- and y-axis. Furthermore, defined 3D substrates might offer a unique way of conducting research in this area, as differential and selective coating of the substrate is conceivable (Richter et. al 2017). Therefore, ligands specifying dorsal and ventral character could be selectively coated to different areas of the substrate. To increase the complexity of the system even more, one could attempt to additionally include a gradient stimulating naso-temporal specification. A system like this would offer incredible opportunity to replicate a complex and multifactorial process like pattern formation and eye development in a controlled and reliable manner. If the practical realization of this system would work, this would offer a platform to examine changes and modifications to the basic system with relative ease compared to model organisms. As we demonstrate here, the cultivation of organoid derived retinal cells in pillar arrays is feasible, laying the foundation for a plethora of potential *in vitro* systems.

7.4.4 Self-organization of Retinal Tissues in Vitro

In the last few decades, retinal development and self-organization processes during retinogenesis have peaked the interest of researchers. Even in modern organoid culture, the self-organization of stem cell-derived retinal cells is of great significance. Seminal work about self-organization was conducted by Aron Moscona and Paul Layer and colleagues. Working on chick retina, they dissociated retinae and reaggregated them in a bioreactor (Sheffield and Moscona 1969). A correlation of ordered aggregate formation and the age of the retinal cells at the beginning of the experiment was identified, with E6 retina yielding the highest percent of ordered aggregates (Vollmer and Layer 1986b). Reaggregation experiments have also been conducted in zebrafish, showing that the underlying principles might be valid for a wide range of species (M. K. Eldred et. al 2017). These experiments indicate a basic propensity of retinal cells to recognize appropriate cell types and spatially orient accordingly, even after dissociation and lacking spatial cues.

We also observed some level of self-organization in retinal cells cultivated in pillar arrays, showing a preferential localization of Rcvrn$^+$ PR-like cells to the top of the array, while Sox9+ Müller glial-like cells were rather located to the center or bottom of the array. Similar observations were also made for Pax6 and Otx2, however, markers like calbindin and calretinin were quite evenly distributed throughout the pillar array. Additionally, these markers were also

often colocalized. Given their combined expression in GCs (Pasteels et. al 1990), the colocalization is not surprising. However, many markers were distributed throughout the whole *z*-axis, indicating that formation of pronounced layers like in the retina is still missing. This indication is reinforced by the fact that the synaptic vesicle marker synaptophysin was distributed throughout the whole retinal tissue, not condensing in defined plexiform-like layers. This would mean that synaptic connections might form, but they are randomly localized and not organized in a distinct layer. The question arises, if the synaptic connections are formed between the correct signaling partners or if target acquisition is perturbed. Hence, the architecture and level of synaptic organization would have to be further analysed. Immunostainings of prominent synapse markers like Bassoon or RIBEYE could shed light on the synaptic organization in retinal tissues cultivated in 3D substrates. Synapse-like structures in organoids could be used as a comparison to potentially identify beneficial effects of the 3D substrates.

Reports in literature of dissociated retinae cultivated in 3D substrates match our observations. In these experiments, dissociated cells showed preferential localization in *z*-axis in PLGA-channel substrates. However, the direction of organization was inverse, as $Pax6^+$ cells were rather localized to the top of the structure, while $Otx2^+$ cells were more frequent in central and lower position. The same was true for human embryonic stem cell derived retinal cells generated from protocols based on 2D cultivation (McUsic et. al 2012).

Given that both, retinal reaggregation systems as well as organoids, are able to form structures of varying degree of organization, avenues of improving the organization within the pillar arrays might have been established already. Indeed, some publications discuss modifications to the system, which result in improved laminar organization. Co-culture with RPE and Müller glial cells improved the organization in a fraction of cultivated aggregates (Layer and Willbold 1989; Vollmer and Layer 1986b; Vollmer et. al 1984; Willbold et. al 1995, 2000). In both cases, the sheer presence of the corresponding cell type was sufficient to improve laminar organization within the reaggregated retinal cells. Direct co-culture and application of conditioned media were compared in both setups. These two conditions lead to similar frequency of stratified reaggregates, suggesting the presence of soluble factors required for laminar organization (Rothermel et. al 1997; Willbold et. al 2000).

In 2003, Shinichi Nakagawa and colleagues identified anterior rim cells to have a similar capacity, inhibiting rosette formation and inducing laminar organization in reaggregated chick retinae. Ultimately, they were able to identify WNT2b as the reason for the correct layer formation, terming this agent the laminar-inducing factor (Nakagawa et. al 2003). Unfortunately, no follow-up work linking WNT2b with functions in layer formation was conducted. Instead, WNT2b's influence on cell proliferation at the ciliary marginal zone, determination of peripheral fate and function in RPE specification have been analysed (Cho, S.H.

Cepko, C. L. 2006; Kubo et. al 2003, 2005; Steinfeld et. al 2013). Still, further analysis on WNT2b's function as laminar-inducing factor would be of great interest. Potentially, other WNT-ligands might also be candidates to influence the cellular behaviour and organization during *in vitro* retinal differentiation. Mototsugu Eiraku and colleagues also cultivated their retinal organoids in the presence of WNT3a-expressing L cells. This cultivation setup led to a higher level of OC-like structure formation (Eiraku et. al 2011).

Combining retinal cells cultivated in 3D substrates with RPE or Müller glial cells or the corresponding conditioned media might also be beneficial to the organization in an *in vitro* culture. Starting from conditioned media, positive effects on laminar organization could then be traced back to single components of the media. Based on literature, WNT2b would be an interesting candidate to incorporate in an *in vitro* cultivation system using two-photon lithography fabricated substrates. As extrinsic cues are missing, addition of soluble factors known to have functions in the organization and lamination of retinal tissues might improve the overall outcome of the system. Factors along this line could for example be BMP4, FGF3 and FGF8.

More insight on the mechanisms and processes underlying the self-organization has also been gained quite recently. Central to this mechanism is the well-known eye field transcription factor Pax6, which is also regarded as a master control gene of eye development (Cvekl and Callaerts 2017; Shaham et. al 2012). Pax6 interacts with two morphogen-coding genes, *Tgfb2* and *Fst*. Timothy Grocott and colleagues used computer simulations to examine the networks influence on developmental processes. Pax6 and Fst function as a short-range auto-regulating activator, while Tgfb2 would be a long-range inhibitor, establishing an Activator-Inhibitor Turing nework (Turing 1952). Given these premises, computer simulations attribute this system a self-organizing capacity, which could also be verified with explant culture experiments. Lacking extrinsic positional information, OVs cultivated as explants still show organization events, which suggests an intrinsic organization capacity (Grocott et. al 2020).

Taken together, *in vitro* systems are capable of forming patterns and organized tissue constructs in the absence of surrounding tissues, which usually function as organizing centers. Even when dissociated, retinal cells are able to reform and reorganize to some level, both in the absence and presence of 3D structures. Some factors like WNT2b have been implicated with functions in cellular organization into laminar structures. It remains to be seen if these factors can also improve self-organization in 3D substrates.

7.5 Role of the RPE

The RPE is a key structure of the eye, not only taking on important functions in absorbing scattered light and as a barrier structure between the choroid and retina, but it is also a necessary support structure. As a support structure its main functions are in supplying the closely related PRs with nutrients and also recycling and regenerating visual pigments from PR outer segments (Kwon and Freeman 2020; Strauss 2005). In addition to these important functions, various studies implicated the RPE as an important signaling niche during developmental processes (Dutt et. al 2010; Ha et. al 2017; Sheedlo et. al 2007). The crucial role of the RPE becomes apparent when looking at diseases linked to RPE degeneration. In many cases, the primary degeneration of RPE cells leads to a secondary degeneration of PRs, resulting in vision impairment or complete loss of vision (Carullo et. al 2020; Guziewicz et. al 2017; Nowak 2006; Sparrow et. al 2010). In order to achieve reliable *in vitro* models, generation of RPE cells and the combination with neural retina tissue is of utmost importance.

7.5.1 Differentiation of RPE in Vitro

Already ten years before the rise of retinal organoids, RPE was differentiated *in vitro* using cynomolgus monkey embryonic stem cells. These stem cells were induced via cultivation on mouse stromal cells, leading to the generation of both dopaminergic neurons as well as RPE cells (Kawasaki et. al 2002). In the following years, methods for obtaining RPE *in vitro* were refined and spontaneus as well as directed differentiation protocols were established (Artero-Castro et. al 2019; Buchholz et. al 2009, 2013; Meyer et. al 2011).

By now, quite a number of reports show the generation of RPE from patient-derived iPSCs, leading to a robust *in vitro* disease model which reliably replicates the characteristics of the various diseases (Deng et. al 2018; Gong et. al 2020; Guo et. al 2019; Nguyen et. al 2015). Protocols for generating RPE are mostly focused on human cells, as they are also of great interest for regenerative medicine approaches (da Cruz et. al 2018). However, using a culture system based on mouse embryonic stem cells, we sought to derive RPE from mouse stem cells. Thus far, one report of RPE derived from murine iPSCs is available by Yuko Iwasaki and colleagues (Iwasaki et. al 2016).

In the master thesis of Kai Richler under my supervision, this protocol was established. Starting from retinal organoids, the aggregates were broken up and cultivated on flat 2D substrates from D7 onwards in the presence of the Wnt-activator CHIR99021 and FGF-receptor inhibitor SU5402. This protocol quite reliably lead to the differentiation of cell sheets demonstrating the typical honey-

combed morphology and expression of RPE markers like RPE65, Mitf, Sox9, Otx2 and Zo-1. Additionally, the cell sheet showed an apico-basal polarity and some level of functionality via the internalization of fluorescently labeled latex beads.

An important feature for downstream application of the differentiated RPE cells is the ability to passage the cells. While reports demonstrate the capacity of hESC derived RPE to get passaged, Yuko Iwasaki and colleagues attempted passaging, but they report loss of and inability to regain epithelial structure upon reseeding (Croze et. al 2014; Iwasaki et. al 2016). We also attempted passages of the obtained RPE sheets, however, our observations match the reports by Yuko Iwasaki and colleagues. This might indicate different stages of development of cells obtained from the various protocols. Potentially, mouse ESC-derived RPE cells rather quickly differentiate terminally, while human iPSC-derived RPE cells retain some level of progenitor-like state, allowing proliferation and, thus, passaging of the cells (Salero et. al 2012).

To circumvent the problems of passaging the cells, instead of using normal tissue culture plates, cultivation and differentiation on moveable substrates would be feasible. We attempted and succeeded in the cultivation on Corning Transwell-inserts ™, offering some level of flexibility. Other membrane-systems as cell culture surface would also be feasible. Many polymer-based products are available, but there are also commercial extracellular matrix protein-based membranes available for cell culture, for example Collagen Cell Carrier membranes by Viscofan Bio Engineering. These products could offer much needed flexibility to the mouse ESC-derived RPE cells.

7.5.2 Co-culture of RPE and Retinal Tissues

Given that the interactions of RPE and neural retina, especially the PR layer, are of great importance for correct development and function of the tissues, the lack of direct contact of these tissues in most *in vitro* systems is critical. Many reports regarding retinal organoids identified RPE-like regions within the aggregate, but in most cases they were distant to the neural retina sections (Eiraku et. al 2011). Along these lines, in order to create a more relevant system, a combination of RPE and neural retina *in vitro* would be desirable. Various reports have shown beneficial effects of co-cultured RPE cells and neural retina, leading to reduced apoptosis in explant co-cultures compared to only neural retina cultures, better maintenance of tissue structure and cellular organization as well as reduced level of immunoreaction (Di Lauro et. al 2016; Ghareeb et. al 2020; Kaempf et. al 2008).

In the recent past, co-cultures of stem cell-derived tissues have also been conducted. They showed accelerated PR differentiation, an effect which could not be achieved by conditioned media addition (Akhtar et. al 2019). Furthermore, in a sophisticated co-culture setup using also a microfluidic system, enhanced outer

segment formation was observed in co-cultured retinal organoids (Achberger et. al 2019). These examples clearly demonstrate the beneficial effects of direct co-culture of RPE and neural retina.

Initially, we aimed for a co-culture setup seeding RPE cells inside a 3D substrate and adding neural retina cells afterwards. However, as the RPE cells did not regain their morphology after passaging, this approach could not be realized. Keeping the cellular organization of the retinal cells cultivated in pillar arrays in mind, with PR-like cells preferentially localizing to the upper part of the cellular construct, a direct co-culture system would be conceivable where a monolayer of RPE cells is cultivated on a 2D substrate and the cover slip with the pillar array is turned upside down, to allow contact of the PR-like cells with the separately cultivated RPE. Similar to the procedure described by Kevin Achberger and colleagues, to avoid direct contact of RPE and neural retina cells, a hydrogel could be incorporated in this setup (ibid.). Furthermore, a culture system without direct contact of RPE and neural retina cells could be conceivable. In this case, the differentiation and maturation of the neural retinal cells would be modified via secreted proteins and factors from the RPE-layer. Consequently, an organotypic culture system containing all retinal cell types could be achieved, offering more options of unraveling basic developmental and tissue organizational questions as well as improving the outcome of *in vitro* retinal cell culture.

8 Chapter 8
Conclusion and Outlook

The overarching aim of this thesis was the differentiation of retinal cells, design and fabrication of 3D substrates and ultimately the combination of these two components. While we attempted different protocols for the generation of retinal cells, only the retinal organoid protocol lead to retinal induction in our hands. The addition of AGN193109 and differentiation media containing 5% KSR drastically improved the outcome of the protocol, leading to induction of retinal fate in most aggregates. However, no retinal induction was observed when using various small molecules and growth factors to induce retinal fate in stem cell aggregates. More focused work will have to be put into the induction of retinal fate using other protocols than organoids. A lot of work has been done in this direction using human stem cells, but in order to replicate these results with mouse embryonic stem cells, deviations in concentration and time of addition would have to be tested.

Retinal organoids show the presence of most cell types and an organization relatively close to the *in vivo* situation. However, in many cases the RPE is completely missing, or is in areas distant to the retinal parts. Hence, we also differentiated RPE cells in a separate 2D culture system. The purity of the obtained cell sheets was to a rather high degree and the presence of key marker proteins validated the fate of the obtained cell type. Furthermore, a polarization of the cells was also evident and they were able to internalize fluorescently labeled latex beads, indicating some level of normal functionality. However, these cells proved impossible to be passaged, which renders them quite inflexible and inefficient for experimental application.

To fabricate 3D substrates, we employed a commercial direct laser writing setup. A quite simple substrate design was chosen: a pillar array with 28x28 pillars of 70 µm height, distanced 20 µm from edge to edge. With this 3D substrate design we attempt to replicate the dimensions of the retina to some extend. The pillars are supposed to adopt stabilizing functions characteristic for Müller glial cells. Scanning electron microscopy validated the substrates design and

immunocytochemical stainings of pillar arrays coated with LN proved the protein-adhesive properties of the pillars, while the area surrounding the pillars were written in a protein-repellent photoresist.

In order to combine retinal cells generated via organoids with 3D substrates produced via DLW, we enzymatically and mechanically dissociate the organoids at D14, a stage where they mostly consist of retinal progenitor-like cells. Prior to seeding, the pillar arrays were coated with LN. Per substrate, three dissociated organoids were seeded, resulting in a thin layer of progenitor-like cells. The cells started to coalesce and form smaller clusters. With prolonged cultivation, the progenitor-like clusters continued to proliferate, ultimately leading to the formation of a uniform cell layer within the confines of the pillar array. Throughout cultivation, we did not detect a detrimental effect of the 3D substrate on the survival of the cells. The cell layer remained GFP^+ and also retained their morphology and integrity to a higher degree than age-matched organoids. This suggests a positive effect of the 3D substrates on the long-term morphology and integrity of the cell sheets.

The cellular organization within the pillar arrays was also assessed via immunocytochemistry, revealing the presence of all retinal cell types but RPE. Even the presence of synaptic vesicle markers was observed. In some cases, the markers examined showed a preferential localization. The PR markers Rcvrn and Otx2 were often localized to the upper part of the pillar arrays, while INL markers like Sox9 and Pax6 rather localized to the central and lower parts of the pillar arrays. This suggests some level of intrinsic self-organization programs within retinal organoid-derived cell sheets. Additionally, the cells cultivated in pillar arrays could be maintained for a longer time than was the case for free-floating organoids.

In this thesis, a basic cultivation system combining retinal cells and 3D substrates was successfully established. However, there are still many different avenues to improve the cultivation system. Some of these options will be shortly introduced in the following:

1. Different 3D substrate designs

The 3D substrate design was chosen within the scope of technical options and the dimensions observed in the retina. However, the direct laser writing setup is quite flexible in which types of architectures to fabricate. Basically, any given design can be produced, as long as it is structurally stable. As the general idea of combining retinal cells and DLW-produced substrates proved successful, the influence of different substrate designs on the behaviour and differentiation potential of the cultivated cells can be examined. 3D substrate designs like the microchannels known from previous publications, bowl-like structures, stacked beams leading to a 'woodpile'-like structure or interlinked pillar arrays could be tested. Biodegradable photoresists have also been applied in 3D substrate

production, which could be tested for these applications as well.

2. Combination with growth/lamination factors

Development and cellular organization *in vivo* is orchestrated by a combination of different morphogens. While retinal organoids differentiate in the absence of these inducing factors, they might nonetheless have a positive influence on the outcome of the differentiation process, both, in organoids and when cultivating organoid-derived retinal cells on 3D substrates. Thus, a combination of the 3D substrate cultivation system with different growth and lamination factors could be tested. These factors could either be added to the culture media in a soluble form, or in contrast to the organoid system, the 3D substrates would also allow for a surface coating. Hence, a gradient of factors or a coating restricted to certain areas of the 3D substrate would be conceivable. While in this work the pillar arrays were coated with LN, surface coatings with other ECM-proteins would also be an option.

3. Composite scaffolds

By now, a plethora of different production methods for 3D substrates are available, each catering to different niches regarding material property, dimension and downstream modifications and applications. In order to generate an organotypic system, multiple fabrication methods can be combined to use the advantages of different methods to their fullest. We started a cooperation to combine the pillar arrays with electrospun nanofibers (Bentele et. al 2019). A polymer suspension is ejected through a needle, the application of a high voltage electrical field leads to the elongation of the solution droplet and the deposition of the resulting stream as a fiber to the substrate. Both, the dimension and the composition of the fibers can be modified. These fibers could function as additional substrates and anchoring points for retinal cells cultivated in the pillar arrays, potentially offering a closer replication of the *in vivo* situation.

Three-dimensional scaffolds could also address the earlier stages of organoid development. A key event during retinogenesis is the optic vesicle and successive optic cup formation. The OV gets into close contact with the surface ectoderm, an important signaling niche, leading to the invagination and OC formation. Morphogens secreted by the surface ectoderm are crucially involved in the OC formation and retinal differentiation.

The structure and function of the surface ectoderm could be mimicked by some type of substrate. On the one hand, this structure would have to offer the limiting function of the surface ectoderm, on the other hand it would also function as a secretion hub for morphogens. This could be achieved via prior loading of the substrate with the corresponding morphogens. To this end, a lot of work has been conducted in the field of controlled drug release. Polymeric film-based systems allow an automatic and gradual release of contained drugs. Along the same lines,

the application of surface-anchored metal-organic frameworks (SURMOFs) could also achieve the same goal of controlled and gradual morphogen release (Begum et. al 2019). A combination of such polymeric films and 3D-fabricated structures could offer a system closely resembling the *in vivo* situation.

4. Co-cultivation with RPE

The RPE is a key structure for the maintenance and functionality of the retina. In most *in vitro* systems for differentiating retinal tissue, the RPE is lacking or not in direct contact to the neural retina. In order to design a more reliable and meaningful *in vitro* cultivation system, the combination of neural retina and RPE to one co-cultivation system is of utmost importance. We already have the tools at hand, now the combination of the components needs to be tested in the laboratory. To initially get a grasp on the system, co-cultivation of RPE and organoids would be the first step. With the insights gained from this system, the co-cultivation of RPE and retinal tissues cultivated in 3D substrates could be subsequently attempted.

5. Transition to a human stem cell based system

A system based on mouse pluripotent stem cells has a number of advantages: the cultivation time of 25 to 50 days is rather short, making it quite flexible and perfect to establish the basic system. Already, a lot of work with murine retinal organoids has been done, offering a large fundus of knowledge about the system and how to manipulate it. However, some differences between the murine and human system exist, which also become apparent in the possible cultivation time while still maintaining the morphology, the level of differentiation and cellular organization achieved. However, one massive downside is the extended time required to obtain retinal fate and for the differentiation process to take place. Therefore, after establishing the basic system for cultivating retinal cells in 3D substrates, starting work on a human based system in parallel would be interesting. On the one hand it would be interesting to see if depending on the cell source, the cultivation in 3D substrates differs, on the other hand, potentially having medical downstream applications in mind, a system based on human cells would have a higher impact.

To summarize, in this thesis the generation of retinal organoids is shown and their combination with DLW-produced pillar arrays. The substrates had no negative effect on the viability of the cells and served as a defined cultivation environment. Retinal cells cultivated in LN coated pillar arrays proliferated readily to ultimately fill the whole confines of the substrate. The cultivation time could be extended in the 3D substrates compared to the free-floating organoid system, while still maintaining some level of structure. Furthermore, the seeded retinal progenitor-like cells continued their differentiation program, giving rise to cells

expressing in total all markers of the retinal cell types. In some cases we also observed a preferential distribution of cells positive for certain markers within the pillar array, indicating some level of self-organization within the retinal cells.

This demonstrates the general feasibility of combining retinal cell culture with defined 3D substrates for long-term cultivation. In subsequent work, a plethora of changes and modifications to the system would be conceivable (some of them listed above), potentially leading to the generation of more meaningful *in vitro* cultivation systems.

9 Chapter 9
Abbreviations

Table 9.1: **Abbreviations**

AC	Amacrine cell
AF	AlexaFluor
BC	Bipolar cell
BMP	Bone morphogenetic protein
D	Day of differentiation protocol
DAPI	4′6-Diamidin-2-phenylindol
DKK	Dickkopf
DLW	Direct laser writing
DV	Dorso-ventral
ECM	Extracellular matrix
EFTF	Eye field transcription factor
FGF	Fibroblast growth factor
GC	Ganglion cell
GCL	Ganglion cell layer
(e)GFP	(enhanced) Green fluorescent protein
GFAP	Glial fibrillary acidic protein
HC	Horizontal cell
(S)HH	(Sonig)Hedgehog
INL	Inner nuclear layer
IPL	Outer nuclear layer
Islet1	Insulin gene enhancer protein 1
LN	Laminin
m/h ESC	mouse/human embryonic stem cells
m/h iPSC	mouse/human induced pluripotent stem cells
Mitf	Microphthalmia-associated transcription factor
OC	Optic cup
ONL	Outer nuclear layer

Table 9.1: **Abbreviations**

OPL	Outer plexiform layer
Otx2	Orthodenticle homeobox
OV	Optic vesicle
o/n	over night
Pax6	Paired box protein 6
PDMS	Polydimethylsiloxane
PFA/GA	Paraformaldehyde/Gluaraldehyde
PI	Propidium Iodide
PR	Photoreceptor
RPC	Retinal progenitor cell
RPE	Retinal pigment epithelium
Rx	Retinal homeobox
SEM	Scanning electron microscopy
Sox9	SRY-box transcription factor 9
Vsx2	Visual system homeobox 2
WNT	Wingless and Int-1
ZO-1	Zonula occludens-1

List of Figures

List of Tables

Chapter 10

10 List of Publications

Authors	Y. Hu, C. M. Domínguez, J. Bauer, S. Weigel, A. Schipperges, C. Ölschläger, N. Willenbacher, **S. Keppler**, M. Bastmeyer, S. Heißler, C. Wöll, T. Scharnweber, K. S. Rabe, C. M. Niemeyer
Title	Carbon-nanotube reinforcement of DNA-silica nanocomposites yields programmable and cell-instructive biocoatings
Journal	Nature communications, 2019

Contribution: *Preliminary experiments, Introduction to stem cell culture, Support during culture and experiments, Verification of experiments and performance of control experiments*

Bibliography

Abbot, A. (2003). "Cell culture biology's new dimension". In: *Nature*.

Accardo, A., M.-C. Blatché, R. Courson, I. Loubinoux, C. Thibault, L. Malaquin, and C. Vieu (2017). "Multiphoton Direct Laser Writing and 3D Imaging of Polymeric Freestanding Architectures for Cell Colonization". In: *Small (Weinheim an der Bergstrasse, Germany)* 13.27. DOI: 10.1002/smll.201700621.

Achberger, K. et. al (2019). "Merging organoid and organ-on-a-chip technology to generate complex multi-layer tissue models in a human retina-on-a-chip platform". In: *eLife*. DOI: 10.7554/eLife.46188.001.

Adamis, A. P., D. T. Shima, K.-T. Yeo, T.-K. Yeo, Brown, L. F., Berse, B., P. A. D'Amore, and J. Folkman (1993). "Synthesis and secretion of vascular permeability factor/vascular endothelial growth factor by human retinal pigment epithelial cells". In: 193, pp. 631–638.

Agathocleous, M., I. Iordanova, M. I. Willardsen, X. Y. Xue, M. L. Vetter, W. A. Harris, and K. B. Moore (2009). "A directional Wnt/beta-catenin-Sox2-proneural pathway regulates the transition from proliferation to differentiation in the Xenopus retina". In: *Development (Cambridge, England)* 136.19, pp. 3289–3299. DOI: 10.1242/dev.040451.

Ahmad, M. T., P. Zhang, C. Dufresne, L. Ferrucci, and R. D. Semba (2018). "The Human Eye Proteome Project: Updates on an Emerging Proteome". In: *Proteomics* 18.5-6, e1700394. DOI: 10.1002/pmic.201700394.

Ail, D. and M. Perron (2017). "Retinal Degeneration and Regeneration-Lessons From Fishes and Amphibians". In: *Current pathobiology reports* 5.1, pp. 67–78. ISSN: 2167-485X. DOI: 10.1007/s40139-017-0127-9.

Akhtar, T., H. Xie, M. I. Khan, H. Zhao, J. Bao, M. Zhang, and T. Xue (2019). "Accelerated photoreceptor differentiation of hiPSC-derived retinal organoids by contact co-culture with retinal pigment epithelium". In: *Stem cell research* 39, p. 101491. DOI: 10.1016/j.scr.2019.101491.

Aldiri, I. et. al (2017). "The Dynamic Epigenetic Landscape of the Retina During Development, Reprogramming, and Tumorigenesis". In: *Neuron* 94.3, 550–568.e10. DOI: 10.1016/j.neuron.2017.04.022.

Amin, N. D. and S. P. Paşca (2018). "Building Models of Brain Disorders with Three-Dimensional Organoids". In: *Neuron* 100.2, pp. 389–405. DOI: 10.1016/j.neuron.2018.10.007.

Anderson, F. E. and C. B. Green (2000). "Symphony of rhythms in the Xenopus laevis retina". In: *Microscopy Research and Techniques*.

Anderson, R. M., A. R. Lawrence, R. W. Stottmann, D. Bachiller, and J. Klingensmith (2002). "Chordin and noggin promote organizing centers of forebrain development in the mouse". In: *Development* 129, pp. 4975–4987.

Aoki, S., T. Takezawa, H. Sugihara, and S. Toda (2016). "Progress in cell culture systems for pathological research". In: *Pathology international* 66.10, pp. 554–562. DOI: 10.1111/pin.12443.

Araújo, R. S., D. F. Santos, and G. A. Silva (2018). "The role of the retinal pigment epithelium and Müller cells secretome in neovascular retinal pathologies". In: *Biochimie* 155, pp. 104–108. DOI: 10.1016/j.biochi.2018.06.019.

Artero-Castro, A., S. Popelka, P. Jendelova, J. Motlik, T. Ardan, F. J. R. Jimenez, and S. Erceg (2019). "The identification of small molecules that stimulate retinal pigment epithelial cells: potential novel therapeutic options for treating retinopathies". In: *Expert opinion on drug discovery* 14.2, pp. 169–177. DOI: 10.1080/17460441.2019.1559148.

Assawachananont, J., M. Mandai, S. Okamoto, C. Yamada, M. Eiraku, S. Yonemura, Y. Sasai, and M. Takahashi (2014). "Transplantation of embryonic and induced pluripotent stem cell-derived 3D retinal sheets into retinal degenerative mice". In: *Stem cell reports* 2.5, pp. 662–674. ISSN: 2213-6711. DOI: 10.1016/j.stemcr.2014.03.011.

Autenrieth, T. J., S. C. Frank, A. M. Greiner, D. Klumpp, B. Richter, M. Hauser, S.-I. Lee, J. Levine, and M. Bastmeyer (2016). "Actomyosin contractility and RhoGTPases affect cell-polarity and directional migration during haptotaxis". In: *Integrative biology : quantitative biosciences from nano to macro* 8.10, pp. 1067–1078. DOI: 10.1039/c6ib00152a.

Bagley, J. A., D. Reumann, S. Bian, J. Lévi-Strauss, and J. A. Knoblich (2017). "Fused cerebral organoids model interactions between brain regions". In: *Nature methods* 14.7, pp. 743–751. DOI: 10.1038/nmeth.4304.

Barer, R. and Sidman R. L. (1955). "The absorption spectrum of rhodopsin in solution and in intact rods". In: *J. Physiol.* 1955.129/3.

Bassett, E. A. and V. A. Wallace (2012). "Cell fate determination in the vertebrate retina". In: *Trends in neurosciences* 35.9, pp. 565–573. DOI: 10.1016/j.tins.2012.05.004.

Basson, M. A. (2012). "Signaling in cell differentiation and morphogenesis". In: *Cold Spring Harbor perspectives in biology* 4.6. DOI: 10.1101/cshperspect.a008151.

Beatty, S., H.-H. Koh, D. Henson, and M. Bouton (2000). "The Role of Oxidative Stress in the Pathogenesis of Age-Related Macular Degeneration". In: *Survey of Ophthalmology* 45/2. DOI: 10.1016/s0039-6257(00)00140-5.

Begum, S., Z. Hassan, S. Bräse, C. Wöll, and M. Tsotsalas (2019). "Metal-Organic Framework-Templated Biomaterials: Recent Progress in Synthesis, Functionalization, and Applications". In: *Accounts of chemical research* 52.6, pp. 1598–1610. DOI: 10.1021/acs.accounts.9b00039.

Bentele, T. et. al (2019). "New Class of Crosslinker-Free Nanofiber Biomaterials from Hydra Nematocyst Proteins". In: *Scientific reports*.

Bertuzzi, S., R. Hindges, S. H. Mui, D. D. M. O'Leary, and G. Lemke (1999). "The homeodomain protein Vax2 is required for axon guidance and major tract formation in the devloping forebrain". In: *Genes & development* 13, pp. 3092–3105. ISSN: 0890-9369. DOI: 10.1101/gad.13.23.3092.

Bharti, K. (2019). *Pluripotent Stem Cells in Eye Disease Therapy*. Vol. 1186. Cham: Springer International Publishing. ISBN: 978-3-030-28470-1. DOI: 10.1007/978-3-030-28471-8.

Bharti, K., M. Gasper, J. Ou, M. Brucato, K. Clore-Gronenborn, J. Pickel, and H. Arnheiter (2012). "A regulatory loop involving PAX6, MITF, and WNT signaling controls retinal pigment epithelium development". In: *PLoS genetics* 8.7, e1002757. DOI: 10.1371/journal.pgen.1002757.

Bonnans, C., J. Chou, and Z. Werb (2014). "Remodelling the extracellular matrix in development and disease". In: *Nature reviews. Molecular cell biology* 15.12, pp. 786–801. DOI: 10.1038/nrm3904.

Borday, C. et. al (2012). "Antagonistic cross-regulation between Wnt and Hedgehog signalling pathways controls post-embryonic retinal proliferation". In: *Development (Cambridge, England)* 139.19, pp. 3499–3509. DOI: 10.1242/dev.079582.

Brooks, M. J., H. Y. Chen, R. A. Kelley, A. K. Mondal, K. Nagashima, N. de Val, T. Li, V. Chaitankar, and A. Swaroop (2019). "Improved Retinal Organoid Differentiation by Modulating Signaling Pathways Revealed by Comparative Transcriptome Analyses with Development In Vivo". In: *Stem cell reports* 13.5, pp. 891–905. ISSN: 2213-6711. DOI: 10.1016/j.stemcr.2019.09.009.

Brzezinski, J. A. and T. A. Reh (2015). "Photoreceptor cell fate specification in vertebrates". In: *Development (Cambridge, England)* 142.19, pp. 3263–3273. DOI: 10.1242/dev.127043.

Buchholz, D. E., S. T. Hikita, T. J. Rowland, A. M. Friedrich, C. R. Hinman, L. V. Johnson, and D. O. Clegg (2009). "Derivation of Functional Retinal Pigmented Epithelium from Induced Pluripotent Stem Cells". In: *stem cells* 27, pp. 2427–2434.

Buchholz, D. E., B. O. Pennington, R. H. Croze, C. R. Hinman, P. J. Coffey, and D. O. Clegg (2013). "Rapid and efficient directed differentiation of human pluripotent stem cells into retinal pigmented epithelium". In: *Stem cells translational medicine* 2.5, pp. 384–393. ISSN: 2157-6564. DOI: 10.5966/sctm.2012-0163.

Burns, M. S. and M. J. Hartz (1992). "The retinal pigment epithelium induces fenestration of endothelial cells in vivo". In: *Current eye research* 11.9, pp. 863–873. DOI: 10.3109/02713689209033484.

Cakir, B. Xiang, Yangfei et. al (2019). "Engineering of human brain organoids with a functional vascular-like system". In: *Nature methods* 16.11, pp. 1169–1175. DOI: 10.1038/s41592-019-0586-5.

Cangiano, L., S. Asteriti, L. Cervetto, and C. Gargini (2012). "The photovoltage of rods and cones in the dark-adapted mouse retina". In: *The Journal of physiology* 590.16, pp. 3841–3855. DOI: 10.1113/jphysiol.2011.226878.

Cao, W., J. Tombran-Tink, W. Chen, D. Mrazek, R. Elias, and J. F. McGinnis (1999). "Pigment epithelium–derived factor protects cultured retinal neurons against hydrogen peroxide–induced cell death". In: *Journal of neuroscience research* 57, pp. 789–800.

Capowski, E. E. et. al (2014). "Loss of MITF expression during human embryonic stem cell differentiation disrupts retinal pigment epithelium development and optic vesicle cell proliferation". In: *Human molecular genetics* 23.23, pp. 6332–6344. DOI: 10.1093/hmg/ddu351.

Cardozo, M. J., M. Almuedo-Castillo, Bovolenta, P.Cardozo, M. J., and P. Bovolenta (2019). "Patterning the Vertebrate Retina with Morphogenetic Signaling Pathways". In: *The Neuroscientist : a review journal bringing neurobiology, neurology and psychiatry*, p. 1073858419874016. DOI: 10.1177/1073858419874016.

Carpenter, A. C., A. N. Smith, H. Wagner, Y. Cohen-Tayar, S. Rao, V. Wallace, R. Ashery-Padan, and R. A. Lang (2015). "Wnt ligands from the embryonic surface ectoderm regulate 'bimetallic strip' optic cup morphogenesis in mouse". In: *Development (Cambridge, England)* 142.5, pp. 972–982. DOI: 10.1242/dev.120022.

Carullo, G., S. Federico, N. Relitti, S. Gemma, S. Butini, and G. Campiani (2020). "Retinitis Pigmentosa and Retinal Degenerations: Deciphering Pathways and Targets for Drug Discovery and Development". In: *ACS chemical neuroscience* 11.15, pp. 2173–2191. DOI: 10.1021/acschemneuro.0c00358.

Cattaneo, C. M., K. K. Dijkstra, L. F. Fanchi, S. Kelderman, S. Kaing, N. van Rooij, S. van den Brink, T. N. Schumacher, and E. E. Voest (2020). "Tumor organoid-T-cell coculture systems". In: *Nature protocols* 15.1, pp. 15–39. DOI: 10.1038/s41596-019-0232-9.

Cepko, C. L., C. P. Austin, X. Yang, M. Alexiades, and D. Ezzeddine (1996). "Cell fate determination in the vertebrate retina". In: *Proceedings of the National Academy of Sciences of the United States of America* 93, pp. 589–595.

Chambon, P. (1996). "A decade of molecular biology of retinoic acid receptors". In: *FASEB journal : official publication of the Federation of American Societies for Experimental Biology*.

Chan, S. Y. et. al (2017). "Electrospun Pectin-Polyhydroxybutyrate Nanofibers for Retinal Tissue Engineering". In: *ACS omega* 2.12, pp. 8959–8968. ISSN: 2470-1343. DOI: 10.1021/acsomega.7b01604.

Chen, G. and Y. Lv (2018). "Decellularized Bone Matrix Scaffold for Bone Regeneration". In: *Methods in molecular biology (Clifton, N.J.)* 1577, pp. 239–254. DOI: 10.1007/7651$_$2017$_$50.

Chen, H. Y., K. D. Kaya, L. Dong, and A. Swaroop (2016). "Three-dimensional retinal organoids from mouse pluripotent stem cells mimic in vivo development with enhanced stratification and rod photoreceptor differentiation." In: *Molecular Vision* 22, pp. 1077–1094.

Chen, T.-C. et. al (2019). "Polybenzyl Glutamate Biocompatible Scaffold Promotes the Efficiency of Retinal Differentiation toward Retinal Ganglion Cell Lineage from Human-Induced Pluripotent Stem Cells". In: *International journal of molecular sciences* 20.1. DOI: 10.3390/ijms20010178.

Chhabra, S., L. Liu, R. Goh, X. Kong, and A. Warmflash (2019). "Dissecting the dynamics of signaling events in the BMP, WNT, and NODAL cascade during self-organized fate patterning in human gastruloids". In: *PLoS biology* 17.10, e3000498. DOI: 10.1371/journal.pbio.3000498.

Cho, S.H. Cepko, C. L. (2006). "Wnt2b/beta-catenin-mediated canonical Wnt signaling determines the peripheral fates of the chick eye". In: *Development (Cambridge, England)* 133.16, pp. 3167–3177. DOI: 10.1242/dev.02474.

Chun, H. J., C. H. Park, I. K. Kwon, and G. Khang (2018). *Cutting-Edge Enabling Technologies for Regenerative Medicine*. Vol. 1078. Singapore: Springer Singapore. ISBN: 978-981-13-0949-6. DOI: 10.1007/978-981-13-0950-2.

Clark, B. S. et. al (2019). "Single-Cell RNA-Seq Analysis of Retinal Development Identifies NFI Factors as Regulating Mitotic Exit and Late-Born Cell Specification". In: DOI: 10.1016/j.neuron.2019.04.010.

Clevers, H. (2006). "Wnt/beta-catenin signaling in development and disease". In: *Cell* 127.3, pp. 469–480. DOI: 10.1016/j.cell.2006.10.018.

– (2016). "Modeling Development and Disease with Organoids". In: *Cell* 165.7, pp. 1586–1597. DOI: 10.1016/j.cell.2016.05.082.

Collin, J., R. Queen, D. Zerti, B. Dorgau, R. Hussain, J. Coxhead, S. Cockell, and M. Lako (2019). "Deconstructing Retinal Organoids: Single Cell RNA-Seq Reveals the Cellular Components of Human Pluripotent Stem Cell-Derived Retina". In: *Stem cells (Dayton, Ohio)* 37.5, pp. 593–598. DOI: 10.1002/stem.2963.

Country, M. W. (2017). "Retinal metabolism: A comparative look at energetics in the retina". In: *Brain research* 1672, pp. 50–57. DOI: 10.1016/j.brainres.2017.07.025.

Cowan, C. S. et. al (2020). "Cell Types of the Human Retina and Its Organoids at Single-Cell Resolution". In: *Cell* 182.6, 1623–1640.e34. DOI: 10.1016/j.cell.2020.08.013.

Cringle, S. J. and D.-Y. Yu (2010). "Oxygen supply and consumption in the retina: implications for studies of retinopathy of prematurity". In: *Documenta ophthalmologica. Advances in ophthalmology* 120.1, pp. 99–109. DOI: 10.1007/s10633-009-9197-2.

Cringle, S. J., P. K. Yu, E.-N. Su, and D.-Y. Yu (2006). "Oxygen distribution and consumption in the developing rat retina". In: *Investigative ophthalmology & visual science* 47.9, pp. 4072–4076. DOI: 10.1167/iovs.05-1638.

Croze, R. H., D. E. Buchholz, M. J. Radeke, W. J. Thi, Q. Hu, P. J. Coffey, and D. O. Clegg (2014). "ROCK Inhibition Extends Passage of Pluripotent Stem Cell-Derived Retinal Pigmented Epithelium". In: *Stem cells translational medicine* 3.9, pp. 1066–1078. ISSN: 2157-6564. DOI: 10.5966/sctm.2014-0079.

Cruz-Acuña, R. et. al (2017). "Synthetic hydrogels for human intestinal organoid generation and colonic wound repair". In: *Nature cell biology* 19.11, pp. 1326–1335. DOI: 10.1038/ncb3632.

Cui, X., T. Boland, D. D. D'Lima, and M. K. Lotz (2012a). "Thermal Inkjet Printing in Tissue Engineering and Regenerative Medicine". In: *Recent Pat Drug Deliv Formul.* DOI: 10.2174/187221112800672949.

Cui, X., K. Breitenkamp, M. G. Finn, M. Lotz, and D. D. D'Lima (2012b). "Direct human cartilage repair using three-dimensional bioprinting technology". In: *Tissue engineering. Part A* 18.11-12, pp. 1304–1312. DOI: 10.1089/ten.TEA.2011.0543.

Cui, Z. et. al (2020). "Transcriptomic Analysis of the Developmental Similarities and Differences Between the Native Retina and Retinal Organoids". In: *Investigative ophthalmology & visual science* 61.3, p. 6. DOI: 10.1167/iovs.61.3.6.

Cvekl, A. and P. Callaerts (2017). "PAX6: 25th anniversary and more to learn". In: *Experimental eye research* 156, pp. 10–21. DOI: 10.1016/j.exer.2016.04.017.

da Cruz, L. et. al (2018). "Phase 1 clinical study of an embryonic stem cell-derived retinal pigment epithelium patch in age-related macular degeneration". In: *Nature biotechnology* 36.4, pp. 328–337. DOI: 10.1038/nbt.4114.

Dakubo, G. D. and V. A. Wallace (2004). "Hedgehogs and retinal ganglion cells organizers of the mammalian retina". In: *Neuroreport* 15, No. 3. DOI: 10.1097/00001756-200403010-00019.

Dakubo, G. D., Y. P. Wang, C. Mazerolle, K. Campsall, A. P. McMahon, and V. A. Wallace (2003). "Retinal ganglion cell-derived sonic hedgehog signaling is required for optic disc and stalk neuroepithelial cell development". In: *Development (Cambridge, England)* 130.13, pp. 2967–2980. DOI: 10.1242/dev.00515.

Dalke, C. and J. Graw (2005). "Mouse mutants as models for congenital retinal disorders". In: *Experimental eye research* 81.5, pp. 503–512. DOI: 10.1016/j.exer.2005.06.004.

DeForest, C. A. and K. S. Anseth (2012). "Advances in bioactive hydrogels to probe and direct cell fate". In: *Annual review of chemical and biomolecular engineering* 3, pp. 421–444. ISSN: 1947-5438. DOI: 10.1146/annurev-chembioeng-062011-080945.

DelMonte, D. W. and T. Kim (2011). "Anatomy and physiology of the cornea". In: *Journal of cataract and refractive surgery* 37.3, pp. 588–598. DOI: 10.1016/j.jcrs.2010.12.037.

Deng, W.-L. et. al (2018). "Gene Correction Reverses Ciliopathy and Photoreceptor Loss in iPSC-Derived Retinal Organoids from Retinitis Pigmentosa Patients". In: *Stem cell reports* 10.4, pp. 1267–1281. ISSN: 2213-6711. DOI: 10.1016/j.stemcr.2018.02.003.

Derby, B. (2010). "Inkjet Printing of Functional and Structural Materials: Fluid Property Requirements, Feature Stability, and Resolution". In: *Annual Review of Materials Research* 40.1, pp. 395–414. ISSN: 1531-7331. DOI: 10.1146/annurev-matsci-070909-104502.

Di Lauro, S., D. Rodriguez-Crespo, M. J. Gayoso, M. T. Garcia-Gutierrez, J. C. Pastor, G. K. Srivastava, and I. Fernandez-Bueno (2016). "A novel coculture model of porcine central neuroretina explants and retinal pigment epithelium cells". In: *Molecular Vision* 22, pp. 243–253.

Diao, Y., Y. Chen, P. Zhang, L. Cui, and J. Zhang (2018). "Molecular guidance cues in the development of visual pathway". In: *Protein & cell* 9.11, pp. 909–929. DOI: 10.1007/s13238-017-0490-7.

Dijkstra, K. K. et. al (2018). "Generation of Tumor-Reactive T Cells by Co-culture of Peripheral Blood Lymphocytes and Tumor Organoids". In: *Cell* 174.6, 1586–1598.e12. DOI: 10.1016/j.cell.2018.07.009.

DiStefano, T., H. Yu Chen, C. Panebianco, K. D. Kaya, M. J. Brooks, L. Gieser, N. Y. Morgan, T. Pohida, and A. Swaroop (2018). "Accelerated and Improved Differentiation of Retinal Organoids from Pluripotent Stem Cells in Rotating-Wall Vessel Bioreactors". In: *Stem cell reports* 10.1, pp. 300–313. ISSN: 2213-6711. DOI: 10.1016/j.stemcr.2017.11.001.

Dorgau, B., M. Felemban, A. Sharpe, R. Bauer, D. Hallam, D. H. Steel, S. Lindsay, C. Mellough, and M. Lako (2018). "Laminin Gamma 3 plays an important role in retinal lamination, photoreceptor organisation and ganglion cell differentiation". In: *Cell death & disease* 9.6, p. 615. DOI: 10.1038/s41419-018-0648-0.

Dowling, J. E. (1965). "Foveal Receptors of the Monkey Retina: Fine Structure". In: *Science (New York, N.Y.)* 147.3653, pp. 57–59. DOI: 10.1126/science.147.3653.57.

Drost, J. and H. Clevers (2017). "Translational applications of adult stem cell-derived organoids". In: *Development (Cambridge, England)* 144.6, pp. 968–975. DOI: 10.1242/dev.140566.

Duester, G. (2009). "Keeping an eye on retinoic acid signaling during eye development". In: *Chemico-biological interactions* 178.1-3, pp. 178–181. DOI: 10.1016/j.cbi.2008.09.004.

Dutt, K., P. Douglas, and Y. Cao (2010). "RPE-secreted factors: influence differentiation in human retinal cell line in dose- and density-dependent manner". In: *Journal of ocular biology, diseases, and informatics* 3.4, pp. 144–160. DOI: 10.1007/s12177-011-9076-4.

Dutta, D., I. Heo, and H. Clevers (2017). "Disease Modeling in Stem Cell-Derived 3D Organoid Systems". In: *Trends in molecular medicine* 23.5, pp. 393–410. DOI: 10.1016/j.molmed.2017.02.007.

Eckert, P., M. D. Knickmeyer, L. Schütz, J. Wittbrodt, and S. Heermann (2019). "Morphogenesis and axis specification occur in parallel during optic cup and optic fissure formation, differentially modulated by BMP and Wnt". In: *Open biology* 9.2, p. 180179. DOI: 10.1098/rsob.180179.

Eghrari, A. O., S. A. Riazuddin, and J. D. Gottsch (2015). "Overview of the Cornea: Structure, Function, and Development". In: *Progress in molecular biology and translational science* 134, pp. 7–23. DOI: 10.1016/bs.pmbts.2015.04.001.

Eiraku, M. and Y. Sasai (2011). "Mouse embryonic stem cell culture for generation of three-dimensional retinal and cortical tissues". In: *Nature protocols* 7.1, pp. 69–79. DOI: 10.1038/nprot.2011.429.

Eiraku, M., N. Takata, H. Ishibashi, M. Kawada, E. Sakakura, S. Okuda, K. Sekiguchi, T. Adachi, and Y. Sasai (2011). "Self-organizing optic-cup morphogenesis in three-dimensional culture". In: *Nature* 472.7341, pp. 51–56. DOI: 10.1038/nature09941.

Eiraku, M. et. al (2008). "Self-organized formation of polarized cortical tissues from ESCs and its active manipulation by extrinsic signals". In: *Cell stem cell* 3.5, pp. 519–532. DOI: 10.1016/j.stem.2008.09.002.

Eldred, K. C. et. al (2018). "Thyroid hormone signaling specifies cone subtypes in human retinal organoids". In: *Science (New York, N.Y.)* 362.6411. DOI: 10.1126/science.aau6348.

Eldred, M. K., M. Charlton-Perkins, L. Muresan, and W. A. Harris (2017). "Self-organising aggregates of zebrafish retinal cells for investigating mechanisms of neural lamination". In: *Development (Cambridge, England)* 144.6, pp. 1097–1106. DOI: 10.1242/dev.142760.

Evans, G. S., N. Flint, A. S. Somers, B. Eyden, and C. S. Potten (1992). "The development of a method for the preparation of rat intestinal epithelial cell primary cultures". In: *Journal of cell science* 101 (Pt 1), pp. 219–231.

Ewart, J. C. and G. Thin (1874). "On the Structure of the Retina". In: *Journal of Anatomy and Physiology*.

Fan, X. et. al (2003). "Targeted Disruption of Aldh1a1 (Raldh1) Provides Evidence for a Complex Mechanism of Retinoic Acid Synthesis in the Developing Retina". In: *Molecular and cellular biology* 23/13, pp. 4637–4648. DOI: 10.1128/MCB.23.13.4637-4648.2003.

Felemban, M. et. al (2018). "Extracellular matrix component expression in human pluripotent stem cell-derived retinal organoids recapitulates retinogenesis in vivo and reveals an important role for IMPG1 and CD44 in the development of photoreceptors and interphotoreceptor matrix". In: *Acta biomaterialia* 74, pp. 207–221. DOI: 10.1016/j.actbio.2018.05.023.

Fendler, C., C. Denker, J. Harberts, P. Bayat, R. Zierold, G. Loers, M. Münzenberg, and R. H. Blick (2019). "Microscaffolds by Direct Laser Writing for Neurite Guidance Leading to Tailor-Made Neuronal Networks". In: *Advanced biosystems* 3.5, e1800329. ISSN: 2366-7478. DOI: 10.1002/adbi.201800329.

Foltz, L. P. and D. O. Clegg (2017). "Rapid, Directed Differentiation of Retinal Pigment Epithelial Cells from Human Embryonic or Induced Pluripotent Stem Cells". In: *Journal of visualized experiments : JoVE* 128. DOI: 10.3791/56274.

Frank, R. N., R. H. Amin, and J. E. Puklin (1999). "Antioxidant Enzymes in the Macular Retinal Pigment Epithelium of Eyes With Neovascular Age-related Macular Degeneration". In: *American Journal of Ophthalomology* 127/6. DOI: 10.1016/s0002-9394(99)00032-x.

Fuhrmann, S., E. M. Levine, and T. A. Reh (2000). "Extraocular mesenchyme patterns the optic vesicle during early eye development in the embryonic chick". In: *Development*.

Gale, E., V. Prince, A. Lumsden, J. Clarke, N. Holden, and M. Maden (1996). "Late effects of retinoic acid on neural crest and aspects of rhombomere". In: *Development* 122, pp. 783–793.

Gallemore, R. P., B. A. Hughes, and S. S. Miller (1997). "Retinal Pigment Epithelial Transport Mechanisms and Their Contriubutions to the Electroretinogram". In: *Progress in retinal and eye research* 16, pp. 509–566. ISSN: 1350-9462. DOI: 10.1016/S1350-9462(96)00037-7.

Gao, L. et. al (2016). "Intermittent high oxygen influences the formation of neural retinal tissue from human embryonic stem cells". In: *Scientific reports* 6, p. 29944. DOI: 10.1038/srep29944.

Ghareeb, A. E., M. Lako, and D. H. Steel (2020). "Coculture techniques for modeling retinal development and disease, and enabling regenerative medicine". In: *Stem cells translational medicine*. ISSN: 2157-6564. DOI: 10.1002/sctm.20-0201.

Giobbe, G. G. et. al (2019). "Extracellular matrix hydrogel derived from decellularized tissues enables endodermal organoid culture". In: *Nature communications* 10.1, p. 5658. DOI: 10.1038/s41467-019-13605-4.

Girotti, A. W. and T. Kriska (2004). "Role of Lipid Hydroperoxides in Photo-Oxidative Stress Signaling". In: *Antioxidants & Redox Signaling* 6, 2.

Glaser, T., L. Jepeal, J. G. Edwards, S. R. Young, J. Favor, and R. L. Maas (1994). In: *Nature genetics*. DOI: 10.1038/ng0894-463.

Glaser, T., D. S. Walton, and R. L. Maas (1992). "Genomic structure, evolutionary conservation and aniridia mutations in the human PAX6 gene". In: *Nature genetics*. DOI: 10.1038/ng1192-232.

Glass, A. S. and R. Dahm (2004). "The zebrafish as a model organism for eye development". In: *Ophthalmic research* 36.1, pp. 4–24. DOI: 10.1159/000076105.

Glinka, A., W. Wu, H. Delius, A. P. Monaghan, C. Blumenstock, and C. Niehrs (1998). "Dickkopf-1 is a member of a new family of secreted proteins and functions in head induction". In: *Nature* 391. DOI: 10.1038/34848.

Glover, J. C., J.-S. Renaud, and F. M. Rijli (2006). "Retinoic acid and hindbrain patterning". In: *Journal of neurobiology* 66.7, pp. 705–725. ISSN: 0022-3034. DOI: 10.1002/neu.20272.

Goel, R. et. al (2013). "Characterizing the normal proteome of human ciliary body". In: *Clinical Proteomics* 9. DOI: 10.1186/1559-0275-10-9.

Gong, J., H. Cai, S. Noggle, D. Paull, L. J. Rizzolo, L. V. Del Priore, and M. A. Fields (2020). "Stem cell-derived retinal pigment epithelium from patients with age-related macular degeneration exhibit reduced metabolism and matrix interactions". In: *Stem cells translational medicine* 9.3, pp. 364–376. ISSN: 2157-6564. DOI: 10.1002/sctm.19-0321.

Gonzalez-Cordero, A. et. al (2017). "Recapitulation of Human Retinal Development from Human Pluripotent Stem Cells Generates Transplantable Populations of Cone Photoreceptors". In: *Stem cell reports* 9.3, pp. 820–837. ISSN: 2213-6711. DOI: 10.1016/j.stemcr.2017.07.022.

Grapin-Botton, A., M.-A. Bonnin, L. A. McNaughton, R. Krumlauf, and N. M. Le Douarin (1995). "Plasticity of transposed rhombomeres Hox gene induction is correlated with phenotypic modifications". In: *Development* 121, pp. 2707–2721.

Green, E. S., J. L. Stubbs, and E. M. Levine (2003). "Genetic rescue of cell number in a mouse model of microphthalmia: interactions between Chx10 and G1-phase cell cycle regulators". In: *Development (Cambridge, England)* 130.3, pp. 539–552. DOI: 10.1242/dev.00275.

Grenier, K., J. Kao, and P. Diamandis (2020). "Three-dimensional modeling of human neurodegeneration: brain organoids coming of age". In: *Molecular psychiatry* 25.2, pp. 254–274. DOI: 10.1038/s41380-019-0500-7.

Grocott, T., E. Lozano-Velasco, G. F. Mok, and A. E. Münsterberg (2020). "The Pax6 master control gene initiates spontaneous retinal development via a self-organising Turing network". In: *Development (Cambridge, England)*. DOI: 10.1242/dev.185827.

Guo, Y. et. al (2019). "Modeling Retinitis Pigmentosa: Retinal Organoids Generated From the iPSCs of a Patient With the USH2A Mutation Show Early Developmental Abnormalities". In: *Frontiers in cellular neuroscience* 13, p. 361. ISSN: 1662-5102. DOI: 10.3389/fncel.2019.00361.

Guziewicz, K. E. et. al (2017). "Bestrophinopathy: An RPE-photoreceptor interface disease". In: *Progress in retinal and eye research* 58, pp. 70–88. ISSN: 1350-9462. DOI: 10.1016/j.preteyeres.2017.01.005.

Ha, T., K. H. Moon, L. Dai, J. Hatakeyama, K. Yoon, H.-S. Park, Y.-Y. Kong, K. Shimamura, and J. W. Kim (2017). "The Retinal Pigment Epithelium Is a Notch Signaling Niche in the Mouse Retina". In: *Cell reports* 19.2, pp. 351–363. DOI: 10.1016/j.celrep.2017.03.040.

Hägglund, A. C., L. Dahl, and L. Carlsson (2011). "Lhx2 is required for patterning and expansion of a distinct progenitor cell population committed to eye development". In: *PloS one* 6.8, e23387. DOI: 10.1371/journal.pone.0023387.

Hasegawa, Y., N. Takata, S. Okuda, M. Kawada, M. Eiraku, and Y. Sasai (2016). "Emergence of dorsal-ventral polarity in ESC-derived retinal tissue". In: *Development (Cambridge, England)* 143.21, pp. 3895–3906. DOI: 10.1242/dev.134601.

Hausman, R. E. (2007). "Ocular extracellular matrices in development". In: *Progress in retinal and eye research* 26.2, pp. 162–188. ISSN: 1350-9462. DOI: 10.1016/j.preteyeres.2006.11.001.

Heavner, W. and L. Pevny (2012). "Eye development and retinogenesis". In: *Cold Spring Harbor perspectives in biology* 4.12. DOI: 10.1101/cshperspect.a008391.

Hever, A. M., K. A. Williamson, and V. van Heyningen (2006). "Developmental malformations of the eye: the role of PAX6, SOX2 and OTX2". In: *Clinical genetics* 69.6, pp. 459–470. ISSN: 0009-9163. DOI: 10.1111/j.1399-0004.2006.00619.x.

Hiler, D. et. al (2015). "Quantification of Retinogenesis in 3D Cultures Reveals Epigenetic Memory and Higher Efficiency in iPSCs Derived from Rod Photoreceptors". In: *Cell stem cell* 17.1, pp. 101–115. DOI: 10.1016/j.stem.2015.05.015.

Hippler, M., E. Blasco, J. Qu, M. Tanaka, Christopher Barner-K., Martin W., and M. Bastmeyer (2019). "Controlling the shape of 3D microstructures by temperature and light". In: *Nature communications* 10.1, p. 232. DOI: 10.1038/s41467-018-08175-w.

Honjo, M., H. Tanibara, S. Suzuki, T. Tanaka, Y. Honda, and M. Takeichi (2000). "Differntial Expression of Cadherin Adhesion Receptors in Neural Retina of the Postnatal Mouse". In: *Investigative ophthalmology & visual science* 41, pp. 546–551.

Hoon, M., H. Okawa, L. Della Santina, and R. O. L. Wong (2014). "Functional architecture of the retina: development and disease". In: *Progress in retinal and eye research* 42, pp. 44–84. ISSN: 1350-9462. DOI: 10.1016/j.preteyeres.2014.06.003.

Horsford, J. D., M.-T. T. Nguyen, G. C. Sellar, R. Kothary, H. Arnheiter, and R. R. McInnes (2005). "Chx10 repression of Mitf is required for the maintenance of mammalian neuroretinal identity". In: *Development (Cambridge, England)* 132.1, pp. 177–187. DOI: 10.1242/dev.01571.

Hoshino, A. et. al (2017). "Molecular Anatomy of the Developing Human Retina: comparison mouse and human retina". In: *Developmental cell* 43.6, 763–779.e4. DOI: 10.1016/j.devcel.2017.10.029.

Hotaling, N. A., V. Khristov, Q. Wan, R. Sharma, B. S. Jha, M. Lotfi, A. Maminishkis, C. G. Simon, and K. Bharti (2016). "Nanofiber Scaffold-Based Tissue-Engineered Retinal Pigment Epithelium to Treat Degenerative Eye Diseases". In: *Journal of ocular pharmacology and therapeutics : the official journal of the Association for Ocular Pharmacology and Therapeutics* 32.5, pp. 272–285. DOI: 10.1089/jop.2015.0157.

Huang, J., Y. Liu, A. Oltean, and D. C. Beebe (2015). "Bmp4 from the optic vesicle specifies murine retina formation". In: *Developmental biology* 402.1, pp. 119–126. DOI: 10.1016/j.ydbio.2015.03.006.

Huch, M., J. A. Knoblich, M. P. Lutolf, and A. Martinez-Arias (2017). "The hope and the hype of organoid research". In: *Development (Cambridge, England)* 144.6, pp. 938–941. DOI: 10.1242/dev.150201.

Huebsch, N., P. R. Arany, A. S. Mao, D. Shvartsman, O. A. Ali, S. A. Bencherif, J. Rivera-Feliciano, and D. J. Mooney (2010). "Harnessing traction-mediated manipulation of the cell/matrix interface to control stem-cell fate". In: *Nature materials* 9.6, pp. 518–526. ISSN: 1476-1122. DOI: 10.1038/nmat2732.

Hughes, C. S., L. M. Postovit, and G. A. Lajoie (2010). "Matrigel: a complex protein mixture required for optimal growth of cell culture". In: *Proteomics* 10.9, pp. 1886–1890. DOI: 10.1002/pmic.200900758.

Hyer, J., J. Kuhlman, E. Afif, and T. Mikawa (2003). "Optic cup morphogenesis requires pre-lens ectoderm but not lens differentiation". In: *Developmental biology* 259.2, pp. 351–363. DOI: 10.1016/S0012-1606(03)00205-7.

Hynes, R. O. (1992). "Integrins: Versatility, Modulation, and Signaling in Cell Adhesion". In: *Cell* 69, pp. 11–25. DOI: 10.1016/0092-8674(92)90115-s.

Iwasaki, Y., S. Sugita, M. Mandai, S.u Yonemura, A. Onishi, S.-I. Ito, M. Mochizuki, K. Ohno-Matsui, and M. Takahashi (2016). "Differentiation/Purification Protocol for Retinal Pigment Epithelium from Mouse Induced Pluripotent Stem Cells as a Research Tool". In: *PloS one* 11.7, e0158282. DOI: 10.1371/journal.pone.0158282.

J. Hyer, T. Mima and T. Mikawa (1998). "FGF1 pattern the optic vesicle by directing the placement of the neural retina domain". In: *Development* 125, pp. 869–877.

Jackson, C. G. (1981). "Prenatal development of the microphthalmic eye in the golden hamster". In: *Journal of Morphology* 167, pp. 65–90. DOI: 10.1002/jmor.1051670107.

Jeong, S. Y., S. Lee, W. H. Choi, J. H. Jee, H.-R. Kim, and J. Yoo (2020). "Fabrication of Dentin-Pulp-Like Organoids Using Dental-Pulp Stem Cells". In: *Cells* 9.3. ISSN: 2073-4409. DOI: 10.3390/cells9030642.

Jiang, X., Y. Peng, C. Yang, W. Liu, and B. Han (2018). "The feasibility study of an in situ marine polysaccharide-based hydrogel as the vitreous substitute". In: *Journal of biomedical materials research. Part A* 106.7, pp. 1997–2006. DOI: 10.1002/jbm.a.36403.

Johnson, A. T., L. Wang, and S. J. Gillett (1999). "High affinity retinoic acid receptor antagonists: analogs of AGN193109". In: *Bioorganig & Medicinal Chemistry Letters* 9, pp. 573–576. DOI: 10.1016/s0960-894x(99)00047-5.

Kadowaki, M., S. Nakamura, O. Machon, S. Krauss, G. L. Radice, and M. Takeichi (2007). "N-cadherin mediates cortical organization in the mouse brain". In: *Developmental biology* 304.1, pp. 22–33. DOI: 10.1016/j.ydbio.2006.12.014.

Kaempf, S., P. Walter, A. K. Salz, and G. Thumann (2008). "Novel organotypic culture model of adult mammalian neurosensory retina in co-culture with retinal pigment epithelium". In: *Journal of neuroscience methods* 173.1, pp. 47–58. ISSN: 0165-0270. DOI: 10.1016/j.jneumeth.2008.05.018.

Kaewkhaw, R., K. D. Kaya, M. Brooks, K. Homma, J. Zou, V. Chaitankar, M. Rao, and A. Swaroop (2015). "Transcriptome Dynamics of Developing Photoreceptors in Three-Dimensional Retina Cultures Recapitulates Temporal Sequence of Human Cone and Rod Differentiation Revealing Cell Surface Markers and Gene Networks". In: *Stem cells (Dayton, Ohio)* 33.12, pp. 3504–3518. DOI: 10.1002/stem.2122.

Kaewkhaw, R. et. al (2016). "Treatment Paradigms for Retinal and Macular Diseases Using 3-D Retina Cultures Derived From Human Reporter Pluripotent Stem Cell Lines". In: *Investigative ophthalmology & visual science* 57.5, ORSFl1–ORSFl11. DOI: 10.1167/iovs.15-17639.

Kanamoto, T., T. Ue, T. Yokoyama, N. Souchelnytskyi, and Y. Kiuchi (2009). "Proteomic study of DBA/2J mice retina: Down-regulation of Integrin beta7 correlated with retinal ganglion cell death". In: *Proteomics* 9.21, pp. 4962–4969. DOI: 10.1002/pmic.200800978.

Kar, S. K., B. van der Hee, L. M. P. Loonen, N. Taverne, J. J. Taverne-Thiele, D. Schokker, M. A. Smits, A. J. M. Jansman, and J. M. Wells (2020). "Effects of undigested protein-rich ingredients on polarised small intestinal organoid monolayers". In: *Journal of animal science and biotechnology* 11, p. 51. ISSN: 1674-9782. DOI: 10.1186/s40104-020-00443-4.

Kassen, S. C., R. Thummel, C. T. Burket, L. A. Campochiaro, M. J. Harding, and D. R. Hyde (2008). "The Tg(ccnb1:EGFP) transgenic zebrafish line labels proliferating cells during retinal development and regeneration". In: *Molecular Vision* 14, pp. 951–963.

Kaufman, M. L., K. U. Park, N. B. Goodson, S. Chew, S. Bersie, K. L. Jones, D. A. Lamba, and J. A. Brzezinski (2019). "Transcriptional profiling of murine retinas undergoing semi-synchronous cone photoreceptor differentiation". In: *Developmental biology* 453.2, pp. 155–167. DOI: 10.1016/j.ydbio.2019.05.016.

Kawasaki, H. et. al (2002). "Generation of dopaminergic neurons and pigmented epithelia from primate ES cells by stromal cell-derived inducing activity". In: *Proceedings of the National Academy of Sciences of the United States of America* 99, pp. 1580–1585.

Kaya, K. D., H. Y. Chen, M. J. Brooks, and A. Swaroop (2019). "Transcriptome-based molecular staging of human stem cell-derived retinal organoids uncovers accelerated photoreceptor differentiation by 9-cis retinal". In: *Molecular Vision*.

Kelley, M. W., J. K. Turner, and T. A. Reh (1994). "Retinoic acid promotes differentiation of photoreceptors in vitro". In: *Development* 120, pp. 2091–2102.

Kendall, K. (2015). "Cell adhesion century: culture breakthrough". In: *Philosophical transactions of the Royal Society of London. Series B, Biological sciences* 370.1661, p. 20140025. DOI: 10.1098/rstb.2014.0025.

Kim, E. K., H.-Y. L. Park, and C. K. Park (2017). "Relationship between Retinal Inner Nuclear Layer Thickness and Severity of Visual Field Loss in Glaucoma". In: *Scientific reports* 7.1, p. 5543. DOI: 10.1038/s41598-017-05282-4.

Kim, S. et. al (2019). "Generation, transcriptome profiling, and functional validation of cone-rich human retinal organoids". In: *Proceedings of the National Academy of Sciences of the United States of America* 116.22, pp. 10824–10833. DOI: 10.1073/pnas.1901572116.

Kim, S. E., K. Mi Shim, K. Jang, J.-H. Shim, and S. S. Kang (2018). "Three-Dimensional Printing-based Reconstruction of a Maxillary Bone Defect in a Dog Following Tumor Removal". In: *In vivo (Athens, Greece)* 32.1, pp. 63–70. DOI: 10.21873/invivo.11205.

Kim, Y., J. Jeong, and D. Choi (2020). "Small-molecule-mediated reprogramming: a silver lining for regenerative medicine". In: *Experimental & molecular medicine*. DOI: 10.1038/s12276-020-0383-3.

Kleinman, H. K. and G. R. Martin (2005). "Matrigel: basement membrane matrix with biological activity". In: *Seminars in cancer biology* 15.5, pp. 378–386. ISSN: 1044-579X. DOI: 10.1016/j.semcancer.2005.05.004.

Kleinman, H. K., M. L. McGarvey, L. A. Liotta, P. G. Robey, K. Tryggvason, and G. R. Martin (1982). "Isolation and characterization of type IV procollagen, laminin, and heparan sulfate proteoglycan from the EHS sarcoma". In: *Biochemistry* 21.24, pp. 6188–6193. ISSN: 0006-2960. DOI: 10.1021/bi00267a025.

Koike, C., A. Nishida, K. Akimoto, M.-a. Nakaya, T. Noda, S. Ohno, and T. Furukawa (2005). "Function of atypical protein kinase C lambda in differentiating photoreceptors is required for proper lamination of mouse retina". In: *The Journal of neuroscience : the official journal of the Society for Neuroscience* 25.44, pp. 10290–10298. DOI: 10.1523/JNEUROSCI.3657-05.2005.

Krencik, R. et. al (2017). "Systematic Three-Dimensional Coculture Rapidly Recapitulates Interactions between Human Neurons and Astrocytes". In: *Stem cell reports* 9.6, pp. 1745–1753. ISSN: 2213-6711. DOI: 10.1016/j.stemcr.2017.10.026.

Kruczek, K. and A. Swaroop (2020). "Pluripotent stem cell-derived retinal organoids for disease modeling and development of therapies". In: *Stem cells (Dayton, Ohio)*. DOI: 10.1002/stem.3239.

Kruczek, K. et. al (2017). "Differentiation and Transplantation of Embryonic Stem Cell-Derived Cone Photoreceptors into a Mouse Model of End-Stage Retinal Degeneration". In: *Stem cell reports* 8.6, pp. 1659–1674. ISSN: 2213-6711. DOI: 10.1016/j.stemcr.2017.04.030.

Kubo, F. and S. Nakagawa (2008). "Wnt signaling in retinal stem cells and regeneration". In: *Development, growth & differentiation* 50.4, pp. 245–251. DOI: 10.1111/j.1440-169X.2008.01033.x.

Kubo, F., M. Takeichi, and S. Nakagawa (2003). "Wnt2b controls retinal cell differentiation at the ciliary marginal zone". In: *Development (Cambridge, England)* 130.3, pp. 587–598. DOI: 10.1242/dev.00244.

– (2005). “Wnt2b inhibits differentiation of retinal progenitor cells in the absence of Notch activity by downregulating the expression of proneural genes”. In: *Development (Cambridge, England)* 132.12, pp. 2759–2770. DOI: 10.1242/dev.01856.

Kundu, J., A. Michaelson, K. Talbot, P. Baranov, M. J. Young, and R. L. Carrier (2016). “Decellularized retinal matrix: Natural platforms for human retinal progenitor cell culture”. In: *Acta biomaterialia* 31, pp. 61–70. DOI: 10.1016/j.actbio.2015.11.028.

Kusakabe, T. G., N. Takimoto, M. Jin, and M. Tsuda (2009). “Evolution and the origin of the visual retinoid cycle in vertebrates”. In: *Philosophical transactions of the Royal Society of London. Series B, Biological sciences* 364.1531, pp. 2897–2910. DOI: 10.1098/rstb.2009.0043.

Kuwahara, A., C. Ozone, T. Nakano, K. Saito, M. Eiraku, and Y. Sasai (2015). “Generation of a ciliary margin-like stem cell niche from self-organizing human retinal tissue”. In: *Nature communications* 6, p. 6286. DOI: 10.1038/ncomms7286.

Kwon, W. and S. A. Freeman (2020). “Phagocytosis by the Retinal Pigment Epithelium: Recognition, Resolution, Recycling”. In: *Frontiers in immunology* 11, p. 604205. DOI: 10.3389/fimmu.2020.604205.

Lamba, D., M. O. Karl, C. B. Ware, and T. A. Reh (2006). “Efficient generation of retinal progenitor cells from human embryonic stem cells”. In: *PNAS*. DOI: 10.1073/pnas.0601990103.

Lamba, D. A., J. Gust, and T. A. Reh (2009). “Transplantation of human embryonic stem cell-derived photoreceptors restores some visual function in Crx-deficient mice”. In: *Cell stem cell* 4.1, pp. 73–79. DOI: 10.1016/j.stem.2008.10.015.

Lancaster, M. A. et. al (2013). “Cerebral organoids model human brain development and microcephaly”. In: *Nature* 501.7467, pp. 373–379. DOI: 10.1038/nature12517.

Layer, P. G., A. Robitzki, A. Rothermel, and E. Willbold (2002). “Of layers and spheres: the reaggregate approach in tissue engineering”. In: *Trends in neurosciences* 25.3, pp. 131–134. DOI: 10.1016/s0166-2236(00)02036-1.

Layer, P. G. and E. Willbold (1989). “Embryonic chicken retinal cells can regenerate all cell layers in vitro, but ciliary pigmented cells induce their correct polarity”. In: *Cell and tissue research* 258.2, pp. 233–242. ISSN: 0302-766X. DOI: 10.1007/BF00239443.

Lee, C., T. Herman, T. R. Clandini, R. Lee, and S. L. Zipursky (2001). “N-Cadherin Regulates Target Specificity in the Drosophila Visual System”. In: *Neuron*.

Leu, S. T. et. al (2004). “Integrin alpha4beta1 function is required for cell survival in developing retina”. In: *Developmental biology* 276.2, pp. 416–430. DOI: 10.1016/j.ydbio.2004.09.003.

Li, H.-s., C. Tierney, L. Wen, J. Y. Wu, and Y. Rao (1997). “A single morphogenetic field gives rise to two retinal primordia under the influence of the prechordal plate”. In: *Development* 124, pp. 603–615.

Li, K. et. al (2017). "HiPSC-derived retinal ganglion cells grow dendritic arbors and functional axons on a tissue-engineered scaffold". In: *Acta biomaterialia* 54, pp. 117–127. DOI: 10.1016/j.actbio.2017.02.032.

Li, M. and D. S. Sakaguchi (2004). "Inhibition of integrin-mediated adhesion and signaling disrupts retinal development". In: *Developmental biology* 275.1, pp. 202–214. DOI: 10.1016/j.ydbio.2004.08.005.

Li, X., B. Liu, B. Pei, J. Chen, D. Zhou, J. Peng, X. Zhang, W. Jia, and T. Xu (2020). "Inkjet Bioprinting of Biomaterials". In: *Chemical reviews*. DOI: 10.1021/acs.chemrev.0c00008.

Ligon, S. C., R. Liska, J. Stampfl, M. Gurr, and R. Mülhaupt (2017). "Polymers for 3D Printing and Customized Additive Manufacturing". In: *Chemical reviews* 117.15, pp. 10212–10290. DOI: 10.1021/acs.chemrev.7b00074.

Lindborg, B. A. et. al (2016). "Rapid Induction of Cerebral Organoids From Human Induced Pluripotent Stem Cells Using a Chemically Defined Hydrogel and Defined Cell Culture Medium". In: *Stem cells translational medicine* 5.7, pp. 970–979. ISSN: 2157-6564. DOI: 10.5966/sctm.2015-0305.

Liu, I. S. C., J.-d. Chen, L. Ploder, D. Vidgen, D. van der Kooy, V. I. Kalnins, and R. R. McInnes (1994). "Developmental Expression of a Novel Murine Homeobox Gene (Chx10): Evidence for ROles in Determination of the Neuroretina and Inner Nuclear Layer". In: *Neuron* 13, pp. 377–393. DOI: 10.1016/0896-6273(94)90354-9.

Liu, W., O. Lagutin, E. Swindell, M. Jamrich, and G. Oliver (2010). "Neuroretina specification in mouse embryos requires Six3-mediated suppression of Wnt8b in the anterior neural plate". In: *The Journal of clinical investigation* 120.10, pp. 3568–3577. DOI: 10.1172/JCI43219.

Liu, Z., N. Yu, F. G. Holz, F. Yang, and B. V. Stanzel (2014). "Enhancement of retinal pigment epithelial culture characteristics and subretinal space tolerance of scaffolds with 200 nm fiber topography". In: *Biomaterials* 35.9, pp. 2837–2850. ISSN: 0142-9612. DOI: 10.1016/j.biomaterials.2013.12.069.

Lorber, B., W.-K. Hsiao, I. M. Hutchings, and K. R. Martin (2014). "Adult rat retinal ganglion cells and glia can be printed by piezoelectric inkjet printing". In: *Biofabrication* 6.1, p. 015001. DOI: 10.1088/1758-5082/6/1/015001.

Lukovic, D. et. al (2020). "Retinal Organoids derived from hiPSCs of an AIPL1-LCA Patient Maintain Cytoarchitecture despite Reduced levels of Mutant AIPL1". In: *Scientific Reports* 10.1, p. 391. DOI: 10.1038/s41598-020-62047-2.

M. Carl, F. Loosli and J. Wittbrodt (2002). "Loss of Six3 function in medaka fish". In: *Development* 129, pp. 4057–4063.

M.-T. T. Nguyen and H. Arnheiter (2000). "Role of FGF and MITF in eye development". In: *Development* 127, pp. 3581–3591.

Mangelsdorf, D. J. and R. M. Evans (1995). "The RXR Heterodimers and Orphan Receptors". In: *Cell* 83, pp. 841–850. DOI: 10.1016/0092-8674(95)90200-7.

Mansour, A. A. et. al (2018). "An in vivo model of functional and vascularized human brain organoids". In: *Nature biotechnology* 36.5, pp. 432–441. DOI: 10.1038/nbt.4127.

Mao, X. et. al (2019). "Single-Cell RNA Sequencing of hESC-Derived 3D Retinal Organoids Reveals Novel Genes Regulating RPC Commitment in Early Human Retinogenesis". In: *Stem cell reports* 13.4, pp. 747–760. ISSN: 2213-6711. DOI: 10.1016/j.stemcr.2019.08.012.

Martin, G. R. (1981). "Isolation of a pluripotent cell line from early mouse embryos cultured in medium conditioned by teratocarcinoma stem cells". In: *Proceedings of the National Academy of Sciences of the United States of America* 78.12, pp. 7634–7638. DOI: 10.1073/pnas.78.12.7634.

Martinez-Morales, J. R., F. Del Bene, G. Nica, M. Hammerschmidt, P. Bovolenta, and J. Wittbrodt (2005). "Differentiation of the vertebrate retina is coordinated by an FGF signaling center". In: *Developmental cell* 8.4, pp. 565–574. DOI: 10.1016/j.devcel.2005.01.022.

Martinez-Morales, J. R. and J. Wittbrodt (2009). "Shaping the vertebrate eye". In: *Current opinion in genetics & development* 19.5, pp. 511–517. DOI: 10.1016/j.gde.2009.08.003.

Martyn, I., E. D. Siggia, and A. H. Brivanlou (2019). "Mapping cell migrations and fates in a gastruloid model to the human primitive streak". In: *Development (Cambridge, England)* 146.17. DOI: 10.1242/dev.179564.

Maruo, S., O. Nakamura, and S. Kawata (1997). "Three-dimensional microfabrication with two-photon-absorbed photopolymerization". In: *Optic Letters* 22/2. DOI: 10.1364/OL.22.000132.

Maruotti, J. et. al (2015). "Small-molecule-directed, efficient generation of retinal pigment epithelium from human pluripotent stem cells". In: *Proceedings of the National Academy of Sciences of the United States of America* 112.35, pp. 10950–10955. DOI: 10.1073/pnas.1422818112.

Masai, I. et. al (2003). "N-cadherin mediates retinal lamination, maintenance of forebrain compartments and patterning of retinal neurites". In: *Development (Cambridge, England)* 130.11, pp. 2479–2494. DOI: 10.1242/dev.00465.

Masters, K. S., D. N. Shah, G. Walker, L. A. Leinwand, and K. S. Anseth (2004). "Designing scaffolds for valvular interstitial cells: cell adhesion and function on naturally derived materials". In: *Journal of biomedical materials research. Part A* 71.1, pp. 172–180. DOI: 10.1002/jbm.a.30149.

Matsunaga, M., K. Hatta, and M. Takeichi (1988). "Role of N-Cadherin Cell Adhesion Molecules in the Histogenesis of Neural Retina". In: *Neuron* 1, pp. 289–295.

Matsuoka, R. L., Z. Jiang, I. S. Samuels, K. T. Nguyen-Ba-Charvet, L. O. Sun, N. S. Peachey, A. Chédotal, K.-W. Yau, and A. L. Kolodkin (2012). "Guidance-cue control of horizontal cell morphology, lamination, and synapse formation in

the mammalian outer retina". In: *The Journal of neuroscience : the official journal of the Society for Neuroscience* 32.20, pp. 6859–6868. DOI: 10.1523/JNEUROSCI.0267-12.2012.

Matsuoka, R. L. et. al (2011). "Class 5 transmembrane semaphorins control selective Mammalian retinal lamination and function". In: *Neuron* 71.3, pp. 460–473. DOI: 10.1016/j.neuron.2011.06.009.

McUsic, A. C., D. A. Lamba, and T. A. Reh (2012). "Guiding the morphogenesis of dissociated newborn mouse retinal cells and hES cell-derived retinal cells by soft lithography-patterned microchannel PLGA scaffolds". In: *Biomaterials* 33.5, pp. 1396–1405. ISSN: 0142-9612. DOI: 10.1016/j.biomaterials.2011.10.083.

Medina-Martinez, O., F. Amaya-Manzanares, C. Liu, M. Mendoza, R. Shah, L. Zhang, R. R. Behringer, K. A. Mahon, and M. Jamrich (2009). "Cell-autonomous requirement for rx function in the mammalian retina and posterior pituitary". In: *PloS one* 4.2, e4513. DOI: 10.1371/journal.pone.0004513.

Mellough, C. B., J. Collin, M. Khazim, K. White, E. Sernagor, D. H. W. Steel, and M. Lako (2015). "IGF-1 Signaling Plays an Important Role in the Formation of Three-Dimensional Laminated Neural Retina and Other Ocular Structures From Human Embryonic Stem Cells". In: *Stem cells (Dayton, Ohio)* 33.8, pp. 2416–2430. DOI: 10.1002/stem.2023.

Mellough, C. B. et. al (2019). "Systematic Comparison of Retinal Organoid Differentiation from Human Pluripotent Stem Cells Reveals Stage Specific, Cell Line, and Methodological Differences". In: *Stem cells translational medicine* 8.7, pp. 694–706. ISSN: 2157-6564. DOI: 10.1002/sctm.18-0267.

Meyer, J. S., R. L. Shearer, E. E. Capowski, L. S. Wright, K. A. Wallace, E. L. McMillan, Zhang S.-C., and D. M. Gamm (2009). "Modeling early retinal development with human embryonic and induced pluripotent stem cells". In: *PNAS* 106/39. DOI: 10.1073/pnas.0905245106.

Meyer, J. S. et. al (2011). "Optic Vesicle–like Structures Derived from Human Pluripotent Stem Cells Facilitate a Customized Approach to Retinal Disease Treatment". In: *Stem Cell* 29, pp. 1206–1218.

Miesfeld, J. B. and N. L. Brown (2019). "Eye organogenesis: A hierarchical view of ocular development". In: *Current topics in developmental biology* 132, pp. 351–393. DOI: 10.1016/bs.ctdb.2018.12.008.

Minn, K. T., Y. C. Fu, S. He, S. Dietmann, S. C.. George, M. A. Anastasio, S. A. Morris, and L. Solnica-Krezel (2020). "High-resolution transcriptional and morphogenetic profiling of cells from micropatterned human ESC gastruloid cultures". In: *eLife*.

Mitchell, P., G. Liew, B. Gopinath, and T. Y. Wong (2018). "Age-related macular degeneration". In: *The Lancet* 392.10153, pp. 1147–1159. ISSN: 01406736. DOI: 10.1016/S0140-6736(18)31550-2.

Molotkov, A., N. Molotkova, and G. Duester (2006). "Retinoic acid guides eye morphogenetic movements via paracrine signaling but is unnecessary for retinal dorsoventral patterning". In: *Development (Cambridge, England)* 133.10, pp. 1901–1910. DOI: 10.1242/dev.02328.

Moris, N., K. Anlas, S. C. van den Brink, A. Alemany, J. Schröder, S. Ghimire, T. Balayo, A. van Oudenaarden, and A. Martinez Arias (2020). "An in vitro model of early anteroposterior organization during human development". In: *Nature* 582.7812, pp. 410–415. DOI: 10.1038/s41586-020-2383-9.

Müller, F., H. Rohrer, and A. Vogel-Höpker (2007). "Bone morphogenetic proteins specify the retinal pigment epithelium in the chick embryo". In: *Development (Cambridge, England)* 134.19, pp. 3483–3493. DOI: 10.1242/dev.02884.

Murali, D., S. Yoshikawa, R. R. Corrigan, D. J. Plas, M. C. Crair, G. Oliver, K. M. Lyons, Y. Mishina, and Y. Furuta (2005). "Distinct developmental programs require different levels of Bmp signaling during mouse retinal development". In: *Development (Cambridge, England)* 132.5, pp. 913–923. DOI: 10.1242/dev.01673.

Murphy, A. R., A. Laslett, C. M. O'Brien, and N. R. Cameron (2017). "Scaffolds for 3D in vitro culture of neural lineage cells". In: *Acta biomaterialia* 54, pp. 1–20. DOI: 10.1016/j.actbio.2017.02.046.

Mussard, E. et. al (2020). "Culture of rabbit caecum organoids by reconstituting the intestinal stem cell niche in vitro with pharmacological inhibitors or L-WRN conditioned medium". In: *Stem cell research* 48, p. 101980. DOI: 10.1016/j.scr.2020.101980.

Mustafi, D., A. H. Engel, and K. Palczewski (2009). "Structure of cone photoreceptors". In: *Progress in retinal and eye research* 28.4, pp. 289–302. ISSN: 1350-9462. DOI: 10.1016/j.preteyeres.2009.05.003.

Nakagawa, S., S. Takada, R. Takada, and M. Takeichi (2003). "Identification of the laminar-inducing factor: Wnt-signal from the anterior rim induces correct laminar formation of the neural retina in vitro". In: *Developmental biology* 260.2, pp. 414–425. DOI: 10.1016/S0012-1606(03)00320-8.

Nakano, T. et. al (2012). "Self-formation of optic cups and storable stratified neural retina from human ESCs". In: *Cell stem cell* 10.6, pp. 771–785. DOI: 10.1016/j.stem.2012.05.009.

Nava, M. M., T. Zandrini, G. Cerullo, R. Osellame, and M. T. Raimondi (2017). "3D Stem Cell Niche Engineering via Two-Photon Laser Polymerization". In: *Methods in molecular biology (Clifton, N.J.)* 1612, pp. 253–266. DOI: 10.1007/978-1-4939-7021-6$_$19.

Naylor, A., A. Hopkins, N. Hudson, and M. Campbell (2019). "Tight Junctions of the Outer Blood Retina Barrier". In: *International journal of molecular sciences* 21.1. DOI: 10.3390/ijms21010211.

Neumann, C. J. and C. Nuesslein-Volhard (2000). "Patterning of the zebrafish retina by a wave of sonic hedgehog activity". In: *Science (New York, N.Y.)* 289.5487, pp. 2137–2139. DOI: 10.1126/science.289.5487.2137.

Nguyen, H. V., Y. Li, and S. H. Tsang (2015). "Patient-Specific iPSC-Derived RPE for Modeling of Retinal Diseases". In: *Journal of clinical medicine* 4.4, pp. 567–578. ISSN: 2077-0383. DOI: 10.3390/jcm4040567.

Nickels, S. L., J. Modamio, B. Mendes-Pinheiro, A. S. Monzel, F. Betsou, and J. C. Schwamborn (2020). "Reproducible generation of human midbrain organoids for in vitro modeling of Parkinson's disease". In: *Stem cell research* 46, p. 101870. DOI: 10.1016/j.scr.2020.101870.

Nornes, H. O., G. R. Dressler, E. W. Knapik, U. Deutsch, and P. Gruss (1990). "Spatially and temporally restricted expression of Pax2 during murine neurogenesis". In: *Development* 109, pp. 797–809.

Nowak, J. Z. (2006). "Age-related macular degeneration (AMD): pathogenesis and therapy". In: *Pharmacological Reports* 58, pp. 353–363.

Nozaki, K., W. Mochizuki, Y. Matsumoto, T. Matsumoto, M. Fukuda, T. Mizutani, M. Watanabe, and T. Nakamura (2016). "Co-culture with intestinal epithelial organoids allows efficient expansion and motility analysis of intraepithelial lymphocytes". In: *Journal of gastroenterology* 51.3, pp. 206–213. DOI: 10.1007/s00535-016-1170-8.

Osakada, F., Z.-B. Jin, Y. Hirami, H. Ikeda, T. Danjyo, K. Watanabe, Y. Sasai, and M. Takahashi (2009). "In vitro differentiation of retinal cells from human pluripotent stem cells by small-molecule induction". In: *Journal of cell science* 122.Pt 17, pp. 3169–3179. DOI: 10.1242/jcs.050393.

"Osteogenic differentiation of human mesenchymal stem cells in 3-D Zr-Si organic-inorganic scaffolds produced by two-photon polymerization technique" (2015). In: *PloS one* 10.2, e0118164. DOI: 10.1371/journal.pone.0118164.

Ovando-Roche, P. et. al (2018). "Use of bioreactors for culturing human retinal organoids improves photoreceptor yields". In: *Stem cell research & therapy* 9.1, p. 156. DOI: 10.1186/s13287-018-0907-0.

Pandit, T., V. K. Jidigam, C. Patthey, and L. Gunhaga (2015). "Neural retina identity is specified by lens-derived BMP signals". In: *Development (Cambridge, England)* 142.10, pp. 1850–1859. DOI: 10.1242/dev.123653.

Pao, Y.–H. and P. M. Rentzepis (1965). "Multiphoton Absorption and Optical–Harmonic Generation in Highly Absorbing Molecular Crystals". In: *The Journal of Chemical Physics* 43.4, pp. 1281–1286. ISSN: 0021-9606. DOI: 10.1063/1.1696915.

Pariser, H. P., J. Zhang, and R. E. Hausman (2000). "The cell adhesion molecule retina cognin is a cell surface protein disulfide isomerase that uses disulfide exchange activity to modulate cell adhesion". In: *Experimental cell research* 258.1, pp. 42–52. DOI: 10.1006/excr.2000.4931.

Park, J., P. Baranov, A. Aydin, H. Abdelgawad, D. Singh, W. Niu, M. Kurisawa, M. Spector, and M. J. Young (2019). "In Situ Cross-linking Hydrogel as a Vehicle for Retinal Progenitor Cell Transplantation". In: *Cell transplantation* 28.5, pp. 596–606. DOI: 10.1177/0963689719825614.

Park, S. Y., J. Park, S. H. Sim, M. G. Sung, K. S. Kim, B. H. Hong, and S. Hong (2011). "Enhanced differentiation of human neural stem cells into neurons on graphene". In: *Advanced materials (Deerfield Beach, Fla.)* 23.36, H263–7. DOI: 10.1002/adma.201101503.

Pascolini, D. and S. P. Mariotti (2012). "Global estimates of visual impairment: 2010". In: *The British journal of ophthalmology* 96.5, pp. 614–618. DOI: 10.1136/bjophthalmol-2011-300539.

Pasteels, B., J. Rogers, F. Blachier, and R. Pochet (1990). "Calbindin and calretinin localization in retina from different species". In: *Visual neuroscience* 5, pp. 1–16. DOI: 10.1017/s0952523800000031.

Pearson, R. A. et. al (2016). "Donor and host photoreceptors engage in material transfer following transplantation of post-mitotic photoreceptor precursors". In: *Nature communications* 7, p. 13029. DOI: 10.1038/ncomms13029.

Pera, E. M., O. Wessely, S.-Y. Li, and E. M. de Robertis (2001). "Neural and Head induction by Insulin-like Growth Factor Signaling". In: *Developmental cell*. DOI: 10.1016/s1534-5807(01)00069-7.

Perepelkina, Tatiana, Evgenii Kegeles, and Petr Baranov (2019). "Optimizing the Conditions and Use of Synthetic Matrix for Three-Dimensional In Vitro Retinal Differentiation from Mouse Pluripotent Cells". In: *Tissue engineering. Part C, Methods* 25.7, pp. 433–445. DOI: 10.1089/ten.TEC.2019.0053.

Pham, M. T., K. M. Pollock, M. D. Rose, W. A. Cary, H. R. Stewart, P. Zhou, J. A. Nolta, and B. Waldau (2018). "Generation of human vascularized brain organoids". In: *Neuroreport* 29.7, pp. 588–593. DOI: 10.1097/WNR.0000000000001014.

Philippeos, C., R. D. Hughes, A. Dhawan, and R. R. Mitry (2012). "Introduction to cell culture". In: *Methods in molecular biology (Clifton, N.J.)* 806, pp. 1–13. DOI: 10.1007/978-1-61779-367-7$_$1.

Picker, A. and M. Brand (2005). "Fgf signals from a novel signaling center determine axial patterning of the prospective neural retina". In: *Development (Cambridge, England)* 132.22, pp. 4951–4962. DOI: 10.1242/dev.02071.

Picker, A., F. Cavodeassi, A. Machate, S. Bernauer, S. Hans, G. Abe, K. Kawakami, S. W. Wilson, and M. Brand (2009). "Dynamic coupling of pattern formation and morphogenesis in the developing vertebrate retina". In: *PLoS biology* 7.10, e1000214. DOI: 10.1371/journal.pbio.1000214.

Pokutta, S. and W. I. Weis (2007). "Structure and mechanism of cadherins and catenins in cell-cell contacts". In: *Annual review of cell and developmental biology* 23, pp. 237–261. ISSN: 1081-0706. DOI: 10.1146/annurev.cellbio.22.010305.104241.

Ponnalagu, M., M. Subramani, C. Jayadev, R. Shetty, and D. Das (2017). "Retinal pigment epithelium-secretome: A diabetic retinopathy perspective". In: *Cytokine* 95, pp. 126–135. DOI: 10.1016/j.cyto.2017.02.013.

Poskanzler, K., L. A. Needleman, O. Bozdai, and G. W. Hutley (2003). "N-cadherin regulates ingrowth and laminar targeting of thalamocortical axons". In: *Journal of neuroscience research*.

Qian, X. et. al (2016). "Brain-Region-Specific Organoids Using Mini-bioreactors for Modeling ZIKV Exposure". In: *Cell* 165.5, pp. 1238–1254. DOI: 10.1016/j.cell.2016.04.032.

Qin, H., A. Zhao, and X. Fu (2017). "Small molecules for reprogramming and transdifferentiation". In: *Cellular and molecular life sciences : CMLS* 74.19, pp. 3553–3575. DOI: 10.1007/s00018-017-2586-x.

Quadrato, G. et. al (2017). "Cell diversity and network dynamics in photosensitive human brain organoids". In: *Nature* 2017.545. DOI: 10.1038/nature22047.

Quarta, M. et. al (2016). "An artificial niche preserves the quiescence of muscle stem cells and enhances their therapeutic efficacy". In: *Nature biotechnology* 34.7, pp. 752–759. DOI: 10.1038/nbt.3576.

Raimondi, M. T., S. M. Eaton, M. Laganà, V. Aprile, M. M. Nava, G. Cerullo, and R. Osellame (2013). "Three-dimensional structural niches engineered via two-photon laser polymerization promote stem cell homing". In: *Acta biomaterialia* 9.1, pp. 4579–4584. DOI: 10.1016/j.actbio.2012.08.022.

Rasin, M.-R. et. al (2007). "Numb and Numbl are required for maintenance of cadherin-based adhesion and polarity of neural progenitors". In: *Nature neuroscience* 10.7, pp. 819–827. DOI: 10.1038/nn1924.

Rault, I., V. Frei, and D. Herbage (1996). "Evaluation of different chemical methods for cros-linking collagen gel, films and sponges". In: *Journal of materials science. Materials in medicine*.

Reichman, S. et. al (2017). "Generation of Storable Retinal Organoids and Retinal Pigmented Epithelium from Adherent Human iPS Cells in Xeno-Free and Feeder-Free Conditions". In: *Stem cells (Dayton, Ohio)* 35.5, pp. 1176–1188. DOI: 10.1002/stem.2586.

Richler, Kai (2019). "Differentiation of mouse embryonic stem cells to retinal pigment epithelium". In: *Master Thesis*.

Richter, B., V. Hahn, S. Bertels, T. K. Claus, M. Wegener, G. Delaittre, C. Barner-Kowollik, and M. Bastmeyer (2017). "Guiding Cell Attachment in 3D Microscaffolds Selectively Functionalized with Two Distinct Adhesion Proteins". In: *Advanced materials (Deerfield Beach, Fla.)* 29.5. DOI: 10.1002/adma.201604342.

Rizzolo, L. J., S. Peng, Y. Luo, and W. Xiao (2011). "Integration of tight junctions and claudins with the barrier functions of the retinal pigment epithelium". In: *Progress in retinal and eye research* 30.5, pp. 296–323. ISSN: 1350-9462. DOI: 10.1016/j.preteyeres.2011.06.002.

Robertis, E. de and A. Lasansky (1958). "Submicroscopic Organization of Retinal Cones of the Rabbit". In: *J. Biophysic. and Biochem. Cytol.* 4. DOI: 10.1083/jcb.4.6.743.

Robles, E. and H. Baier (2012). "Assembly of synaptic laminae by axon guidance molecules". In: *Current opinion in neurobiology* 22.5, pp. 799–804. DOI: 10.1016/j.conb.2012.04.014.

Rothermel, A., E. Willbold, Willem J. Degrip, and P. G. Layer (1997). "Pigmented epithelium induces complete retinal reconstitution from dispersed embryonic chick retinae in reaggregation culture". In: *Proc. R. Soc. Lond.*, pp. 1293–1302.

Rowan, S. and C. L. Cepko (2005). "A POU factor binding site upstream of the Chx10 homeobox gene is required for Chx10 expression in subsets of retinal progenitor cells and bipolar cells". In: *Developmental biology* 281.2, pp. 240–255. DOI: 10.1016/j.ydbio.2005.02.023.

Ruberte, E., P. Dolle, P. Chambon, and G. Morriss-Kay (1991). "Retinoic acid receptors and cellular retinoid binding proteins. Their differential pattern of transcription during early morphogenesis in mouse embryos". In: *Development* 111, pp. 45–60.

Ruberte, E., P. Dolle, A. Krust, A. Zelent, G. Morriss-Kay, and P. Chambon (1990). "Specific spatial and temporal distribution of retinoic acid receptor gamma transcripts during mouse embryogenesis". In: *Development* 108, pp. 213–222.

Saari, J. C. (2016). *The Biochemistry of Retinoid Signaling II*. Vol. 81. Dordrecht: Springer Netherlands. ISBN: 978-94-024-0943-7. DOI: 10.1007/978-94-024-0945-1.

Sakaguchi, H., Y. Ozaki, T. Ashida, T.i Matsubara, N. Oishi, S. Kihara, and J. Takahashi (2019). "Self-Organized Synchronous Calcium Transients in a Cultured Human Neural Network Derived from Cerebral Organoids". In: *Stem cell reports* 13.3, pp. 458–473. ISSN: 2213-6711. DOI: 10.1016/j.stemcr.2019.05.029.

Sakakura, E., M. Eiraku, and N. Takata (2016). "Specification of embryonic stem cell-derived tissues into eye fields by Wnt signaling using rostral diencephalic tissue-inducing culture". In: *Mechanisms of development* 141, pp. 90–99. DOI: 10.1016/j.mod.2016.05.001.

Salero, E., T. A. Blenkinsop, B. Corneo, A. Harris, D. Rabin, J. H. Stern, and S. Temple (2012). "Adult human RPE can be activated into a multipotent stem cell that produces mesenchymal derivatives". In: *Cell stem cell* 10.1, pp. 88–95. DOI: 10.1016/j.stem.2011.11.018.

Samal, P., P. Maurer, C. van Blitterswijk, R. Truckenmüller, and S. Giselbrecht (2020). "A New Microengineered Platform for 4D Tracking of Single Cells in a Stem-Cell-Based In Vitro Morphogenesis Model". In: *Advanced materials (Deerfield Beach, Fla.)* 32.24, e1907966. DOI: 10.1002/adma.201907966.

Santos-Ferreira, T. et. al (2016). "Stem Cell-Derived Photoreceptor Transplants Differentially Integrate Into Mouse Models of Cone-Rod Dystrophy". In: *Investigative ophthalmology & visual science* 57.7, pp. 3509–3520. DOI: 10.1167/iovs.16-19087.

Sato, T. et. al (2009). "Single Lgr5 stem cells build crypt-villus structures in vitro without a mesenchymal niche". In: *Nature* 459.7244, pp. 262–265. DOI: 10.1038/nature07935.

Scalia, F. and K. Fite (1974). "A retinotopic analysis of the central connections of the optic nerve in the frog". In: *J. Comp. Neur.* 158, pp. 455–478. DOI: 10.1002/cne.901580406.

Seabra, Rita and Nirmala Bhogal (2010). "In Vivo Research Using Early Life Stage Models". In: *In vivo (Athens, Greece)* 24, pp. 457–462.

Selden, Clare and Barry Fuller (2018). "Role of Bioreactor Technology in Tissue Engineering for Clinical Use and Therapeutic Target Design". In: *Bioengineering (Basel, Switzerland)* 5.2. ISSN: 2306-5354. DOI: 10.3390/bioengineering5020032.

Sen, J., S. Harpavat, M. A. Peters, and C. L. Cepko (2005). "Retinoic acid regulates the expression of dorsoventral topographic guidance molecules in the chick retina". In: *Development (Cambridge, England)* 132.23, pp. 5147–5159. DOI: 10.1242/dev.02100.

Shafiee, A. and A. Atala (2017). "Tissue Engineering: Toward a New Era of Medicine". In: *Annual review of medicine* 68, pp. 29–40. DOI: 10.1146/annurev-med-102715-092331.

Shaham, O., Y. Menuchin, C. Farhy, and R. Ashery-Padan (2012). "Pax6: a multi-level regulator of ocular development". In: *Progress in retinal and eye research* 31.5, pp. 351–376. ISSN: 1350-9462. DOI: 10.1016/j.preteyeres.2012.04.002.

Sheedlo, H. J., T. J. Bartosh, Z. Wang, B. Srinivasan, A. M. Brun-Zinkernagel, and R. S. Roque (2007). "RPE-derived factors modulate photoreceptor differentiation: a possible role in the retinal stem cell niche". In: *In vitro cellular & developmental biology. Animal* 43.10, pp. 361–370. ISSN: 1071-2690. DOI: 10.1007/s11626-007-9051-3.

Sheedlo, H. J. and J. E. Turner (1992). "Effects of RPE-cell factors secreted from permselective fibers on retinal cells in vitro". In: *Brain research* 587, pp. 327–337. DOI: 10.1016/0006-8993(92)91015-7.

Sheffield, J. B. and A. A. Moscona (1969). "Early stages in the reaggregation of embryonic chick neural retina cells". In: *Experimental cell research*.

Shin, E. Y., J. H. Park, M. E. Shin, J. E. Song, M. Thangavelu, C. Carlomagno, A. Motta, C. Migliaresi, and G. Khang (2019). "Injectable taurine-loaded alginate hydrogels for retinal pigment epithelium (RPE) regeneration". In: *Materials science & engineering. C, Materials for biological applications* 103, p. 109787. DOI: 10.1016/j.msec.2019.109787.

Shkumatava, A., S. Fischer, F. Müller, U. Strahle, and C. J. Neumann (2004). "Sonic hedgehog, secreted by amacrine cells, acts as a short-range signal to direct differentiation and lamination in the zebrafish retina". In: *Development (Cambridge, England)* 131.16, pp. 3849–3858. DOI: 10.1242/dev.01247.

Shrestha, A., B. N. Allen, L. A. Wiley, B. A. Tucker, and K. S. Worthington (2020). "Development of High-Resolution Three-Dimensional-Printed Extracellular Ma-

trix Scaffolds and Their Compatibility with Pluripotent Stem Cells and Early Retinal Cells". In: *Journal of ocular pharmacology and therapeutics : the official journal of the Association for Ocular Pharmacology and Therapeutics* 36.1, pp. 42–55. DOI: 10.1089/jop.2018.0146.

Sigulinsky, C. L., E. S. Green, A. M. Clark, and E. M. Levine (2008). "Vsx2/Chx10 ensures the correct timing and magnitude of Hedgehog signaling in the mouse retina". In: *Developmental biology* 317.2, pp. 560–575. DOI: 10.1016/j.ydbio.2008.02.055.

Singh, M., H. M. Haverinen, P. Dhagat, and G. E. Jabbour (2010). "Inkjet printing-process and its applications". In: *Advanced materials (Deerfield Beach, Fla.)* 22.6, pp. 673–685. DOI: 10.1002/adma.200901141.

Soofi, S. S., J. A. Last, S. J. Liliensiek, P. F. Nealey, and C. J. Murphy (2009). "The elastic modulus of Matrigel as determined by atomic force microscopy". In: *Journal of structural biology* 167.3, pp. 216–219. DOI: 10.1016/j.jsb.2009.05.005.

Soto, F., K. L. Watkins, R. E. Johnson, F. Schottler, and D. Kerschensteiner (2013). "NGL-2 regulates pathway-specific neurite growth and lamination, synapse formation, and signal transmission in the retina". In: *The Journal of neuroscience : the official journal of the Society for Neuroscience* 33.29, pp. 11949–11959. DOI: 10.1523/JNEUROSCI.1521-13.2013.

Sparrow, J. R., D. Hicks, and C. P. Hamel (2010). "The retinal pigment epithelium in health and disease". In: *Current molecular medicine* 10.9, pp. 802–823. DOI: 10.2174/156652410793937813.

Sperling, L. E., K. P. Reis, L. G. Pozzobon, C.a S. Girardi, and P. Pranke (2017). "Influence of random and oriented electrospun fibrous poly(lactic-co-glycolic acid) scaffolds on neural differentiation of mouse embryonic stem cells". In: *Journal of biomedical materials research. Part A* 105.5, pp. 1333–1345. DOI: 10.1002/jbm.a.36012.

Sridhar, A. et. al (2020). "Single-Cell Transcriptomic Comparison of Human Fetal Retina, hPSC-Derived Retinal Organoids, and Long-Term Retinal Cultures". In: *Cell reports* 30.5, 1644–1659.e4. DOI: 10.1016/j.celrep.2020.01.007.

Steinfeld, J., I. Steinfeld, N. Coronato, M.-L. Hampel, P. G. Layer, M. Araki, and A. Vogel-Höpker (2013). "RPE specification in the chick is mediated by surface ectoderm-derived BMP and Wnt signalling". In: *Development (Cambridge, England)* 140.24, pp. 4959–4969. DOI: 10.1242/dev.096990.

Strauss, O. (2005). "The retinal pigment epithelium in visual function". In: *Physiological reviews* 85.3, pp. 845–881. ISSN: 0031-9333. DOI: 10.1152/physrev.00021.2004.

Svoboda, K. K. H. and S. O'Shea (1987). "An analysis of cell shape and the neuroepithelial basal lamina during optic vesicle formation in the mouse embryo". In: *Development* 100, pp. 185–200.

Takahashi, K. and S. Yamanaka (2006). "Induction of pluripotent stem cells from mouse embryonic and adult fibroblast cultures by defined factors". In: *Cell* 126.4, pp. 663–676. DOI: 10.1016/j.cell.2006.07.024.

Takeichi, M. (1995). "Morphogenetic roles of classic cadherins". In: *Current biology : CB*.

Talbot, N. C. and T. J. Caperna (2015). "Proteome array identification of bioactive soluble proteins/peptides in Matrigel: relevance to stem cell responses". In: *Cytotechnology* 67.5, pp. 873–883. ISSN: 0920-9069. DOI: 10.1007/s10616-014-9727-y.

Tang, Z. et. al (2019). "Mussel-inspired injectable hydrogel and its counterpart for actuating proliferation and neuronal differentiation of retinal progenitor cells". In: *Biomaterials* 194, pp. 57–72. ISSN: 0142-9612. DOI: 10.1016/j.biomaterials.2018.12.015.

Taylor, L., K. Arnér, K. Engelsberg, and F. Ghosh (2015). "Scaffolding the retina: the interstitial extracellular matrix during rat retinal development". In: *International journal of developmental neuroscience : the official journal of the International Society for Developmental Neuroscience* 42, pp. 46–58. DOI: 10.1016/j.ijdevneu.2015.03.002.

Tétreault, N., M.-P. Champagne, and G. Bernier (2009). "The LIM homeobox transcription factor Lhx2 is required to specify the retina field and synergistically cooperates with Pax6 for Six6 trans-activation". In: *Developmental biology* 327.2, pp. 541–550. DOI: 10.1016/j.ydbio.2008.12.022.

Thompson, J. R. et. al (2019). "Two-photon polymerized poly(caprolactone) retinal cell delivery scaffolds and their systemic and retinal biocompatibility". In: *Acta biomaterialia* 94, pp. 204–218. DOI: 10.1016/j.actbio.2019.04.057.

Tomaskovic-Crook, E. and J. M. Crook (2019). "Clinically Amendable, Defined, and Rapid Induction of Human Brain Organoids from Induced Pluripotent Stem Cells". In: *Methods in molecular biology (Clifton, N.J.)* 1576, pp. 13–22. DOI: 10.1007/7651$_$2017$_$95.

Turing, A. M. (1952). "The chemical basis of morphogenesis". In: *The Royal Society* 237.

Turner, D. L. and C. L. Cepko (1987). "A common progenitor for neurons and glia persists in rat retina late in development". In: *Nature* 1987.328. DOI: 10.1038/328131a0.

Turunen, S., T. Joki, M. L. Hiltunen, T. O. Ihalainen, S. Narkilahti, and M. Kellomäki (2017). "Direct Laser Writing of Tubular Microtowers for 3D Culture of Human Pluripotent Stem Cell-Derived Neuronal Cells". In: *ACS applied materials & interfaces* 9.31, pp. 25717–25730. DOI: 10.1021/acsami.7b05536.

Ueda, K., A.i Onishi, S.-I. Ito, M. Nakamura, and M. Takahashi (2018). "Generation of three-dimensional retinal organoids expressing rhodopsin and S- and M-cone opsins from mouse stem cells". In: *Biochemical and biophysical research communications* 495.4, pp. 2595–2601. DOI: 10.1016/j.bbrc.2017.12.092.

Vancamp, P. and V. M. Darras (2017). "Dissecting the role of regulators of thyroid hormone availability in early brain development: Merits and potential of the chicken embryo model". In: *Molecular and cellular endocrinology* 459, pp. 71–78. DOI: 10.1016/j.mce.2017.01.045.

Veien, E. S., J. S. Rosenthal, R. C. Kruse-Bend, C.-B. Chien, and R. I. Dorsky (2008). "Canonical Wnt signaling is required for the maintenance of dorsal retinal identity". In: *Development (Cambridge, England)* 135.24, pp. 4101–4111. DOI: 10.1242/dev.027367.

Völkner, M., M. Zschätzsch, M. Rostovskaya, R. W. Overall, V. Busskamp, K. Anastassiadis, and M. O. Karl (2016). "Retinal Organoids from Pluripotent Stem Cells Efficiently Recapitulate Retinogenesis". In: *Stem cell reports* 6.4, pp. 525–538. ISSN: 2213-6711. DOI: 10.1016/j.stemcr.2016.03.001.

Vollmer, G. (1984). "Reaggregation of Embryonic Chick Retina Cells: Pigment Epithelial Cells Induce a High Order of Stratification". In: *Neuroscience letters* 48, pp. 191–196. DOI: 10.1016/0304-3940(84)90018-1.

Vollmer, G. and P. G. Layer (1986a). "Reaggregation of chick retinal and mixtures of retinal and pigment epithelial cells: The degree of laminar organization is dependent on age". In: *Neuroscience letters* 63.1, pp. 91–95. DOI: 10.1016/0304-3940(86)90019-4.

– (1986b). "Reaggregation of chick retinal and mixtures of retinal pigment epithelial cells: the degree of laminar organization is dependent on age". In: *Neuroscience letters*.

Vollmer, G., P. G. Layer, and A. Gierer (1984). "Reaggregation of embryonic chick retina cells: pigment epithelial cells induce a high order of stratification". In: *Neuroscience letters* 48, pp. 191–196.

Vukicevic, S., H. K. Kleinman, F. P. Luyten, A. B. Roberts, N. S. Roche, and A. H. Reddi (1992). "Identification of Multiple Active Growth Factors in Basement Membrane Matrigel Suggests Caution in Interpretation of Cellular Activity Related to Extracellular Matrix Components". In: *Experimental cell research* 202, pp. 1–8. DOI: 10.1016/0014-4827(92)90397-q.

Wade, N. J. (2008). "Cajal's retina". In: *Cortex; a journal devoted to the study of the nervous system and behavior* 44.3, pp. 227–228. ISSN: 0010-9452. DOI: 10.1016/j.cortex.2007.12.001.

Wallis, D. E. and M. Muenke (1999). "Molecular Mechanisms of Holoprosencephaly". In: *Molecular genetics and metabolism* 68, pp. 126–138. DOI: 10.1006/mgme.1999.2895.

Wang, J., M. L. O'Sullivan, D. Mukherjee, V. M. Puñal, S. Farsiu, and J. N. Kay (2017). "Anatomy and spatial organization of Müller glia in mouse retina". In: *The Journal of comparative neurology* 525.8, pp. 1759–1777. DOI: 10.1002/cne.24153.

Wang, L. et. al (2018). "Retinal Cell Type DNA Methylation and Histone Modifications Predict Reprogramming Efficiency and Retinogenesis in 3D Organoid Cultures". In: *Cell reports* 22.10, pp. 2601–2614. DOI: 10.1016/j.celrep.2018.01.075.

Wang, S., Y. Wang, L. Song, J. Chen, Y. Ma, Y. Chen, S. Fan, M. Su, and X. Lin (2017). "Decellularized tendon as a prospective scaffold for tendon repair". In: *Materials science & engineering. C, Materials for biological applications* 77, pp. 1290–1301. DOI: 10.1016/j.msec.2017.03.279.

Wawesik S., Maas R. L. (2000). "Vertebrate eye developoment as model in Drosophila". In: *Human molecular genetics* Vol 9, No. 6. DOI: 10.1093/hmg/9.6.917.

Welby, E. et. al (2017). "Isolation and Comparative Transcriptome Analysis of Human Fetal and iPSC-Derived Cone Photoreceptor Cells". In: *Stem cell reports* 9.6, pp. 1898–1915. ISSN: 2213-6711. DOI: 10.1016/j.stemcr.2017.10.018.

West, E. L., A. Gonzalez-Cordero, C. Hippert, F. Osakada, J. P. Martinez-Barbera, R. A. Pearson, J. C. Sowden, M. Takahashi, and R. R. Ali (2012). "Defining the integration capacity of embryonic stem cell-derived photoreceptor precursors". In: *Stem cells (Dayton, Ohio)* 30.7, pp. 1424–1435. DOI: 10.1002/stem.1123.

Westenskow, P., S. Piccolo, and S. Fuhrmann (2009). "Beta-catenin controls differentiation of the retinal pigment epithelium in the mouse optic cup by regulating Mitf and Otx2 expression". In: *Development (Cambridge, England)* 136.15, pp. 2505–2510. DOI: 10.1242/dev.032136.

Willbold, E., M. Reinicke, C. Lance-Jones, C. Lagenaur, V. Lemmon, and P. G. Layer (1995). "Müller Glia Stabilizes Cell Columns During Retinal Development: Lateral Cell Migration but not Neuropil Growth is Inhibited in Mixed Chick-Quail Retinospheroids". In: *European Journal of Neuroscience* 7, pp. 2277–2284.

Willbold, E., A. Rothermel, S. Tomlinson, and P. G. Layer (2000). "Müller glia cells reorganize reaggregating chicken retinal cells into correctly laminated in vitro retinae". In: *Glia* 29.1, pp. 45–57.

Wilson S. W., Houart C. (2004). "Early steps in the development of the forebrain". In: *Developmental cell* 6, pp. 167–181. DOI: 10.1016/s1534-5807(04)00027-9.

Worthington, K. S., L. A. Wiley, E. E. Kaalberg, M. M. Collins, R. F. Mullins, E. M. Stone, and B. A. Tucker (2017). "Two-photon polymerization for production of human iPSC-derived retinal cell grafts". In: *Acta biomaterialia* 55, pp. 385–395. DOI: 10.1016/j.actbio.2017.03.039.

Wright, L. S., I. Pinilla, J. Saha, J. M. Clermont, J. S. Lien, K. D. Borys, E. E. Capowski, M. J. Phillips, and D. M. Gamm (2015). "VSX2 and ASCL1 Are Indicators of Neurogenic Competence in Human Retinal Progenitor Cultures". In: *PloS one* 10.8, e0135830. DOI: 10.1371/journal.pone.0135830.

Xu, T., C. Baicu, M. Aho, M. Zile, and T. Boland (2009). "Fabrication and characterization of bio-engineered cardiac pseudo tissues". In: *Biofabrication* 1.3, p. 035001. DOI: 10.1088/1758-5082/1/3/035001.

Yanez, M., J. Rincon, A. Dones, C. de Maria, R. Gonzales, and T. Boland (2015). "In vivo assessment of printed microvasculature in a bilayer skin graft to treat full-thickness wounds". In: *Tissue engineering. Part A* 21.1-2, pp. 224–233. DOI: 10.1089/ten.TEA.2013.0561.

Yang, W., R. Xia, Y. Zhang, H. Zhang, and L. Bai (2018). "Decellularized Liver Scaffold for Liver Regeneration". In: *Methods in molecular biology (Clifton, N.J.)* 1577, pp. 11–23. DOI: 10.1007/7651$_$2017$_$53.

Yen, L. and R. S. Fager (1984). "Chromatographic resolution of the rod pigment from the four cone pigments of the chick retina". In: *Vision research* 24/11, pp. 1555–1562. DOI: 10.1016/s0042-6989(84)80005-x.

Yonekura, S., L. Xu, C.-Y. Ting, and C.-H. Lee (2007). "Adhesive but not signaling activity of Drosophila N-cadherin is essential for target selection of photoreceptor afferents". In: *Developmental biology* 304.2, pp. 759–770. DOI: 10.1016/j.ydbio.2007.01.030.

Zadeh, M. A., M. Khoder, A. A. Al-Kinani, H. M. Younes, and R. G. Alany (2019). "Retinal cell regeneration using tissue engineered polymeric scaffolds". In: *Drug discovery today* 24.8, pp. 1669–1678. DOI: 10.1016/j.drudis.2019.04.009.

Zandrini, T., O. Shan, V. Parodi, G. Cerullo, M. T. Raimondi, and R. Osellame (2019). "Multi-foci laser microfabrication of 3D polymeric scaffolds for stem cell expansion in regenerative medicine". In: *Scientific reports* 9.1, p. 11761. DOI: 10.1038/s41598-019-48080-w.

Zerti, D., B. Dorgau, M. Felemban, Ghareeb, A, E., Yu. M, Y. Ding, N. Krasnogor, and M. Lako (2020). "Developing a simple method to enhance the generation of cone and rod photoreceptors in pluripotent stem cell-derived retinal organoids". In: *Stem cells (Dayton, Ohio)* 38.1, pp. 45–51. DOI: 10.1002/stem.3082.

Zhang, C., A. L. Kolodkin, R. O. Wong, and R. E. James (2017). "Establishing Wiring Specificity in Visual System Circuits: From the Retina to the Brain". In: *Annual review of neuroscience* 40, pp. 395–424. DOI: 10.1146/annurev-neuro-072116-031607.

Zhong, X. et. al (2014). "Generation of three-dimensional retinal tissue with functional photoreceptors from human iPSCs". In: *Nature communications* 5, p. 4047. DOI: 10.1038/ncomms5047.

Zhu, J. and D. A. Lamba (2018). "Small Molecule-Based Retinal Differentiation of Human Embryonic Stem Cells and Induced Pluripotent Stem Cells". In: *Bio-protocol* 8.12. ISSN: 2331-8325. DOI: 10.21769/BioProtoc.2882.

Zhu, J., J. Reynolds, T. Garcia, H. Cifuentes, S. Chew, X. Zeng, and D. A. Lamba (2018). "Generation of Transplantable Retinal Photoreceptors from a Current Good Manufacturing Practice-Manufactured Human Induced Pluripotent Stem Cell Line". In: *Stem cells translational medicine* 7.2, pp. 210–219. ISSN: 2157-6564. DOI: 10.1002/sctm.17-0205.

Zuber, M. E., G. Gestri, A. S. Viczian, G. Barsacchi, and W. A. Harris (2003). "Specification of the vertebrate eye by a network of eye field transcription factors". In: *Development (Cambridge, England)* 130.21, pp. 5155–5167. DOI: 10.1242/dev.00723.

Acknowledgements

Firstly, I want to thank Prof. Dr. Martin Bastmeyer for giving me the opportunity to prepare my PhD thesis at his institute on a very interesting and visionary project. A balance of independent work and ready support whenever needed was nicely managed. During all this time, I had the opportunity to grow as a scientist and on a personal level - a process which hopefully will never be fully finished.

Furthermore, I want to thank Dr. Dietmar Gradl for taking on the responsibility of being the co-referee for this work.

I want to thank all of my colleagues at the Zoological Institute, who made this journey so enjoyable and memorable. A big thanks goes out to all the voluntary and involuntary bakers, who provided an occasional and tasty snack. Also, thank you all for the friendly and cooperative atmosphere! A special thanks goes to Annemarie, Elisa and Magdalena, for always having a few minutes to listen to my wailing and for always being supportive!

A very big thank you goes out to Sarah Bertels, who endured my presence starting from the Zellbio-F2 way back in 2015, I believe? It was a pleasure doing my master thesis under your supervision and to have you as a colleague and supervisor during the PhD. Also, thank you for the critical and thorough proofreading of not only this dissertation, but so many abstracts and posters beforehand. You are dearly missed at the institute!

Also, a special thanks goes to Marc Hippler, who was always there and eager to help with whichever problems occurred. Thank you for sacrificing your time to introduce me to the DLW, for critical comments and discussion and for introducing me to LaTeX!

I also want to thank Chiara Windsor and Kai Richler for the great work during their master theses. Thank you for letting me use your data in this dissertation. It was a pleasure to have you as students.

Furthermore, I want to thank the cluster of excellence 3DMM2O, especially the members of Thrust C3. The discussions and frequent meetings were helpful in steering my project in the right direction.

I also want to thank all of my friends, who accompanied me during the last few years. Thank you for taking my mind off of work, for making this time quite enjoyable and memorable. A special thanks to all of you who were willing to proofread parts of this dissertation. To name all of you, the list would get quite crowded, so thank you all!

Lastly, I want to thank my family. Throughout the years, you have been a source of strength and peace. Thanks for always being there for me and having my back. A special thanks goes out to my parents, who made this whole endeavour possible. You are the reason I am now sitting here, finishing these lines. Thank you from the bottom of my heart.